University of Calgary

PRISM Repository **https://prism.ucalgary.ca**

The Vault Open Theses and Dissertations

2014-01-30

Synaptic Zinc and Cortical Sensory Processing in the Laboratory Mouse

Wu, Hsia-Pai Patrick

Wu, H. P. (2014). Synaptic Zinc and Cortical Sensory Processing in the Laboratory Mouse (Doctoral thesis, University of Calgary, Calgary, Canada). Retrieved from https://prism.ucalgary.ca. doi:10.11575/PRISM/27948

http://hdl.handle.net/11023/1346

Downloaded from PRISM Repository, University of Calgary

UNIVERSITY OF CALGARY

Synaptic Zinc and Cortical Sensory Processing in the Laboratory Mouse

by

Hsia-Pai Patrick Wu

A THESIS

SUBMITTED TO THE FACULTY OF GRADUATE STUDIES

IN PARTIAL FULFILMENT OF THE REQUIREMENTS FOR THE

DEGREE OF DOCTOR OF PHILOSOPHY

DEPARTMENT OF PSYCHOLOGY

CALGARY, ALBERTA

JANUARY, 2014

© HSIA-PAI PATRICK WU 2014

Abstract

A growing body of evidence indicates that synaptic zinc plays an important role in regulating neocortical neurotransmission. The goal of this thesis was to further examine the pattern of the distribution of synaptic zinc in the mammalian cortex and how synaptic zinc mediates synaptic transmission to affect cortical function and the generation of behaviour.

The mouse visual cortex was used as a model system to observe the experience-dependent regulation of synaptic zinc levels. Histochemical analysis revealed that monocular deprivation dynamically altered the distribution of synaptic zinc in the deprived ocular domains of the visual cortex. Short (1 day) deprivation dramatically increased synaptic zinc density in layer IV of the deprived domains while long-term (3 months) deprivation elevated synaptic zinc levels in layers V and II/III. This result was similar to observations made in the visual cortex of cats and monkeys as well the barrel cortex of mice.

The relationship between synaptic zinc in the barrel cortex and the processing of vibrissal sensory input was examined by assessing barrel cortex-dependent behaviour in a transgenic mouse that does not have synaptic zinc (ZnT3 KO mouse). A novel behavioural test that measured barrel cortex-dependent texture discrimination was devised and used to assay mystacial vibrissae function in ZnT3 KO mice. It was observed that ZnT3 KO mice retained the ability to use vibrissal tactile information to discriminate between textures but the acuity of the vibrissal sensory system was greatly reduced. *In vivo* voltage-sensitive dye imaging revealed that stimulation-evoked activity in the barrel cortex of ZnT3 KO mice is altered.

Together, the results of this thesis suggest that synaptic zinc levels are dynamically modulated by sensory experience and that synaptic zinc contributes to the integration of sensory information within the primary sensory cortices.

Acknowledgements

I would like to thank my supervisor, Dr. Richard Dyck. You have made a trying time for an inexperienced student enjoyable and eye-opening. You have led by example and provided invaluable and much needed guidance on matters not restricted to research and academics. Thank you for always keeping your door open and for all of your seemingly unlimited patience and understanding.

I would also like to thank Drs. Mike Antle, Jos Eggermont, William Stell, and Craig Brown for serving on my defence committee, as well as the past and present members of the Neurodevelopment and Plasticity lab for making an Ontario native feel welcomed and supported here in the Canadian Wild West.

Lastly, I would like to thank my friends and family, who have provided support I could not have done without and given me more latitude than I deserve these past 4 years. Thank you.

Dedication

I would like to dedicate this thesis to my wife Alice and baby boy Eason, both of whom had to make many sacrifices to allow me time to complete this document. I look forward to making Eason sit through a reading when he is old enough.

Table of Contents

List of Figures and Illustrations

List of Symbols, Abbreviations and Nomenclature

Unites of measurement

Symbol	Definition
°C	degrees Celsius
h	hour
min	minute
s	second
ms	millisecond
cm	centimetre
cm	millimetre
µm	micrometre
nm	nanometre
kg	kilogram
mg	milligram
ml	millilitre
M	molar
mM	millimolar
µM	micromolar
nM	nanomolar
pM	picomolar
dB	decibel
kHz	kilohertz
W	Watt
Kd	dissociation constant
pKa	acid dissociation constant
kZn	zinc-binding constant

Abbreviations

Symbol	Definition
2-AG	2-arachidonoylglycerol
A1	Primary auditory cortex
ACSF	Artificial cerebral spinal fluid
AMPA	α-Amino-3-hydroxy-5-methyl-4-isoxazolepropionic acid
AP-3	Floral homeotic protein APETALA 3
BDNF	Brain-derived neurotrophic factor
C57BL/6	C57 black 6 mice
cAMP	Cyclic adenosine monophosphate
CaEDTA	Calcium salt of ethylenediaminetetraacetic acid
CaMKII	Calcium/calmodulin-dependent protein kinase II

CB1	Endocannabinoid receptor 1
DNA	Deoxyribonucleic acid
EDTA	Ethylenediaminetetraacetic acid
EPSP	Excitatory post-synaptic potential
ERK	Extracellular signal-regulated kinases
GABA	γ-aminobutyric acid
GluK	Kainate receptor
GluR	Glutamate receptor
GPCR	G protein-coupled receptor
GPR39	G-protein-coupled receptor 39
HEK	Human embryonic kidney
HEPES	Hydroxyethyl piperazineethanesulfonic acid
KO	Knock out
LTD	Long term depression
LTP	Long term potentiation
MAPK	Mitogen activated protein kinase
MT	Metallothioneins
NMDA	N-methyl-D-aspartate
NR2	NMDA receptor 2
PKA	cAMP-dependent protein kinase A
PKC	cAMP-dependent protein kinase C
SAMP10	senescence-accelerated-prone 10 transgenic mice
TrkB	Tropomyosin-related kinase B
Trycine	N-(2-hydroxy-1,1-bis(hydroxymethyl)ethyl) glycine
TPEN	N,N,N′,N′-tetrakis(2-pyridylmethyl)-ethylenediamine
V1	Primary visual cortex
V1B	Binocular domain of the primary visual cortex
V1M	Monocular domain of the primary visual cortex
VPM	Ventral posterior medial thalamic nucleus
VSD	Moltage-sensitive dye
WT	Wild type
ZIP	Zrt-Irt-like protein

ZnR	Zinc receptor
ZnT	Zinc transporter protein

Epigraph

Mientras el cerebro sea un misterio, el universo continuará siendo un misterio también (While the brain is a mystery, the universe will remain a mystery as well)

— Santiago Ramón y Cajal

CHAPTER ONE: GENERAL INTRODUCTION

The fundamental function of the nervous system is the generation of appropriate behaviour in response to cues from the organism's environment. The nervous system must develop and mature as the organism ages, adapt and learn when presented with novel or fluctuating stimuli, and respond to and recover from injury or pathology. The complexity with which a nervous system can function will dictate its ability to integrate sensory information from the constantly changing environment. The nervous system achieves high levels of complexity through morphology and chemical neuromodulation. Therefore, understanding the myriad of mechanisms that govern neurotransmission is essential to, ultimately, the understanding of nervous system function and the production of complex behaviour. It is the focus of the studies presented herein to examine one potent neuromodulator, synaptic zinc, and its role in cortical processing of sensory information.

In addition to the milieu of systems this nutritionally essential element contributes to in the human body, the divalent cation zinc also participates in neuromodulation within the nervous system. Specifically, a subset of zinc within the brain is concentrated in synaptic vesicles and can be released at the presynaptic terminal (Frederickson, 1989; Qian and Noebels, 2005). The location of zinc releasing (zincergic) neurons and the co-release of zinc with neurotransmitters such as glutamate suggest that synaptic zinc is intimately involved in neuromodulation within the cerebral cortex (see Nakashima and Dyck, 2009). In the studies presented herein, the neuromodulator synaptic zinc was

investigated in the context of sensory information processing in the cerebral cortex and experience-dependent cortical plasticity.

1.1 Zinc Biology

The first evidence that zinc is essential to life was discovered in the mid 1800s, when the mineral was found to be essential for the growth of the common bread mould, *Aspergillus niger* (Raulin, 1869). Since then, it has been discovered that zinc is present in all cells and participates in a variety of systems and functions (Prasad et al., 1963; Cousins et al., 2006). Zinc stabilizes protein and nucleic acid structure and act as a cofactor in hundreds of enzymes (Vallee and Falchuk, 1993; MacDonald, 2000). An estimated 10% of all proteins in humans contain zinc as a cofactor (Blasie and Berg, 2002) while between 40-50% of all proteins that participate in the regulation of DNA transcription have binding sites for zinc (Tupler et al., 2001). Zinc is involved in the regulation of essential functions throughout the body, but also has specialized functions within individual systems.

1.2 Zinc Homeostasis within the Brain

In addition to performing essential structural and regulatory functions, zinc is also concentrated in synaptic vesicles within the brain. Approximately 20% of zinc in the brain is found in vesicles (Frederickson, 1989; Cole et al., 1999). This pool of vesicular zinc is not tightly bound to proteins and exists in its free, ionic form, loosely bound to glutamate. Synaptic activation leads to release of this vesicular zinc and transiently increases the concentration of zinc ions in the synaptic cleft (Vogt et al., 2000; Qian and Noebels, 2005; Frederickson et al., 2006). A variety of transmembrane proteins are

sensitive to extracellular zinc. Zinc may also enter or re-enter the post- and presynaptic cell. A growing body of research indicates that zinc ions play a dynamic role in the physiology of brain function.

Alterations in zinc levels outside of normal physiological concentrations have been implicated in epilepsy, ischemia, and neurological diseases such as Alzheimer's and depression (Frederickson et al., 2005; Galasso and Dyck, 2007). For this reason, zinc homeostasis within neurons is strictly regulated. The cellular influx, efflux, and transport of zinc are maintained by three classes of proteins – Zrt-Irt-like proteins (ZIP), metallothioneins (MT), and zinc transporter (ZnT).

1.2.1 Zinc influx

ZIP transporters are responsible for the influx of zinc into the cytoplasm. The ZIP family transporter 1 (ZIP1) is expressed in all cells, including neurons. ZIP1 is located on the plasma membrane as well as the endoplasmic reticulum and facilitates the transport of extracellular zinc as well as zinc stores within the endoplasmic reticulum, repectively, into the cytoplasm (Gaither and Eide, 2001). Thirteen other mammalian ZIP transporters have been identified. All except ZIP7, which is located at the Golgi apparatus, were observed at the plasma membrane. The characterization, precise locations of expression, and exact mechanism for zinc translocation have yet to be outlined in detail for all fourteen known ZIP transporters.

α-Amino-3-hydroxy-5-methyl-4-isoxazolepropionic acid (AMPA) receptor channels without the GluR2 subunit, and kainate receptor channels, may provide entry into neurons for zinc (Hollmann et al 1991; Yin et al 1998). Zinc influx here is only

possible though AMPA and kainic receptors that are also permeable to calcium. As such, zinc influx has also been reported across voltage-dependent calcium channels (Sensi et al., 1999). N-methyl-D-aspartate (NMDA) receptor channels may also allow for zinc influx. Zinc influx here is proposed to be possible though an inhibitory zinc binding site within the pore of the NMDA receptor. Zinc may disengage following binding to this site and move into the neuron (Koh and Choi, 1994).

1.2.2 Intracellular zinc levels

The cytoplasmic concentration of zinc within the neuron is buffered by metallothioneins (MT), a family of cysteine-rich proteins capable of binding cations. MTs are able to bind up to seven zinc atoms and act as a buffer, temporarily binding zinc at high zinc concentration and releasing zinc when cytoplasmic zinc concentration is low (Vallee, 1995). Four MTs have been characterized in mammals. Of these, MT-I and MT-II can be found in several cell types including astrocytes and glia within the spinal cord, while MT-IV is found in a variety of epithelial cells (see Palmiter, 1998). MT-III is exclusive to neurons, particularly those containing vesicular zinc. Perhaps as a consequence to its association with vesicular zinc, MT-III has been linked to the pathophysiology of zinc-related neurological diseases. It has been suggested that MT-III is down-regulated in Alzheimer's disease and MT-III knock out (KO) mice have increased susceptibility to kainic acid-induced seizures (Edadi et al., 1995; Erickson et al., 1997).

The mitochondrion may serve as an intracellular store of zinc. Zinc influx and efflux has both been observed at the mitochondrion (Colvin et al., 2003). Although sub-micromolar concentrations of zinc are sufficient to cause mitochondrial dysfunction

(Dineley et al., 2005), under normal circumstances the concentrations free zinc in the cytoplasm is low to non-existent (Outten and O'Halloran, 2001). In concert with MTs, the mitochondrion likely facilitates the regulation of cytosolic zinc concentration by acting as a buffer for cytoplasmic zinc.

1.2.3 Efflux of cytosolic zinc

The transport of zinc out of the cytoplasm within mammalian cells depends on a family of zinc transporter proteins (ZnT). ZnTs are responsible for the efflux of cytosolic zinc in order to clear excess zinc and transport zinc into intracellular organelles (Cousins et al., 2006). Within the neuron, ZnT1 facilitates zinc efflux at the plasma membrane while ZnT2 and ZnT4 package zinc ions into endosomes and lysosomes (Palmiter and Huang, 2004). A total of 10 ZnT proteins have been described. Their precise function, however, remains to be characterized, especially in the neuron.

ZnT3 is the most thoroughly characterized ZnT protein and is of particular interest within neurons. ZnT3 is responsible for the movement of cytosolic zinc into synaptic vesicles (Palmiter et al., 1996). The deletion of ZnT3 in ZnT3 KO mice leads to a complete absence of vesicular zinc within the brain (Cole et al., 1999).

1.3 Synaptic Zinc

Synaptic vesicles replete with free zinc (rapidly exchangeable zinc ions) were first described in hippocampal mossy fibre boutons in 1967 (Haug, 1967). Approximately 20% of the neuronal pool of zinc is found in zinc-containing synaptic vesicles (Cole et al., 1999). This vesicular pool of zinc can be visualized through autometallographic

staining with sodium selenite (Danscher, 1982; Frederickson, 1989). Systemically circulated selenite binds with histochemically reactive zinc and the resulting zinc selenite crystals can be stained with silver and developed for visualization (See Section 2.3.2). All histochemically reactive zinc in the brain is vesicular (Danscher, 1985, 1996; Perez-Clausell and Danscher, 1985); with the exception of injured nerons and artifacts, zinc staining exclusively indicates the presence of zinc-filled secretory vesicles, either at the presynaptic bouton or en route in the axon. As previously mentioned, ZnT3 is responsible for the movement of cytoplasmic zinc into synaptic vesicles. The distribution of ZnT3 is identical to the pattern of zinc staining within the brain (Cole et al., 1999). Knockout of ZnT3 corresponds to the loss of approximately 20% of zinc within the brain and complete loss of histochemically reactive zinc (Cole et al., 1999).

Different terminologies are used to refer to this pool of loosely bound zinc ions in the brain, including ‘free’, ‘rapidly exchangeable’, ‘mobile’, ‘histochemically reactive’, ‘chelatable’, ‘vesicular’, and ‘synaptic’ zinc. For this thesis, ‘zinc’ will be used to refer to loosely bound zinc ions in general. Given that the focus of this thesis is the role of zinc in modulating neurotransmission, and also the assumption that vesicular zinc is released at the synaptic cleft, ‘synaptic zinc’ will be used to refer to both the vesicular pool of zinc and zinc released into the synaptic cleft. ‘Vesicular zinc’ will be reserved for reference specifically to zinc within vesicles when distinction between ‘synaptic’ and ‘vesicular’ zinc is necessary.

1.3.1 Localization

Since the pioneering identification of zinc-containing neurons in the hippocampal formation as well as throughout the telencephalon by Haug and Danscher (Haug, 1967, 1975; Danscher et al., 1973, 1975), synaptic zinc-containing terminals has been found in γ-aminobutyric acid (GABA)–ergic, glycinergic, and glutamatergic neurons throughout the body (see Nakashima and Dyck, 2009). However, zincergic neurons within the brain are almost exclusively also glutamatergic (Slomianka et al., 1990; Brown and Dyck, 2004). Although not all glutamatergic neurons contain vesicular zinc, zincergic neurons comprise an estimated 50% of all glutamatergic synapses in measured cortical structures (Sindreu et al., 2003).

Zincergic neurons are found in high concentrations throughout the cerebral cortex as well as within limbic structures such as the hippocampus, amygdala, and olfactory bulb (Dyck et al., 1993). The laminar distribution of synaptic zinc is heterogeneous, concentrated in lamina rich with dendrites and synapses – layers I-III, V, VI – while absent in the layer dense with cell bodies – layer IV (Slomianka, 1992; Dyck et al., 1993). This distribution pattern closely matches that of the NMDA receptor subunits sensitive to zinc (Wenzel et al., 1997). Zincergic projections are exclusively corticocortical, corticolimbic, and limbic-cortical, while thalamocortical projections do not contain synaptic zinc (Slomianka, 1992; Dyck et al., 1993; Casanovas-Aguilar et al., 1995). This suggests that synaptic zinc is integral in neurotransmission and functioning within the synapse-rich, evolutionarily recent, and arguably more complex cortical laminae.

1.3.2 Release

Since the discovery and characterization of vesicular zinc in the brain, it has been proposed that zinc would be released into the synapse and potentially modulate synaptic transmission. The concentration of zinc in synaptic vesicles and its co-localization with glutamate invite the assumption that vesicular zinc may be released in an activity-dependent manner. Subsequent studies in the 1980s demonstrated zinc release in hippocampal slice preparations and established that the release of vesicular zinc is stimulation- and calcium-dependent (Howell et al., 1984; Assaf and Chung, 1984). The development of zinc fluorescence imaging and electrophysiological recordings further provided strong evidence for the quantal release of zinc at hippocampal mossy fibre terminals and CA1-CA3 synapses, *in vitro*, following stimulation by a single action potential (Qian and Noebels, 2005). Numerous other studies, including, most recently, the demonstration that presynaptic stimulation-induced increase in extracellular zinc concentration activates a post synaptic zinc-sensing receptor (Perez-Rosello et al,. 2013), support these initial observations and describe a fundamental role for zinc in synaptic function (see Bitanihirwe and Cunningham, 2009; Nakashima and Dyck, 2009; Paoletti et al., 2009).

The concentration of synaptic zinc that reaches the post-synaptic membrane during synaptic stimulation has been reported to vary from nM levels to as high as 300 μM (Vogt et al., 2000; Kay, 2003; Komatsu et al., 2005; see Paoletti et al., 2009). A controversial zinc veneer hypothesis further proposes that vesicular zinc is not released at all and is instead externalized, where vesicular zinc is membrane-bound following

integration of the synaptic vesicle with the presynaptic membrane, remains restricted to the presynaptic membrane, and does not diffuse across the synaptic cleft (Kay et al., 2003; Kay and Toth, 2006). The disparity in measurements of synaptic zinc concentration may be caused by differences between the age of the animals, the choice of zinc chelators, and the temperature of the tissue slice preparation across different labs (Frederickson et al., 2006). Definitive *in vivo* observation of zinc exocytosis has yet been made, mainly because of limitations of the current zinc imaging techniques. Commonly used zinc chelators suffer from lack of selectivity for synaptic zinc (for summary, see 1.5.2), while the kinetics of available zinc fluorescent markers, with K_d in the μM range, is not sensitive enough to convincingly image zinc release under physiological conditions, which is estimated at nM to low μM levels (see Nakashima and Dyck, 2009). Recent development of novel zinc fluorescent markers and zinc chelators with high sensitivity and fast kinetics is promising for the ability to test and image for zinc release at physiological conditions (Kwon et al., 2012; Radford et al., 2013) Despite the lack of consensus regarding extracellular zinc concentrations, the majority of evidence suggests that zinc is released at the presynaptic terminal and that zinc concentrations in the synapse transiently increase to 1 – 100 μM (Vogt et al., 2000; Qian and Noebels, 2005; Frederickson et al., 2006). Stimulation-evoked release of vesicular zinc can exert an effect on both the pre- and post-synaptic membrane. These observations include the modulation of hippocampal LTP *in vivo* (Pan et al., 2011) and the activation of a putative metabotropic zinc-sensing receptor in the dorsal cochlear nucleus *in vitro* to trigger endocannabinoid synthesis (Perez-Rosello et al., 2013). As such, this thesis will proceed

with the assumption that zinc is released at the presynaptic terminal in an activity-dependent manner.

1.3.3 Signalling

Synaptic zinc can affect a variety of pre- and post-synaptic processes through alteration of receptors, channels, and intracellular signalling cascades. Zinc binding sites have been identified on purinergic, nicotinic, glycinergic, GABAergic, serotoninergic, and dopaminergic receptors (see Nakashima and Dyck, 2009). Zinc can also activate calcium/calmodulin-dependent protein kinase II (CaMKII) and tropomyosin-related kinase B (TrkB) pathways (Manzerra et al., 2000; Sindreu et al., 2011). While a general summary of zinc's effect can be drawn – zinc is primarily inhibitory at higher physiologically relevant concentrations (~100 μM – 300 μM), and potentiation occurs at lower concentrations of zinc (~10 μM) – it is important to note that response to zinc is specific to the receptor and receptor subunits and can be concentration- and membrane voltage-dependent. Chelation of endogenous extracellular zinc, on the other hand, can be proconvulsive (Mitchell and Barnes, 1993). There are numerous processes potentially modulated by zinc. For the purpose of this thesis, focus will be placed on the glutamate signalling system as well the recently identified zinc receptor.

1.3.3.1 Glutamate

1.3.3.1.1 AMPA and kainate receptors

Earlier studies suggest that zinc primarily inhibits kainate receptors and that this inhibition increases with zinc concentration (50 μM – 3 mM; Peters et al., 1987). More

recent studies indicate that zinc modulation of kainate receptor, as is typical of glutamate receptors in general, is dependent on zinc concentration and receptor subunit composition. GluK4- and GluK5-containing receptors are inhibited by lower concentrations of zinc (1 – 2 μM) while GluK1- and GluK2-containing receptors are less sensitive to zinc (~70 μM; Mott et al., 2008). Kainate receptors with GluK3 subunits are potentiated by zinc (10 μM – 100 μM; Veran et al., 2012). The regulation of AMPA receptors by zinc is also concentration dependent. High concentrations of zinc (50 μM – 300 μM) potentiates while extremely high concentrations (1 mM – 3 mM) inhibits AMPA receptors (Peters et al., 1987; Bresink et al., 1996).

1.3.3.1.2 NMDA receptors

Zinc is primarily a non-competitive allosteric, voltage-independent inhibitor of glutamate sensitive NMDA channel opening probability (Mayer & Vyklicky, 1989; Paoletti et al., 1997). The wealth of research performed on the effect of zinc on NMDA receptors further revealed that zinc modulation of NMDA receptor activity is also concentration-dependent and is specific to NMDA receptor subunit composition (for review see Paoletti et al., 2009). Zinc does not uniformly affect all NMDA receptors. Binding sites for zinc were discovered on NMDA receptor 2 (NR2) subunits. This binding site is located on the N-terminal domain of both NR2A and NR2B subunits (Choi and Lipton, 1999; Rachline et al., 2005). No binding site for zinc exists on NR2C or NR2D subunits.

At nM concentrations, zinc is a high-affinity voltage-independent inhibitor of NR2A-containing NMDA receptor-mediated excitatory post-synaptic potentials (EPSP). 1~10 nM of zinc added to the extracellular bath can attenuate up to 80% of

NR2A-dependent EPSP in human embryonic kidney (HEK) cells and *Xenopus* oocytes (Paoletti et al., 1997). At μM concentrations, zinc inhibition of NR2A channel-opening probability becomes voltage-*dependent*. 10~100 μM of zinc at negative membrane potentials can increasingly reduce NR2A-dependent EPSP as the membrane potential drops (Christine and Choi, 1990; Chen et al., 1997). An additional, intra-channel NR2A binding site for zinc at asparagine N595 is likely responsible for this voltage-dependent inhibition. Inhibition of NR2B by zinc, on the other hand, occurs only at 1~10 μM zinc concentrations. This blockage of NR2B-containing NMDA receptor current is voltage-independent as well as near complete (Chen et al., 1997; Paoletti et al., 1997). Since spontaneous release of vesicular zinc is estimated to bring synaptic concentrations of zinc to nM levels while stimulation-evoked release may increase synaptic concentrations of zinc to μM levels (Paoletti et al., 1997), the concentration-dependent effects of synaptic zinc on NMDA receptors suggest that zinc may exert tonic as well as phasic modulation of NMDA receptor activity within the brain. Synaptic zinc is positioned to dynamically modulate NMDA receptor activity in a concentration and voltage dependent manner.

Prolonged exposure to zinc at higher concentrations (0.3 mM ~1 mM for 10 min) can, alternatively, *potentiate* EPSPs mediated by both NR2A- and NR2B-containing NMDA receptors within the hippocampus (Kim et al., 2002). It was also observed that this potentiation is mediated by the activation of Src-family tyrosine kinase and the increase in tyrosine phosphorylation of both NR2A and NR2B. The co-localization of

vesicular zinc in glutamatergic neurons within the brain and zinc's dynamic modulation of NMDA receptor activity both infers a very possible role for zinc in synaptic plasticity.

1.3.3.2 Zinc receptor

As zinc deficiency has a major role in gastrointestinal pathology, it was not surprising that a putative zinc-sensing receptor (ZnR) was first identified in a colonocytic line (Hershfinkel et al., 2001). It was shown that a previously uncharacterized G protein-coupled receptor (GPCR) specifically senses changes in extracellular zinc concentration and triggers intracellular release of calcium in colonocytes. Subsequently, this ZnR was identified as G-protein-coupled receptor 39 (GPR39) in the ghrelin receptor family of GPCRs (Yasuda et al., 2007). GPR39 was found to be expressed in hippocampal CA3 neurons and was demonstrated to initiate the activation of mitogen activated protein kinase (MAPK) and CaMKII pathways in the hippocampus (Besser et al., 2009). Recently, a synaptic zinc- and GPR39-mediated endocannabinoid signalling pathway was described in the zinc-rich dorsal cochlear nucleus (Perez-Rosello et al., 2013). Here, it was demonstrated that synaptic zinc-activation of GPR39 on the postsynaptic neuron triggers the synthesis of 2-arachidonoylglycerol (2-AG) and subsequent presynaptic inhibition of glutamate release. Although research into the function of GPR39 in neurotransmission remains sparse and so far has been restricted to *in vitro* cell and slice preparations, the existence of the ZnR implies that synaptic zinc, acting on GPR39, can modulate release of glutamate from the postsynaptic neuron.

1.4 Synaptic Zinc and Cortical Plasticity

The ubiquity of synaptic zinc in the cortex and the vast variety of zinc-sensitive synaptic signalling pathways suggest that synaptic zinc is a vital component of neuronal functioning. Specifically, the neuromodulatory role of synaptic zinc in NMDA receptor-mediated glutamatergic signalling suggests that zinc may play an integral part in synaptic plasticity.

1.4.1 Experience-dependent plasticity in the visual cortex

The earliest association between synaptic zinc and cortical plasticity was the observation that the level of synaptic zinc within the visual cortex of cats and vervet monkeys is altered by deprivation of visual sensory input (Dyck and Cynder, 1993; Dyck, 2003). Further research into the contribution of synaptic zinc to visual cortex plasticity does not exist. However, the increasing popularity of transgenic mouse models in studies of plasticity in the visual cortex may provide a new avenue for synaptic zinc research in the visual cortex.

1.4.1.1 Visual cortex plasticity

The groundbreaking discovery that the cortical circuits are plastic and are susceptible to changes in sensory experience was made in the 1960s. Examination of the effects of depriving one eye of visual stimulation in kittens led to the discovery that binocular representation in the visual cortex is altered to favour the spared eye (Wiesel and Hubel, 1963; Hubel and Wiesel, 1964). Briefly, transient closure of one eye, through suturing together the upper and lower eyelids or wearing of an eye patch for periods of days to weeks, leads to a shift in the preference of cortical neurons for responding to stimulation

of the eye that remained open. Since then, monocular deprivation and subsequent ocular dominance plasticity have served as a prominent model for exploring mechanisms that govern plasticity in the visual cortex. While the phenomenon has been described in detail in a number of species (Hubel and Wiesel, 1964; Hubel et al., 1977; Dräger, 1978), the use of mice in studying ocular dominance plasticity has gained momentum because of the possibility of genetic manipulations. This allowed for greater access to methods for detailed examination of the cellular and molecular mechanisms that underlie the plasticity of cortical circuits.

The mouse visual cortex lacks the eye-specific columnar organization seen in higher mammals. Instead, the primary visual cortex of mice is divided into monocular and binocularly driven regions; both regions are dominated by inputs from the contralateral eye, but the binocular region also receives weak ipsilateral-eye inputs (van Brussel et al., 2009). The ocular dominance shifts induced by monocular deprivation in mice closely resembles those previously described in other mammals, such as cats and non-human primates (see Hofer et al., 2005). Ocular dominance plasticity has been described in both the juvenile and adult mouse, where visual deprivation produces reorganization of receptive field size in the deprived regions (Frenkel and Bear, 2004; Hofer et al., 2005; Hofer et al., 2006). This is followed by depression of synaptic strength in the deprived regions and potentiation of stimulation-evoked activity in the spared eye.

Multiple neurochemical pathways affect ocular dominance plasticity. Electrophysiological data suggest that long term depression (LTD)-like processes underlie the depression of responses in deprived regions of the visual cortex (Sawtell et al., 2003) There is evidence from electrophysiological studies that ocular dominance

plasticity in the adult mouse is dependent on NMDA receptors and NMDA-dependent generation of LTD (Heynen et al., 2003; Sawtell et al., 2003). Signalling pathway through cyclic adenosine monophosphate (cAMP)-dependent protein kinase A (PKA; Fischer et al., 2004) and activation of α-CaMKII (Taha et al., 2002) and extracellular signal-regulated kinases (ERK; Di Cristo et al., 2001) are also necessary for induction of ocular dominance plasticity. The wealth of research in this area indicates that ocular dominance plasticity, and plasticity of cortical circuits in general, are not mediated by a single signalling cascade, but instead require a number of interacting processes. Given that synaptic zinc has the potential to regulate a number of processes essential to visual cortex plasticity, synaptic zinc may be a potent modulator of the phenomenon.

1.4.1.2 Synaptic zinc in the visual cortex

The laminar distribution of synaptic zinc within the primary sensory cortices of mammals is distinct. The level of staining for synaptic zinc is highest in layers II/III, V, and VI, while staining for synaptic zinc is characteristically sparse in layer IV (Dyck and Cynader, 1993). The induction of visual cortex plasticity through monocular deprivation, a standard manipulation that produces well characterized forms of visual cortex plasticity (Wiesel and Hubel, 1963; Mioche and Singer, 1989; Gilbert and Wiesel, 1992), was found to robustly and dynamically alter synaptic zinc levels within layer IV of the primary visual cortex (Dyck, 2003). Short-term (24 hours) monocular deprivation through tetrodotoxin injection or enucleation resulted in an increase in synaptic zinc levels within the thalamocortical input layer of deprived-eye stripes. Long-term (3 months) monocular deprivation conversely decreased synaptic zinc levels within the same area.

It is postulated that the experience-dependent alteration of synaptic zinc levels in the visual cortex of cats and vervet monkeys serves to facilitate synaptic plasticity in eye-specific cortical domains (Dyck, 2003). Increase in synaptic zinc levels following short term deprivation may suppress neuronal activity within the deprived-eye domains through inhibiting NMDA receptors to induce LTD-like processes, or activate the production of endocannabinoids via metabolic ZnR to depress presynaptic neurotransmission. The reduction in synaptic zinc levels after long-term deprivation could subsequently facilitate the potentiation of spared-eye input. Although synaptic zinc is positioned to be a potential modulator of experience-dependent plasticity in the visual cortex, current research in this area is sparse. A recent addition is the observation that synaptic zinc distribution is also dynamically regulated by sensory experience in the developing ferret (Khalil and Levitt, 2013). Synaptic zinc levels in the visual cortex were observed to decrease with maturation in a lamina-specific manner, as a dramatic decrease in layer IV is associated with the first opening of the eyes in young ferrets. The distribution of synaptic zinc and experience-dependent regulation of synaptic zinc levels have not been described in the visual cortex of mice or rats.

1.4.2 Experience-dependent plasticity in the barrel cortex

The relationship between synaptic zinc and experience-dependent plasticity in the cerebral cortex has been explored in greater detail within the vibrissal somatosensory system of mice. A large portion of the rodent primary somatosensory cortex is devoted to processing sensory information from the mystacial vibrissae. This area is characterized by clearly defined topographic compartments that resemble barrels (Woolsey and Van der Loos, 1970). Each barrel within this barrel cortex receives input from a single

contralateral mystacial vibrissa such that consequences to manipulation of the vibrissae can be mapped with specificity to the corresponding barrels in an isomorphic manner (Simons and Woolsey, 1979; Fig. 1-1). The barrel cortex allows for compartmentalized examination of study of experience-dependent plasticity in the cortex (Feldmeyer et al., 2013).

Figure 1-1: Representation of mystacial vibrissae in the primary somatosensory cortex of the mouse.

Barrel cortex representation of the mystacial vibrissae follows a one-to-one isomorphic arrangement.

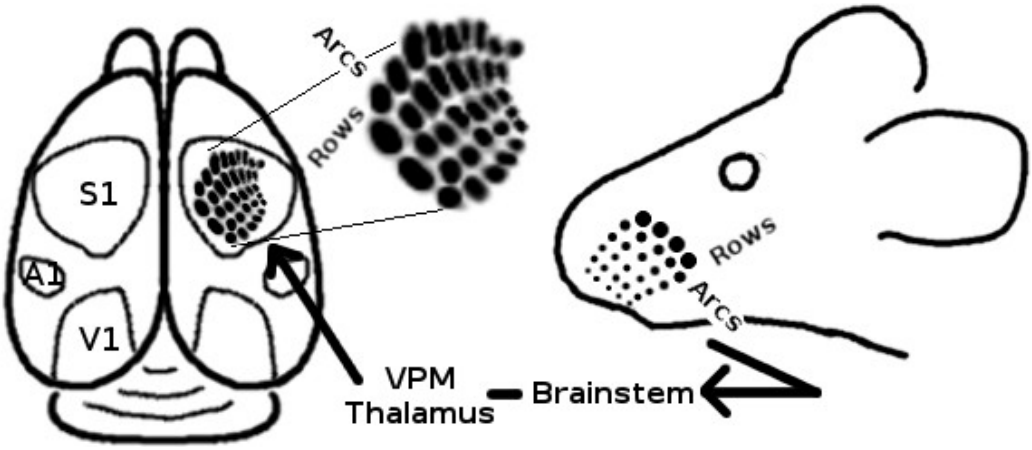
Arcs
Rows
S1
A1
V1
VPM
Thalamus
Brainstem
Rows
Arcs

1.4.2.1 Barrel cortex plasticity

Trimming or removing a subset of the mystacial vibrissae induces well-characterized alterations in the efficacy of neurotransmission within the barrel cortex (see Fox, 2002). Ultimately, cortical activity in deprived barrel fields is suppressed to increase the behavioural salience of stimulations to the spared vibrissae.

Sensory deprivation within the vibrissal-barrel cortex system results in a depression of vibrissa-stimulation-evoked cortical response within the deprived barrels (Glazewski et al., 1998). The magnitude of this response depression in the deprived barrel will increase with proximity to spared, active barrels such that depression is greatest in deprived barrels immediately adjacent to a spared barrel (Glazewski and Fox, 1996). One possible cellular basis to this component of barrel cortex plasticity involves the weakening of layer IV to layer II/III excitatory projection through sensory deprivation-induced LTD and competition between input from active and inactive vibrissae (Allen et al., 2003; Shepherd et al., 2003). Stimulation-evoked cortical response in layers IV and II/III of the spared barrels is further potentiated following removal of the surrounding vibrissae (Barth et al., 2000). This potentiation of cortical response in the spared barrel is also dependent upon intracortical pathways terminating in layer II/III (Wallace et al., 2001; see Fox 2002).

1.4.2.2 Experience-dependent modulation of synaptic zinc levels in the barrel cortex

Removal of the mystacial vibrissae results in a robust increase in synaptic zinc levels within layer IV of corresponding barrels (Quaye et al., 1999; Czupryn and Skangiel-Kramska, 2001a; Brown and Dyck, 2002). This experience-dependent

modulation of synaptic zinc levels is histochemically detectable within 3 hours of deprivation (Brown and Dyck, 2002). Conversely, stimulation of vibrissae induces a decrease in synaptic zinc levels within the corresponding barrels (Fig. 1-2; Brown and Dyck, 2005). These results indicate that the levels of synaptic zinc in the barrel cortex are regulated by vibrissal sensory experience. Although direct evidence to equate the increase in synaptic zinc levels with an increase in zinc release does not yet exist, evidence from electron microscopy identification of zincergic synapses indicates that the experience-dependent modulation of synaptic zinc levels is not an epiphenomenon. Sensory deprivation results in a significant increase in the number of zincergic synapses in the barrel cortex. This increase is not restricted to layer IV and is found in all layers of the deprived barrels (Nakashima and Dyck, 2010).

The changes in synaptic zinc levels in the barrel cortex following vibrissae manipulation also suggest that synaptic zinc plays a role in the modulation of barrel cortex plasticity. Other evidence supports this hypothesis as well. Environmental enrichment is known to sharpen the barrel cortex map such that the receptive fields for each vibrissa within layer II/III of the barrel cortex shrinks and less overlap of the receptive fields occur between neighbouring barrels (Polley et al., 2004). Whisker-stimulation-evoked cortical responses are also weakened. Exposure to enriched environments will enhance the magnitude of sensory deprivation-induced increases in synaptic zinc level within the barrel cortex (Nakashima and Dyck, 2008). Together, these observations indicate that synaptic zinc levels within the barrel cortex are dynamically modulated by sensory experience and further suggest that synaptic zinc is intimately involved with barrel cortex plasticity.

Possible mechanisms through which synaptic zinc may modulate barrel cortex plasticity are numerous. An obvious candidate is NMDA receptor mediated long term potentiation (LTP) and LTD. It is generally accepted that experience-dependent changes in the adult cerebral cortex are affected, at the synaptic level, by LTP- and LTD-like processes. Specifically, activation of NMDA receptors is necessary for the induction of well-characterized forms of LTP and LTD within the hippocampus as well as throughout the cerebral cortex (Bear and Kirkwood, 1993; Kirkwood et al., 1993; Murphy et al., 1997). Synaptic zinc, through its potent inhibition of NR2A and NR2B containing NMDA receptors, may therefore be a potential modulator of LTP and LTD. There is currently no published literature that examines the effect of synaptic zinc on LTP and LTD in the primary sensory cortices, however synaptic zinc has been demonstrated to modulate NMDA receptor-mediated forms of LTP and LTD in the hippocampus (Pan et al., 2011; Sindreu et al., 2011).

1.5 Synaptic Zinc and Behaviour

Broadly defined, plasticity encompasses any changes to the naive, or "normal", characteristics of neurotransmission. As the production of complex behaviour requires the integration of, and adaptation to, constantly changing sensory input, it is prudent to examine the effect of any potent modulator of cortical plasticity on observable behaviour. To explore the relevance of synaptic zinc for the production of behaviour, researchers manipulated zinc concentrations through dietary, chemical, and genetic means.

1.5.1 Dietary manipulation of synaptic zinc

The earliest known, and most researched, effects of manipulating zinc on behaviour were obtained through studies that examined the behaviour of developing organisms under dietary zinc depletion. Pre- and post-natal zinc deprivation leads to a wide range of behavioural deficits, including major learning and memory deficits (Halas et al., 1983; Golube et al., 1988), aggressive behaviour (Halas et al., 1975; Peters, 1978), and anomalies in motivation such as development of anorexia (Peters, 1979). The limited number of studies that examined the consequences of dietary zinc depletion revealed that a reduction in NMDA receptor expression may be associated with the observed behavioural deficits (Chowanadisai et al., 2005). However, since zinc is essential to many cellular processes, zinc deprivation during development can delay and impair the growth of the subject in general (see Sandstead, 2000). Therefore, behavioural deficits observed following zinc deprivation during development cannot be attributed solely to synaptic zinc depletion in the brain.

Studies that employ dietary zinc deprivation in adult subjects suffer from the same caveat. Although dietary zinc deprivation in adults results in learning deficits and increased sensitivity to kainic acid induced seizures (Caldwell et al., 1970; Turner and Soliman, 2000; Takeda et al., 2003), these effects may not be attributable to the actions of synaptic zinc. In fact, evidence suggests that synaptic zinc levels are not altered by dietary zinc deprivation (Takeda et al., 2005). Homeostatic mechanisms may exist to preserve synaptic zinc levels while other pools of zinc within an animal deprived of dietary zinc is reduced.

1.5.2 Chelation of synaptic zinc

Intracranial infusion of zinc chelators, chemical compounds that sequester and surround zinc to render zinc inactive, provides a more direct method of manipulating synaptic zinc levels. Zinc chelation, *in vivo,* results in impaired Morris water task performance when the hippocampus is targeted (Frederickson et al., 1990) and impaired contextual fear conditioning when the amygdala is targeted (Takeda et al., 2004). The caveat to interpretation of these results is that the zinc chelators available at the time suffered from notable draw backs. The most common membrane-permeable zinc chelator N,N,N′,N ′-tetrakis(2-pyridylmethyl)-ethylenediamine (TPEN) can induce dendritic degeneration (Yang et al., 2007), strip zinc cofactors from metalloproteins (Meeusen et al., 2012), and promote apoptosis (Lee et al., 2008). The most common extracellular zinc chelator ethylenediaminetetraacetic acid (EDTA) also binds to calcium and magnesium with high affinity (see Radford and Lippard, 2013). Employing the calcium salt of EDTA (CaEDTA) avoids disruption of extracelluar calcium levels; but, affinity for zinc and rate of zinc binding is reduced, such that CaEDTA may not be effective under physiologically relevant conditions (Paoletti et al., 2009). N-(2-hydroxy-1,1-bis(hydroxymethyl)ethyl) glycine (tricine) is employed as a faster zinc-binding alternative to CaEDTA, but suffers from weaker affinity for zinc (Paoletti et al., 2009).

The recently developed extracellular zinc chelators ZX1, with high specificity and affinity for zinc (K_d Zn = 1 nM) and fast zinc-binding kinetics (kZn = 0.027 s^{-1}), may be the suitable candidate required to target synaptic zinc under physiological conditions (Pan et al., 2011). In electrophysiological studies, ZX1 was used to demonstrate that synaptic zinc is required for the generation of presynaptic LTP at hippocampal mossy

fibre terminals (Pan et al., 2011). Exploration of the effect of synaptic zinc in behaviour would benefit from the use of ZX1.

1.5.3 Genetic manipulation of synaptic zinc

Three mouse models that display alteration in levels of synaptic zinc exist: *mocha*, Senescence Accelerated Mouse Prone 10 (SAMP10), and ZnT3 KO mice. *Mocha* mice, characterized by distinct coat colour, have a mutation in the floral homeotic protein APETALA 3 (AP-3) gene that enables the placement of ZnT3 onto the vesicle membrane (Kantheti et al., 1998). SAMP10 mice were generated by selectively breeding mice that displayed characteristics of senescence early in life (Takeda et al., 1997). Both *mocha* and SAMP10 mice have reduced levels of synaptic zinc and display behavioural abnormalities (Takeda et al., 1997; Stoltenberg et al., 2004). However, since neither model completely removes synaptic zinc stores, and both models also alter physiological processes unrelated to synaptic zinc, direct association between the behavioural phenotypes observed in these models and synaptic zinc cannot be drawn (Takeda et al., 1997; Salazar et al., 2004)

In contrast, disruption of the ZnT3 gene in ZnT3 KO mice abolishes the transporter responsible for loading synaptic vesicles with zinc (Palmiter et al., 1996; Cole et al., 1999). The development of ZnT3 KO mice therefore allowed researchers to examine the effects of a complete elimination of synaptic zinc. Interestingly, initial studies found no behavioural, electrophysiological, or mutant phenotype in ZnT3 KO mice (Cole et al., 1999; Cole et al., 2001; Lopantsev et al., 2003) except for an increase in susceptibility to kainic acid induced seizures (Cole et al., 2000). Clear evidence that zinc

participates in the regulation of a vast number of cellular processes precludes the conclusion that synaptic zinc simply does not play a major functional role in the brain. The initial theory regarding the lack of observable defects in ZnT3 KO mice is that compensatory mechanisms may have been triggered during development to support recovery of functions lost through the absence of synaptic zinc. However, it has since been revealed that ZnT3 KO mice *do* demonstrate deficiencies in a number of behavioural tasks. Although the methods employed in the initial studies were extensive, they were likely not sensitive enough to detect differences between ZnT3 wild type (WT) and KO mice.

Loss of synaptic zinc in ZnT3 KO mice has been found to lead to deficits in Morris water-task performance in older (6 months) subjects (Adlard et al., 2010). Within the hippocampi of these older ZnT3 KO mice, changes in levels of a number of proteins, including AMPA receptors, NR2A and NR2B receptors, and elements of the brain-derived neurotrophic factor (BDNF) pathway were also detected. Since the levels of ZnT3 expression fall with age in older (1 year) wild type (WT) mice, healthy older humans (48-91 years), and particularly in SAMP10 mice and human subjects with Alzheimer's disease, ZnT3 KO may represent a phenocopy of behavioural deficits in senescence and presenile dementia (Adlard et al., 2010).

Behavioural deficits were also reported in younger ZnT3 KO mice (3-5 months). Deficits in fear conditioning and extinction were observed and associated with loss of synaptic zinc in the amygdala (Kodirov et al., 2006; Martel et al., 2010). Loss of synaptic zinc in the hippocampi of ZnT3 KO was associated with poorer performance in spatial memory and contextual discrimination (Sindreu et al., 2011). In this study, a

potential mechanism for synaptic zinc function in hippocampus-dependent memory was proposed. It was observed that ERK1/2 activation was reduced in ZnT3 KO mice and that this reduction was more pronounced after behavioural training. It was speculated that synaptic zinc inhibits MAPK tyrosine phosphatases at the presynaptic hippocampal mossy fibre terminal to promote ERK1/2 activation and enable contextual discrimination. Although absence of synaptic zinc in ZnT3 KO mice does not lead to overt behavioural deficits, it is evident that synaptic zinc regulates specific forms of cortical function.

1.6 Rationale

Synaptic zinc is positioned to modulate a number of processes essential to neurotransmission in the cerebral cortex. The concentration of synaptic zinc is highest in the hippocampus, amygdala, and throughout the cerebral cortex. Recent studies have demonstrated that synaptic zinc is essential to hippocampus- and amygdala-dependent forms of memory. Although activity-dependent regulation of synaptic zinc in the cerebral cortex was one of the first zincergic phenomenon observed in the cerebral cortex, the role of synaptic zinc in cortical neurotransmission and behaviour remains to be elucidated. The studies reported in this thesis will serve to further explore the basis of synaptic zinc function and behavioural consequences of synaptic zinc in the cerebral cortex.

Experience-dependent regulation of synaptic zinc levels in the cerebral cortex was first described in the visual cortex of cats and non-human primates. However, further research on the relationship between synaptic zinc and visual cortex plasticity in cats and non-human primates is sparse. The use of mice to study visual cortex plasticity has become widespread due to the availability of genetic manipulations. While mouse models

have provided additional insight into the understanding of visual cortex function, the relationship between synaptic zinc and visual cortex plasticity in mice has yet to be explored. In Chapter 2, I report the distribution and experience dependent regulation of synaptic zinc in the visual cortex of mice, to provide groundwork for investigating the role of synaptic zinc in mouse visual cortex plasticity.

In the barrel cortex, as in other primary sensory cortices of mice, the distribution of synaptic zinc follows a distinct laminar pattern. Experience-dependent regulation of synaptic zinc in the mouse barrel cortex is a robust phenomenon, characterized by changes in the density of synaptic zinc and zincergic terminals that are observable within hours of sensory manipulation. However, the role that synaptic zinc plays in behaviour mediated by the barrel cortex remains unexplored. To investigate the role of synaptic zinc in barrel cortex function, the consequences of an absence of synaptic zinc for behaviour mediated by the barrel cortex was examined in the studies reported in Chapters 3 and 4. A novel barrel cortex-dependent texture-discrimination task is described in Chapter 3. In Chapter 4, the performance of ZnT3 KO mice on the texture discrimination task is examined.

The general hypothesis is that synaptic zinc is integral to neurotransmission throughout the neocortex. Within the visual cortex of the mouse, the cortical lamina distribution of synaptic zinc is expected to mirror patterns observed in the visual cortices of other mammals as well as the barrel cortex of mice. Sensory deprivation is expected to result in an increase in synaptic zinc levels particularly within layer IV of the mouse visual cortex. Lastly, the absence of zinc in the barrel cortex of mice is expected to lead to deficits in barrel cortex dependent behaviour.

Chapter 2: Visualizing the Distribution of Synaptic Zinc in the Visual Cortex of Monocularly Enucleated Mice

2.1 Abstract

Zinc is packaged in synaptic vesicles within a subset of glutamatergic neurons in the mammalian telencephalon. This synaptic zinc is co-released with glutamate and has been demonstrated to be a potent neuromodulator. To explore the relationship between synaptic zinc and visual cortex plasticity in the adult mouse, we examined the laminar distribution of synaptic zinc in the primary visual cortex (V1) of 3 month-old C57BL/6 mice following monocular enucleation. Synaptic zinc was visualized through zinc histochemistry 24 h, 3 days, 2 weeks, and 3 months following monocular enucleation. We found that the synaptic zinc levles in layer IV of the deprived monocular domain of V1 (V1M) increased sharply (~70 %) relative to the spared V1M following 24 hours of monocular deprivation. Synaptic zinc levels within layers II-III, and V of the deprived V1M were elevated (~10 %) only after long-term (3 months) monocular deprivation. We demonstrated that levels of synaptic zinc within the visual cortex of mice are dynamically modulated by sensory experience. Short-term deprivation is associated with an increase in synaptic zinc within the thalamocortical input layer of the cortex, while long-term deprivation increases synaptic zinc within the pyramidal layers. The spatial and temporal characteristics of change in synaptic zinc levels coincide with the dynamics of deprivation-induced visual cortex plasticity. This result is consistent with and supports other hypotheses that synaptic zinc is a key modulator in visual cortex function and plasticity.

2.2 Introduction

Since pioneering studies in the early 1960s established the capacity for experience-dependent plasticity within the visual cortex of cats (Wiesel and Hubel, 1963; Hubel and Wiesel, 1964), it has become evident that the adult cerebral cortex remains plastic and is continuously modified by sensory experience (Kaas et al., 1983; Kaas, 1988). Studies performed in higher mammals such as cats and non-human primates demonstrated that visual deprivation produces immediate reorganization of receptive field size and cortical topography within the deprived cortical regions (Mioche and Singer, 1989; Gilbert and Wiesel, 1992) Within several days to several weeks of monocular deprivation, modification of synaptic strength within the deprived ocular dominance columns is effected through decreased expression of neuroactive molecules such as glutamate (Carder and Hendry, 1994), NMDA receptor subunits (Catalano et al., 1997), and cytochrome oxidase (Wong-Riley, 1979). Ultimately, long-term sensory deprivation on the order of months leads to the remodelling of cortical connectivity and anatomy; deprived ocular dominance columns are encroached by afferents that also innervate neighboring spared ocular dominance columns (Darian-Smith and Gilbert, 1994).

It is generally accepted that LTP- and LTD-like processes provide the bases to effect experience-dependent changes in the adult cerebral cortex. Glutamatergic activation of NMDA receptors is necessary for the induction of well-characterized forms of LTP and LTD within the hippocampus as well as the cerebral cortex (Bear and Kirkwood, 1993; Kirkwood et al., 1993; Murphy et al., 1997). The key role that glutamatergic neurotransmission plays in LTP and LTD positions synaptic zinc as a

potential modulator of these processes. Zinc is sequestered in the terminal boutons of a subset of corticopetal glutamatergic neurons in the mammalian telencephalon (Beaulieu et al., 1992; Frederickson and Monclieff, 1994). This synaptic zinc is co-released with glutamate in an activity- and calcium-dependent manner (Assaf and Chung, 1984; Qian and Noebels, 2005), and is a potent inhibitor of NMDA receptors (Chen et al., 1997). As such, synaptic zinc has been demonstrated to modulate NMDA receptor-mediated forms of LTP and LTD in the hippocampus (Pan et al., 2011; Sindreu et al., 2011).

The distribution of synaptic zinc within the primary sensory cortices of mammals follows a laminar pattern that complements the distribution of cytochrome oxidase (Dyck and Cynader, 1993). The level of staining for synaptic zinc is highest in layer Va terminal boutons followed by layers II/III, Vb, and VI. Layer IV is characteristically devoid of synaptic zinc (Dyck and Cynader, 1993; Fig. 2-1). Experience-dependent alteration to this laminar distribution of synaptic zinc was first visualized in the visual cortex of cats and vervet monkeys (Dyck and Cynder, 1993; Dyck, 2003). It was observed that short-term (24 hours) monocular deprivation through tetrodotoxin (TTX) injection into the eye or enucleation resulted in an increase in synaptic zinc staining within layer IV of deprived-eye stripes. Long-term, monocular deprivation of visual input (3 months) was found to decrease synaptic zinc staining in layers III, IV, and VI of the deprived-eye stripes. It is postulated that this dynamic and experience-dependent change in levels of synaptic zinc can modulate NMDA receptor sensitivity to glutamate and finally facilitate synaptic plasticity in eye-specific cortical domains. Although there is evidence to suggest that synaptic zinc contributes to ocular dominance plasticity, current research in this area is sparse.

Figure 2-2: Laminar distribution of synaptic zinc and cytochrome oxidase.

A: Nissl-stained coronal section through cat V1. Roman numerals represent cortical layers; B: Cytochrome oxidase-stained adjacent section of cat V1; C: zin-stained adjacent section of cat V1; bar = 2.0 mm. Figure modified from Dyck and Cynader, 1993.

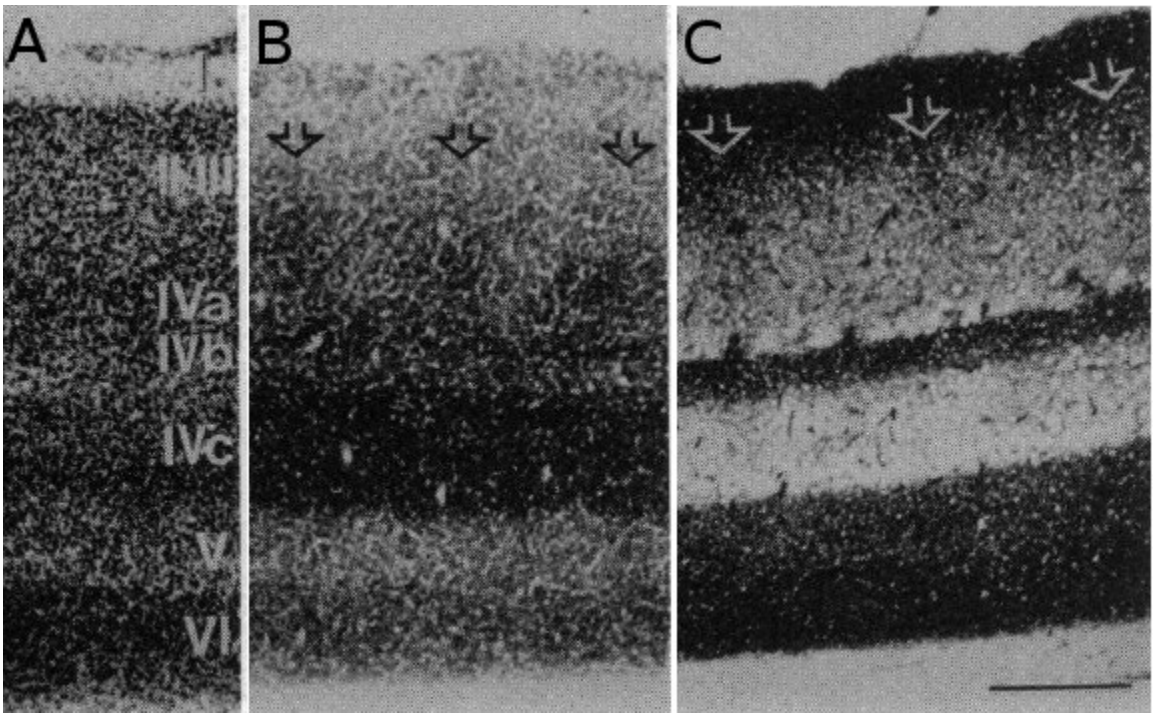
A
B
C
IVa
IVb
IVc

While primates and cats have provided invaluable insight into a wide array of topics in neuroscience not exclusive to visual cortex plasticity, the use of mice to study monocular deprivation-induced reorganization of the visual cortex has become more widespread because of its amenability to genetic manipulation. The mouse visual cortex lacks the eye-specific columnar organization seen in higher mammals, but monocular (V1M) and binocular (V1B) driven regions can be separated and precisely localized (Van Brussel et al., 2009). Monocular deprivation-induced shifts in ocular dominance have been described in both the juvenile and adult mouse (Frenkel and Bear, 2004; Hofer et al., 2005; Hofer et al., 2006). There is also evidence from electrophysiological studies that ocular dominance plasticity in the adult mouse is dependent on NMDA receptors (Sawtell et al., 2003).

The present study aims to provide groundwork for investigating the role of synaptic zinc in mouse visual cortex plasticity. The laminar distribution of synaptic zinc staining within the visual cortex of mice will be described and the effect of periods of monocular deprivation on this distribution quantified. The hypothesis is that synaptic zinc staining patterns and the change in levels of zinc staining in response to experience is conserved across mammalian species as well as conserved throughout the neocortex.

2.3 Methods

2.3.1 Animals and treatment groups

Male C57BL/6 mice at 3 months of age were used for this study. The mice were maintained on standard laboratory diet and water *ad libitum* and kept in standard laboratory housing under a 12-hour light/dark cycle. Mice were placed under isoflourane

anaesthesia and one eye was selected at random and enucleated with fine surgical scissors. Enucleation causes optic nerve degeneration and is irreversible. TTX injections and eye-lid sutures provide, respectively, less traumatic and reversible methods of ocular deprivation (Frenkel and Bear, 2004; Hofer et al., 2006). However, the effect TTX injections on changes in zinc levels in the visual cortex was similar to the effect of enucleation in the monkey (Dyck, 2003), and experience-dependent changes in zinc levels in the barrel cortex of mice were also similar between deprivation models that induce sensory organ damage and those to do not (Czupryn and Skangiel-Kramska, 2001). Enucleation was therefore selected as the most efficient method of ocular deprivation for exploratory examination of the effects of sensory experience on zinc levels in the visual cortex of mice.

Following 24 hours (n = 5), 72 hours (n = 5), 14 days (n = 5), and 3 months (n = 5) of survival inside its home cage, the enucleated mice and age-matched naive mice (n = 5) were killed and their brains removed and prepared (Section 2.3.2) for zinc histochemistry. Pilot studies indicate that the time of surgery, either 30 min to 1 h after the light-cycle or 30 min to 1 h before the dark-cycle, did not affect the level of zinc staining in control animals.

2.3.2 Zinc histochemistry

Synaptic zinc was visualized using a modified version of Danscher's autometallographic staining method (Danscher, 1982; Dyck et al., 1993). A brief description of the staining method is as follows: Sodium selenite (15 mg/kg, i.p.; Sigma) in distilled water (1.5 mg/ml) was injected intraperitoneally. Circulating selenium binds to histochemically reactive zinc; this allows for the visualization of zincergic synaptic terminals following

development with silver (see below). After a survival time of 1 h, the mice were killed with an overdose of sodium pentobarbital. The brains were extracted, rapidly frozen on crushed dry ice, and stored at –80 °C. Coronal sections were cut at 20 μm on a cryostat and thaw mounted onto gelatine-coated slides. The slides were stored at -20 °C. In preparation for staining, the sections were fixed in a descending series of ethanol, and coated with 0.5 % gelatin. Zinc-selinite grains were visualized through development with 37 mM silver lactate and 0.5 M hydroquinone suspended in 50 % gum arabic and buffered with 2.0 M sodium citrate. Sections were developed in darkness for 45 – 60 min. Following staining, the sections were washed in running water, fixed in 5 % sodium thiosulfate, and dehydrated in an increasing series of ethanol. Lastly, the sections were cleared in xylene and coverslipped using Permount.

It is important to note that vesicular zinc, loosely bound zinc ions packaged presynaptic vesicles, is the exclusive source of histochemically reactive zinc (Fredrickson et al., ,2000).

2.3.3 Densitometry and data analysis

Four 20 μm coronal sections that spanned the rostral-caudal extent of the V1M and V1B were selected for analysis for each mouse. Uncompressed, 8-bit grey-scale light photomicrographs were taken for each section (Fig. 2-2A). V1M and V1B on both hemispheres were digitally isolated (Fig. 2-2B) and processed for densitometry. The laminar distribution of synaptic zinc in V1M and V1B was represented as a continuous signal of zinc staining intensity through the cortical layers (Fig. 2-2C). This zinc staining profile consists of the average intensity of zinc staining at consecutive widths of the

cortex from the most superficial to deepest layers. A staining intensity of 255 represents the darkest value possible while 0 represents the lightest.

Figure 2-3: Representative mouse V1M synaptic zinc staining intensity.

A: synaptic zinc-stained coronal section with the isolated V1M shaded; B: isolated V1M section positioned for conversion into zinc staining intensity profile; C: corresponding zinc staining intensity profile.

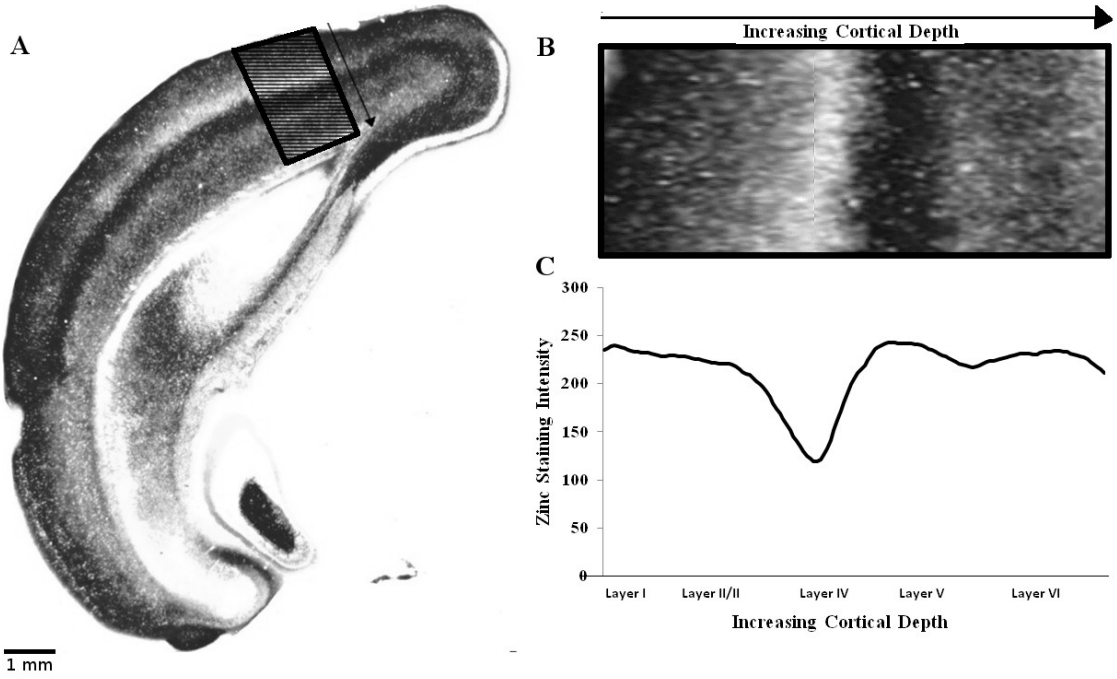
A
1 mm
B
Increasing Cortical Depth
C
Zinc Staining Intensity
300
250
200
150
100
50
0
Layer I
Layer II/II
Layer IV
Layer V
Layer VI
Increasing Cortical Depth

2.4 Results

2.4.1 Distribution of synaptic zinc in V1 of control mice

Consistent with the distribution of histochemically reactive zinc reported in the visual cortex of primates and cats (Dyck, 1993; Dyck et al., 1993) as well as the barrel cortex of mice (Brown and Dyck, 2005), the pattern of mouse V1 innervation by zincergic terminals was lamina-specific (Fig. 2-3). Layers I and V were most heavily stained for zinc, while layer IV was most sparsely stained. Layer IV of V1 is more densely populated with cell bodies and thicker than the same layer in V2L. We verified that the zinc-poor layer of V1 identified as layer IV was also thicker than its more heavily stained counterpart in the lateral secondary visual cortex. V1 can therefore be clearly demarcated from the adjacent medial (V2M) and lateral (V2L) secondary visual cortices by the presence of this characteristically more zinc-poor layer IV in V1. V1M occupies approximately the medial one-half of the rostral-caudal extent of V1 (van Brussel et al., 2009; Fig. 2-3). There were no observable differences in the laminar distribution of synaptic zinc between V1M and V1B in control mice.

Figure 2-4: Synaptic zinc staining in mouse primary visual cortex.

Coronal, 20 μm section. Background image: 10X magnification; Foreground image: 200X magnification; V1: primary visual cortex; M: monocular region of V1; B: binocular region of V1; V2M: medial region of secondary visual cortex; V2L: lateral region of secondary visual cortex; II – VI: cortical layers II through VI.

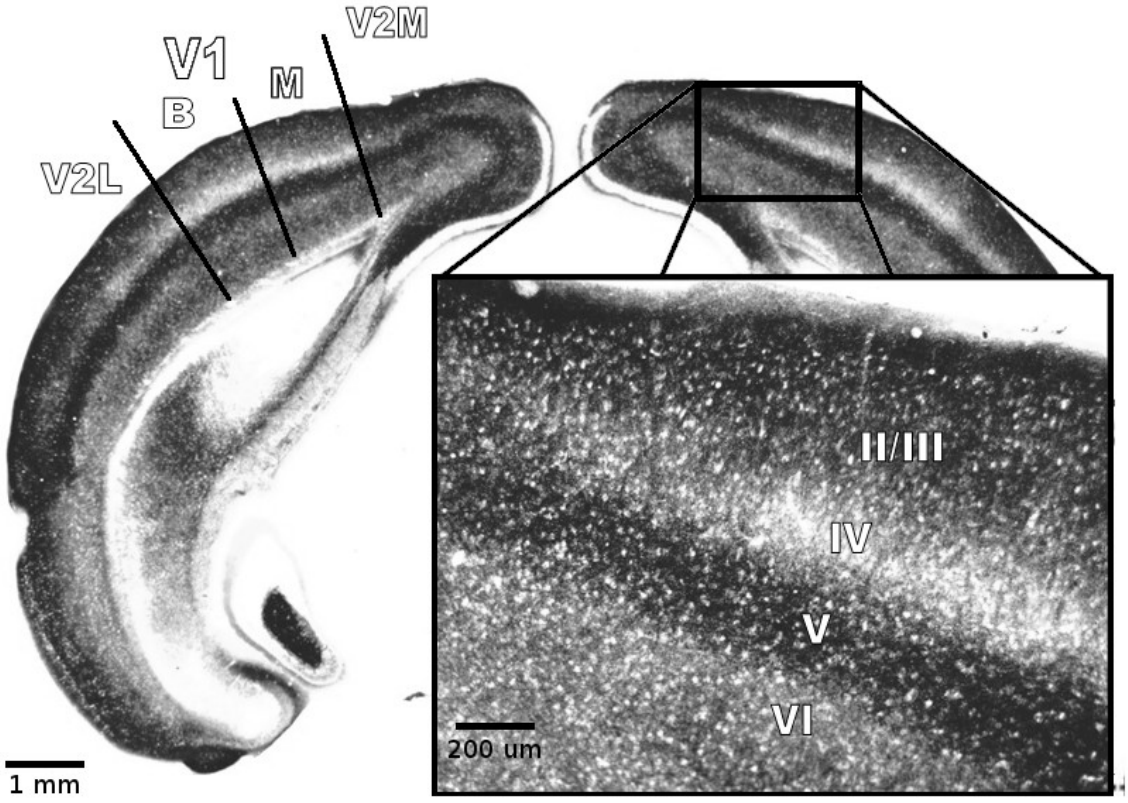
V2M
V1
M
B
V2L
1 mm
II/III
IV
V
VI
200 um

Subtle transitions in the average density of synaptic zinc, both within a particular cortical layer as well as between the cortical layers, were observable the intensity of zinc staining across the layers of the cortex as a continuous signal (Fig. 3). Layer 1 of the mouse V1 was most heavily stained with histochemically detectable zinc. Zinc staining intensity remained high in the most superficial region of layer II, and steadily decreased (approximately 15 %) into the border between layers III and IV. Layers II and III cannot be clearly separated on the basis of zinc staining intensity. Distinct sublaminae were observed in layer IV: IVa, bordering layer II/III and approximately 70 μm thick, was characterized by a sharp decrease (approximately 30 %) in zinc staining intensity; IVb, approximately 90 μm thick, was the most zinc-poor sublamina; and IVc, bordering layer V and 70 μm thick, was characterized by a sharp increase in zinc staining intensity (approximately 75 %). Layer V was homogeneously saturated with synaptic zinc on a level comparable to that in layer I. Zinc staining intensity in layer VI was comparable to layer II/III and was less heavily stained than that in layers I and V. Layers I through VI were divided into 7 laminae for statistical analysis (Fig. 2-4 shading).

Repeated measures analysis of variance revealed that the average zinc staining intensities within each of the cortical layers were significantly different from each other ($F_{(6, 23)} = 137.66$, $p < 0.001$, partial $\eta^2 = 0.98$). This difference was driven by the lower level of synaptic zinc staining in layer IVb compared to all other layers ($p < 0.03$). There was also a significant 6^{th} order fit to the 7-lamina schema (Fig. 2-4 shading) used here to separate different sections of the zinc staining profile for statistic analysis ($F_{(1, 3)} = 441.41$, $p < 0.001$, partial $\eta^2 = 0.99$). The 7-lamina schema validated here with control mice was

therefore used for the statistical analyses of zinc staining intensity profiles in monocularly deprived mice.

The laminar distribution of synaptic zinc tended to vary with age (Fig. 2-5A). Synaptic zinc staining intensity in layer IVb increased (approximately 90%; $F_{(3, 16)} = 5.26$, $p < 0.01$, partial $\eta^2 = 0.55$) in 6 month-old control mice. Zinc staining intensity in layers II/III, V, and VI significantly decreased with age (approximately 25%; Layer II/III: $F_{(3, 16)} = 7.71$, $p < 0.03$, partial $\eta^2 = 0.57$; Layer V: $F_{(3, 16)} = 24.23$, $p < 0.001$, partial $\eta^2 = 0.81$; Layer VI: $F_{(3, 16)} = 17.08$, $p < 0.001$, partial $\eta^2 = 0.75$;). However, comparison of zinc staining profiles between mice must be interpreted with some caution because of the high individual variation (Fig. 2-5B) associated with the zinc staining protocol. Further details are outlined in the Discussions.

Figure 2-5: V1 zinc staining profile for 3 month old naive male mice.

n = 5; Error bars: 95 % confidence interval; X-axis marks: separation of cortical layers as determined by anatomic landmarks and zinc staining intensities; *: significant difference in average zinc staining intensity when compared to that of all other layers at $p < 0.03$; Graphic along the x-axis: sample 2.5 mm thick zinc stained section through V1.

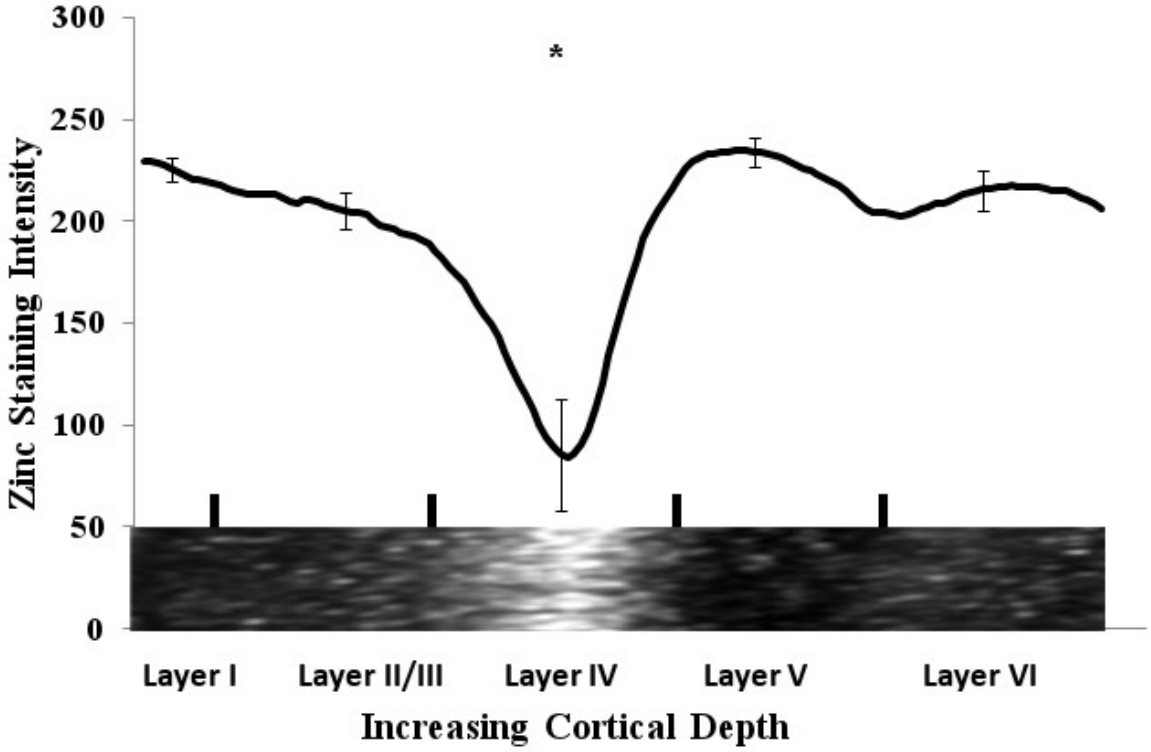
300
250
200
150
100
50
0
Zinc Staining Intensity
*
Layer I
Layer II/III
Layer IV
Layer V
Layer VI
Increasing Cortical Depth

Figure 2-6: Zinc staining profile in V1 of control mice.

A: comparison of the average zinc staining profiles of the control groups (aged matched controls for each of the 4 durations of monocular deprivation examined in this study; n = 5; Error bars: 95% confidence interval); B: raw zinc staining profiles for the individuals for 3 month old group A mice.

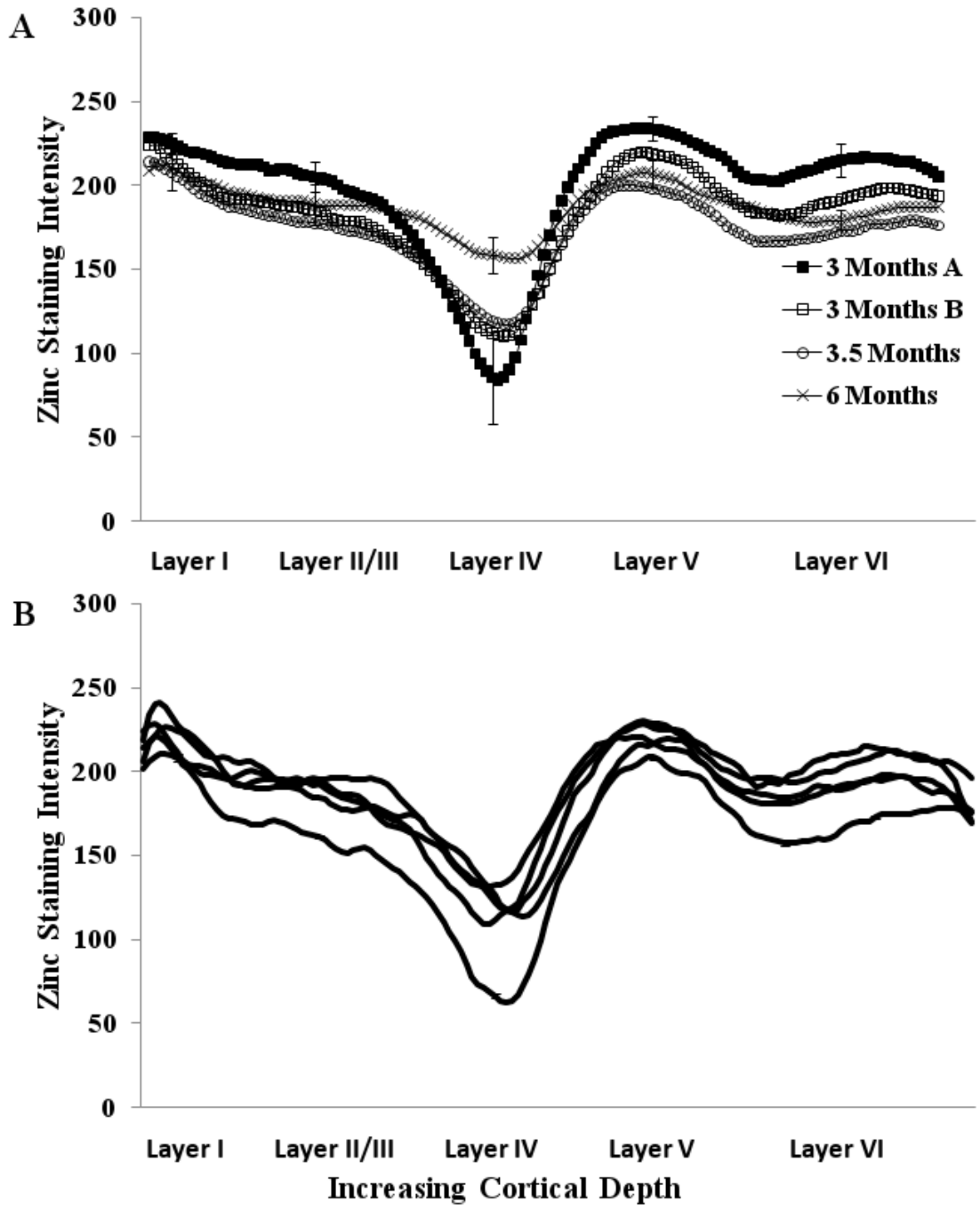
A
300
250
200
150
100
50
0
Zinc Staining Intensity
3 Months A
3 Months B
3.5 Months
6 Months
Layer I
Layer II/III
Layer IV
Layer V
Layer VI
B
300
250
200
150
100
50
0
Zinc Staining Intensity
Layer I
Layer II/III
Layer IV
Layer V
Layer VI
Increasing Cortical Depth

2.4.2 Experience-dependent change in V1 zinc staining intensity

The percent difference in zinc staining intensity between deprived V1M and spared V1M was computed for each monocular deprived mouse and the average plotted against cortical depth (Fig. 2-6A). One day of enucleation resulted in approximately 70 % higher density of synaptic zinc within layer IVb of the deprived *vs* the sparedV1M ($t_{(4)}$ = 3.31, $p < 0.03$). Layer IVb of the deprived V1M remained more intensely stained for synaptic zinc relative to spared V1M, 3 days (35 %; $t_{(4)} = 6.49$, $p < 0.003$), 2 weeks (20 %; $t_{(4)} = 3.45$, $p < 0.04$), and 3 months (5 %; $t_{(4)} = 4.12$, $p < 0.03$) after enucleation. Three months after enucleation, the density of zinc labelling in layers II/III, IVa, IVc, and V in the deprived V1M was approximately 10 % higher in spared V1M (Layer II/III $t_{(4)} = 9.59$, $p < 0.002$; Layer IVa: $t_{(4)} = 9.66$, $p < 0.002$; Layer IVc: $t_{(4)} = 6.9$, $p < 0.006$; Layer V: $t_{(4)}$ = 8.05, $p < 0.004$). The duration of monocular enucleation had a significant effect on the laminar distribution of zinc staining intensity ($F_{(21, 29.27)} = 2.35$, $p < 0.03$, Wilk's $\Lambda = 0.03$, partial $\eta^2 = 0.69$). This effect was driven by a significant decrease in the enucleation-dependent modulation of synaptic zinc levels in layer IVb 3 months after enucleation ($p < 0.025$).

To determine whether the observed difference in V1M zinc staining intensities was due to an increase in synaptic zinc density within the deprived V1M or a reduction of synaptic zinc within spared V1M, comparisons to age-matched controls were made (Fig. 2-6B, 2-6C). Following 1 day of monocular deprivation, there was a larger increase in synaptic zinc density within deprived V1M layer IVb (approximately 60 % compared to age-matched controls; $t_{(4)} = 3.19$, $p < 0.05$; Fig. 2-6B) and a trend for a reduction in synaptic zinc density within spared VIM layer IVb (approximately 15 % compared to

controls; not significant; Fig. 2-6C). Following 3 months of monocular deprivation, synaptic zinc density was greater within V1M layers II/II ($t_{(4)} = 3.98$, $p < 0.03$) and V ($t_{(4)} = 2.74$, $p < 0.05$) compared to age-matched controls.

A similar pattern of monocular deprivation-induced change in zinc staining intensity was observed in V1B (Fig. 2-7). However, significant increase in zinc staining intensity was found only in layer IVb in the deprived V1B relative to spared V1B, 24 hours after monocular deprivation ($t_{(4)} = 4.75$, $p < 0.02$).

Figure 2-7: Percent difference in V1M synaptic zinc staining intensity following periods of monocular deprivation.

A: Difference in zinc staining between deprived V1M and spared V1M; B: Difference in zinc staining between deprived V1M and control V1M; C: Difference in zinc staining between spared V1M and control V1M; Error bars: 95% confidence intervals shown for 1 day and 3 months of monocular deprivation.

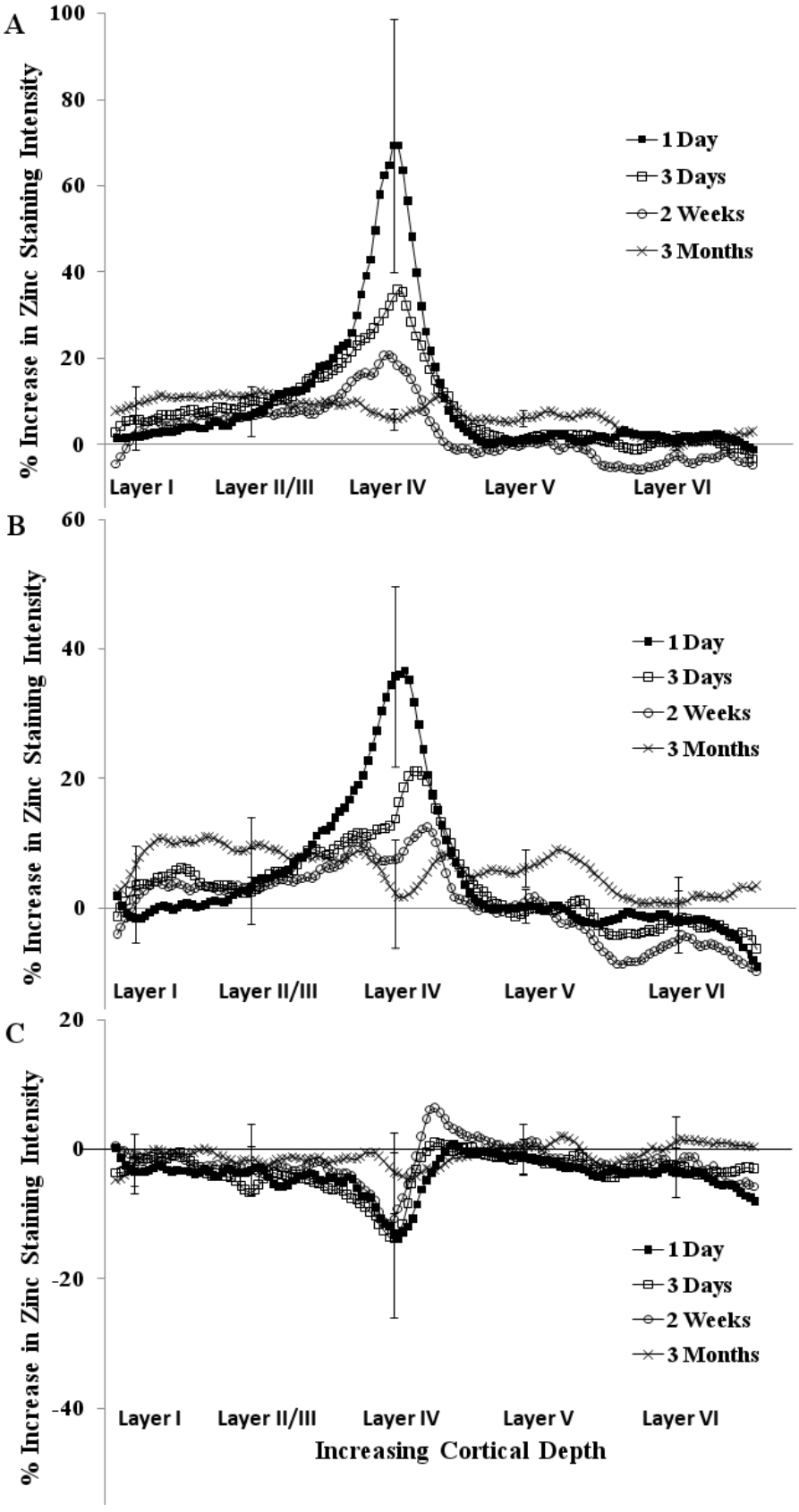
A
100
80
60
40
20
0
% Increase in Zinc Staining Intensity
1 Day
3 Days
2 Weeks
3 Months
Layer I
Layer II/III
Layer IV
Layer V
Layer VI
B
60
40
20
0
% Increase in Zinc Staining Intensity
1 Day
3 Days
2 Weeks
3 Months
Layer I
Layer II/III
Layer IV
Layer V
Layer VI
C
20
0
-20
-40
% Increase in Zinc Staining Intensity
1 Day
3 Days
2 Weeks
3 Months
Layer I
Layer II/III
Layer IV
Layer V
Layer VI
Increasing Cortical Depth

Figure 2-8: Percent difference in V1B synaptic zinc staining intensity at intervals after monocular enucleation.

Error bars: 95% confidence intervals shown for 1 day and 3 months after enucleation.

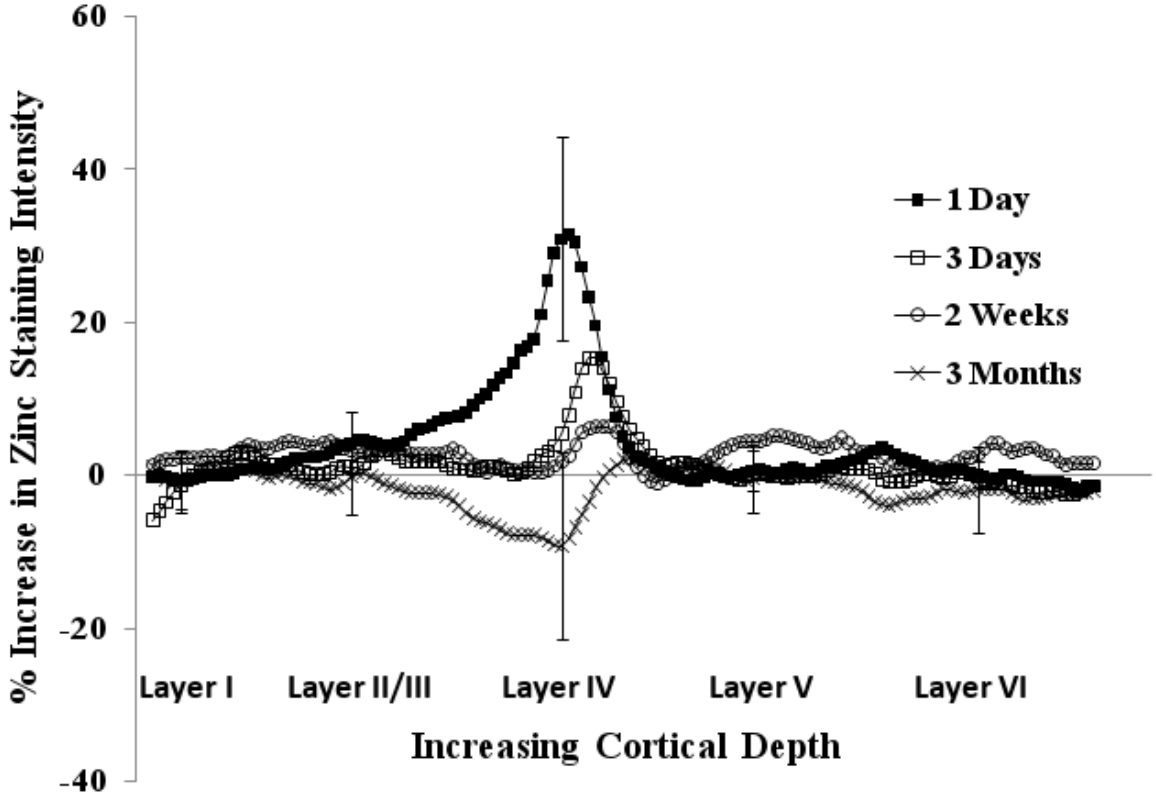
60
40
20
0
-20
-40
% Increase in Zinc Staining Intensity
1 Day
3 Days
2 Weeks
3 Months
Layer I
Layer II/III
Layer IV
Layer V
Layer VI
Increasing Cortical Depth

2.5 Discussion

In higher mammals, such as primates and cats, monocular enucleation-induced plasticity is observed as the shrinkage of receptive field size and depression of activity in deprived ocular dominance columns followed by the expansion and potentiation of activity in spared columns (Hubel and Wiesel, 1964, Shatz and Stryker, 1978). The visual cortex of mice lacks the organization into ocular dominance columns seen in higher mammals (Dräger, 1978; Antonini et al., 1999), and is instead characterized by clearly distinguishable monocularly and binocularly driven regions (Van Brussel et al. 2009; Paulusen et al., 2011). The binocularly driven region does not have clearly separable ocular dominance columns; representation from both retinas are distributed in a loose retinal-topic manner in the binocular region. Monocular deprivation-induced reorganization in the visual cortex has been observed in both young and adult mice as well (see Hofer et al., 2006). We have demonstrated that experience-dependent modulation of synaptic zinc levels previously reported in the visual cortex of higher mammals (Dyck et al., 2003) is also inducible in the adult mouse through monocular deprivation.

The laminar distribution of zinc-containing axon terminals in the adult mouse V1 is similar to, but less complex and distinct than, the patterns observed in the cat and primate. In both mice and the higher mammals, layers I and V are most populated with zincergic terminals, followed by layers VI and II/III. However, layer IV in the mouse V1 is divided into more than one sublaminae given the distribution of synaptic zinc instead of the 4 distinct layers found in higher mammals (layers IVa, IVb, IVcα, and IVcβ; Dyck

and Cynader, 1993 ; Dyck et al., 2003). There were also no clear sublaminae within layers III or VI in the mouse V1. These observations likely correspond to the lack of finer organization of ocular dominance or orientation selectivity in the mouse (Bienenstock et al., 1982).

The density of zincergic terminals in V1 was influenced strongly by the age of the mouse; it appeared to increase with age of in layer IV, but decrease with age in layers II/III, V, and VI. However, caveats to interpreting zinc staining intensities between animals prevent concrete conclusions from being drawn. The autometallographic staining technique used in this study involves systemic circulation of selenium. The intensity of staining in part depends on the rate at, and extent to, which selenium bind to histochemically-reactive zinc. Although dosage of injected sodium selenite and survival time following injection were controlled, there can still be individual difference in the uptake and circulation of selenium ions and, therefore, the amount of zinc-selenium formed and available for physical development. The development process itself involves the use of a viscous developer solution that is light-, temperature-, and time-sensitive. The end point for development is determined visually and the results may not be precisely comparable between different batches of stained sections. This is evident in the average zinc staining profile for 3 month-old control groups A and B, where there is only 1 day of difference in age and no difference in labelling intensitywas expected (Fig. 4A). As such, comparisons made within the same subject, by calculating relative changes in zinc staining intensity between structures on the same section, will most accurately represent manipulation-induced changes. Comparisons made between animals should be interpreted with this in mind.

As in the adult vervet monkey (Dyck et al., 2003), when adult mice were monocularly deprived by enucleation and allowed to survive for 24 hours, a robust and significant increase in zinc staining was observed in layer IVb of the deprived V1M relative to the spared V1M. Long-term monocular deprivation (3 months) reduced this short-term elevation of zinc staining levels in layer IVb to non-significant levels, but did not reverse the direction of change as was reported in monkeys. What was surprising was that long-term deprivation significantly increased zinc staining in layers II/III, V, and VI. Experience-dependent modulation of synaptic zinc levels in layers other than layer IV has only been described in the barrel cortex of mice with electron microscopy (Nakashima and Dyck, 2010). The visualization and quantification techniques described in the present study may be a more sensitive measure of the laminar distributions of zinc staining than traditional densitometry measurements that focus on staining intensity within singular areas *vs* that across the entire region of interest.

Although the use of mice to study the phenomenon of ocular dominance plasticity is relatively recent, the general observation drawn from these studies is that visual cortex plasticity in the mouse closely resembles that reported previously in higher mammals (see Hofer et al., 2006). In the adult mouse, monocular deprivation-induced plasticity has been demonstrated with several methods, including increased expression of the immediate-early gene Arc (Tagawa et al., 2005), increased intrinsic optical imaging signalling in he non-deprived regions of V1 (Hofer et al., 2005), and decreased visual evoked potentials for the deprived eye (Lickey et al., 2004). Monocular deprivation induces an initial weakening of deprived eye responses and later a strengthening of

spared eye responses. These phenomena are both in part mediated by NMDA receptors (Sawtell et al., 2003).

With this in mind, experience-dependent changes in synaptic zinc levels may result in altered modulation of NMDA receptor activity. A number of studies demonstrated that zinc is capable of modulating NMDA receptor-dependent LTP and LTD in the hippocampus (Quinta-Ferreira and Matias, 2004; Qian and Noebel, 2005; Takeda et al., 2010). Increased levels of synaptic zinc in the deprived V1 after short durations of monocular deprivation could therefore function to inhibit NMDA receptors and facilitate LTD-like processes within the deprived V1 regions. The reduction in synaptic zinc levels after long-term deprivation could subsequently facilitate NMDA receptor-dependent strengthening of spared-eye inputs (Sawtell et al., 2003). Electrophysiological studies performed on adult visual cortex suggest that longer deprivation periods (greater than 6 days) are necessary for eliciting maximal ocular dominance shifts (see Hofer et al., 2006). The potentiation of spared eye input coincides with the reduction in synaptic zinc levels observed after 2 weeks and 3 months of monocular deprivation.

Earlier studies that failed to detect an ocular dominance shift in adult mice used barbiturate anaesthesia (Fagiolini and Hensch, 2000). Barbiturates, by enhancing GABA-mediated inhibitory transmission, may have masked monocular deprivation-induced potentiation of spared-eye inputs (Pham et al., 2004). Zinc is a known inhibitor of GABA transporters and elevated levels of synaptic zinc have been proposed to be able to increase synaptic levels of GABA and enhance inhibitory transmission (Cohen-Kfir et al., 2005). The net effect of an increase in zinc levels may

therefore be a combination of reduction of excitation by inhibiting NMDA receptors and promotion of inhibition by augmenting GABA transmission. The time-course of the experience-dependent modulation of synaptic zinc levels observed in this study suggests that, in response to sensory deprivation, synaptic zinc participates first in the immediate and short-term depression of layer IV activity. Following long term deprivation, zinc levels are reduced in layer IV and raised in layers II/III, V, and VI, possibly to facilitate the potentiation of, and encroachment by, neighbouring spared-eye input. Further studies that examine the effects of applied zinc and synaptic zinc chelators are required to support this hypothesis.

Evidence provided in this study suggests that the laminar distribution of synaptic zinc in the visual cortex of adult mice is similar to that observed in higher mammals. Synaptic zinc levels in V1 of adult mice are also dynamically modulated by the presence of absence of an eye to provide normal visual input.. Further studies are required to decipher the role of synaptic zinc in the modulation of short-term and long-term forms of plasticity within the adult cortex.

Chapter 3: Novel, Whisker-Dependent Texture Discrimination Task for Mice

The work contained within this Chapter was previously published:
Hsia-Pai Patrick Wu, Julie C. Ioffe, Michaela M. Iverson, Jacqueline M. Boon, Richard H. Dyck (2012) Novel, Whisker-Dependent Texture Discrimination Task for Mice. Behav. Brain Res. 237:238-242.

The author was responsible for designing the study, designing and fabrication of the behavioural assessment apparatuses, performing the behavioural assessments, analysis of the data, and writing of the manuscript. The author contributed to scoring of the data. Julie C. Ioffe, Michaela M. Iverson, and Jacqueline M. Boon contributed to scoring the behavioural data in the blind, and to revisions of the manuscript. Dr. Richard H. Dyck contributed to study design and revisions of the manuscript.

3.1 Abstract:

Many mammals use their mystacial vibrissae to palpate objects in their environment and encode information such as size, shape and texture. We have developed a novel method to assess the sensitivity with which mice can discriminate textures using their mystacial vibrissae. Our texture discrimination task can be performed within 3 days, requiring approximately 1 hour of handling time, per subject, over the entire testing period. No food or water reward is required. We have demonstrated that this novel texture discrimination task is dependent on intact mystacial vibrissae and can be performed by both young (2 month old) and older (6 month old) C57BL/6 mice. The parameters of the

task can be adjusted to assess the sensitivity of mice using a gradient of textures with different roughness.

3.2 Introduction

Rodents rely on their whiskers to acquire much of the information in their environment. This includes the size, shape, and texture of objects the rodents come in contact with (Brecht, 2007). The barrel cortex is devoted to the processing of sensory input from the facial whiskers and occupies approximately 70% of the primary somatosensory cortex of rodents (Woolsey and Van der Loos, 1970; Simons and Woolsey, 1979). Sensory input from one mystacial vibrissa can be traced with specificity to a defined area of the barrel cortex (Simons and Woolsey, 1979). The barrel cortex system of rodents has been exploited by neuroscientists to examine a wide variety of questions within cellular and systems neuroscience, including cortical map development, cortical plasticity, and neuronal encoding of sensory stimuli (Fox, 2002; Feldman and Brecht, 2005; Brecht, 2007). Where genetic factors are involved, the mouse barrel cortex has been particularly valuable. Many of the studies conducted within the barrel cortex system can be further expanded to observe how the experimental parameters applied can ultimately affect whisker function and whisker-mediated behaviour. Here we describe a task developed specifically to test the whisker sensitivity of mice.

Existing tasks that assess whisker function in mice can be separated into two categories, head-fixed and freely-moving tasks. Head-fixed tasks involve precisely tracking whisker movement with the mouse's head immobilized using implanted rods (O'Connor et al., 2010a-b; Stuttgen, 2010). The immobilized mouse is trained to perform

a discrimination task using its whiskers in a go/no go task with reward from a water-spout. Approximately 10 training sessions are required to reach a criterion of 85 % correct responses. Freely-moving tasks generally consist of training rodents in a Y- or T-maze type enclosure to navigate to the goal arm for a food reward (Guic-Robles et al., 1989; Lipp and Van der Loos, 1991; Guic-Robles et al., 1992; Carvell and Simons, 1996; Krupa et al., 2001). The cue for the goal arm is presented at the junction of the two arms and may consist of textures presented across a gap. The mouse is required to palpate the cue with its whiskers prior to navigating across the gap to the baited arm. Training for these tasks typically requires more than 5 sessions, with each session typically consisting of more than 20 trials.

Although the use of mice in neuroscience research is widespread, behavioural assessment in mice largely involves the use of miniaturized equipment originally tailored to rats and may not be efficient for use with mice (Lipp and Van der Loos, 1991). Training mice typically requires many trials spread across multiple sessions and significant time commitment for each mouse. Food or water deprivation is also required to motivate mice to perform baited tasks. This not only increases the time required to prepare a mouse for testing, but also introduces motivation as another variable that must be accounted for.

In the present study, we demonstrate a novel approach to assess whisker sensitivity in mice. This task does not require food or water rewards, surgery, or extensive commitment in time and equipment. We modified the novel object recognition task (Ennaceur and Delacour, 1988) to create a whisker-dependent texture discrimination task

that can be performed in three days with less than 1 hour of training/testing (in total) per mouse.

3.3 Methods

3.3.1 Animals and treatment groups

Male, C57BL/6 mice at the ages of 2 and 6 months were used for this study. The mice were maintained on standard laboratory diet and water *ad libitum* and kept in standard laboratory housing under a 12-hour light/dark cycle. A whisker-less group was generated to test for the specificity of the texture-discrimination task to the presence of whiskers. Mice were placed under isoflourane anesthesia and all mystacial vibrissae were removed with tweezers. Care was taken to ensure that the plucking of whiskers did not damage the whisker follicles and induce bleeding. The bilateral removal of the mystacial vibrissae was performed 3 days prior to the start of testing. All procedures were approved by the Animal Care Committee of the University of Calgary and conformed to the guidelines set out by the Canadian Council for Animal Care.

3.3.2 Apparatuses

The testing arena was constructed with white corrugated plastic boards (Plaskolite Inc., Ohio) and measured 40 x 40 x 40 cm high (Fig. 3-1A). The base of the arena was carpeted with 2 cm of standard laboratory bedding (Aspen Chip; Nepco, Warrensburg, New York). The target objects used for the texture discrimination task were constructed with rectangular 0.5 cm thick corrugated plastic boards, 4 x 15 cm high, fixed to a 4 x 4 cm base (Fig. 3-1B). Aluminum oxide sand paper (Gator Finishing Products, Ohio) was

affixed to the faces of these upright boards such that the sand paper covered 7.5 cm of the height of the boards starting 2 cm from its base. Different grades of sand paper (80, 100, 120, and 220 grit) were used to create a series of objects that were mainly distinguishable through texture. The roughness of the texture was determined by the average particle diameter of the sandpaper (approximately 190 μm, 140 μm, 115 μm, and 70 μm), evenly distributed across the textured surface (intervals between particles are approximately 200 μm, 150 μm, 120 μm, 75 μm). Three identical objects were created for each grade of sandpaper used in this study, to avoid repeated use of the same object across the testing period. This minimized the possibility that the mice recognized one particular object using olfactory cues.

Plastic transparency film (3M, London, Ontario) was used to cover the faces of the texture discrimination objects to create smooth objects differentiated by the subtle visual differences between the different grades of sandpaper used. The transparent film-covered, "texture-less", objects were used to test the mouse's ability to visually differentiate between the textures. The use of the texture-less objects was included in the study as a means to account for visual cues contributing to the discrimination.

3.3.3 Texture discrimination

All behavioural testing was conducted between 1-2 hours after the start of the dark cycle. The mice were habituated to the testing arena prior to the texture discrimination task. The habituation period was required to acclimatize the mice to the testing arena and promote exploratory behaviour on the testing day. Illumination was provided with two 150 W overhead incandescent floodlights dimmed to approximately 50 % output. Care was taken

to position the arena directly under the light sources such that no shadows were cast on the arena floor by its walls. For two consecutive days prior to the testing day, each animal was placed in the empty arena and allowed to explore for 10 min (Fig. 3-1C). The procedure and specific time intervals used for in this study were derived from parameters used in previously published object recognition tasks (Sik et al., 2003; Spanswick and Sutherland, 2010). Pilot studies indicated that mice were able to perform the texture discrimination task using these parameters.

The animals were transported between the home cage and arena in a clean, empty cage carpeted with bedding. Both the transport cage and arena were cleaned with 70 % ethanol after each animal to mask olfactory cues and accustom the animals to the odour of the cleaning agent. The bedding in the testing arena and transport cage was not replaced for the duration of the experiment.

The testing day consisted of two sessions. The activity of the mouse was recorded with a video camera centered above the arena. For the first session, the learning phase, the mouse was placed in the testing arena equidistant to and facing away from two identically textured objects at the center of the arena. The textured objects were placed in the center of the arena, equidistant to each other and the walls (Fig. 1A). The bedding covered the base of the objects such that the textured surface was immediately above the bedding. The mouse was allowed to explore the objects for 5 min. The mouse was then removed and held in the transport cage for 5 min. This short retention interval was selected to minimize the mnemonic involvement of the hippocampus (Hammon et al., 2004).

Prior to the start of the second session, the two objects in the arena were replaced with a third, identically textured object as well as a novel object with a different texture. The position of the novel versus the familiar textured object was randomized between subjects to account for the possibility of left- or right-side preference. The mouse was then placed back into the arena for the second session, the test phase, and allowed to explore for 3 min (Fig. 1C). The testing arena, objects, and transport cage were cleaned with 70 % ethanol between sessions and between animals to mask olfactory cues.

3.3.4 Data analysis

The amount of time mice spent actively investigating the objects was recorded. Investigation was defined as directing the nose towards the object with a distance of less than 2 cm from the nose to the object or touching the nose to the object. Resting, grooming, and digging next to, or sitting on, the object was not considered as investigation. The total time the mouse spent investigating the two identically textured objects during the learning phase was interpreted as a measure of general exploratory activity. The percentage time spent investigating the novel texture versus the familiar texture during the testing phase served as the discrimination measure. Mice that did not explore the objects during the learning phase, explored only one of the two objects during the testing phase, or had a total investigation time of less than 2 seconds during either phases were excluded from the study for lack of adequate exploratory activity. One-sample T-tests were performed against a chance value of 50 % to determine if the mice were able to discriminate between the novel and previously exposed textures. ANOVAs were performed to reveal between-group effects in the level of general exploratory activity.

Figure 3-9: Schematic of the texture discrimination task.

A) Photograph of the testing apparatus. B) Schematic of the discriminanda. C) Schematic of the procedure for the texture discrimination task. a, a', and a'': 3 objects with identical textures; b: novel object with a different texture to object a.

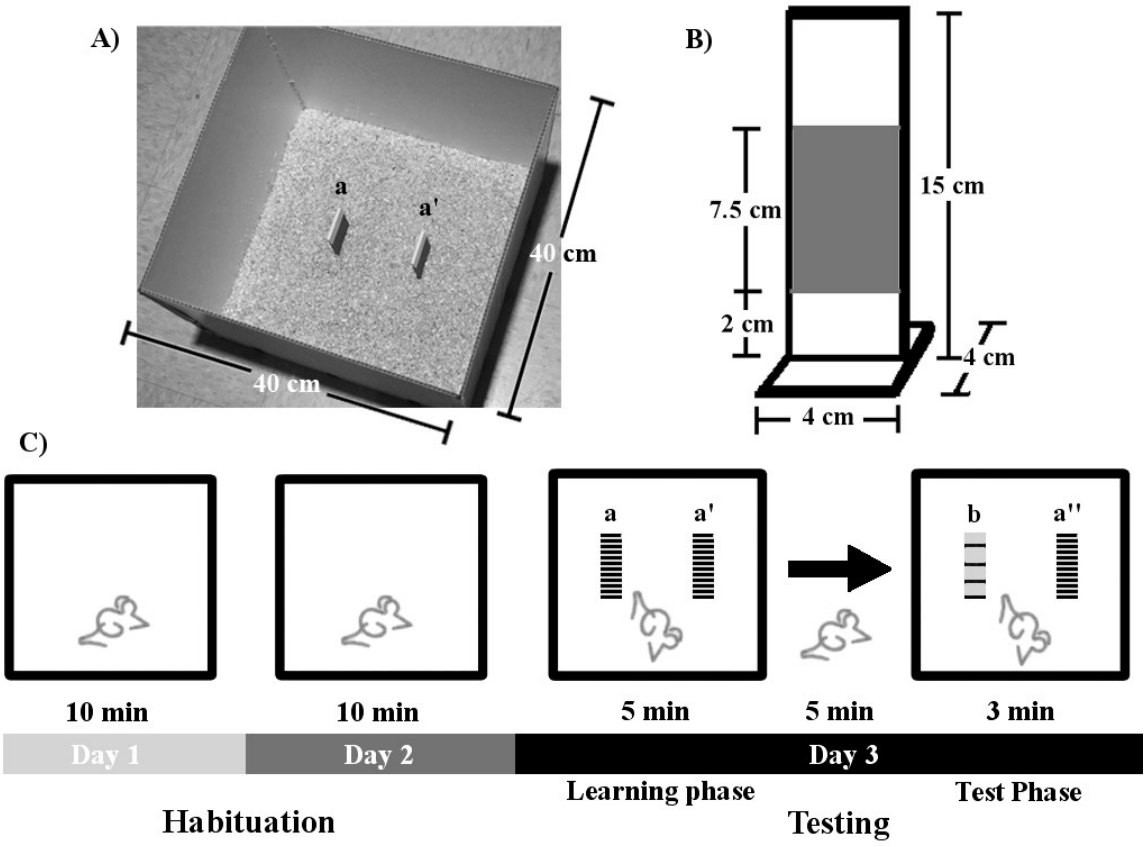
A)
a
a'
40 cm
40 cm
B)
7.5 cm
15 cm
2 cm
4 cm
4 cm
C)
a
a'
b
a''
10 min
10 min
5 min
5 min
3 min
Day 1
Day 2
Day 3
Learning phase
Test Phase
Habituation
Testing

3.4 Results

We found that both 2-month-old ($t_{(5)} = 3.56$, $p = 0.016$) and 6-month-old ($t_{(7)} = 2.65$, $p = 0.033$) mice were able to discriminate between novel and familiar textures that were 25 μm different in roughness (Fig. 3-2A). One 2-month-old and three 6-month-old mice were excluded from analysis for lack of exploratory behaviour. The exploratory activity of the younger adolescent mice was significantly higher during the learning phase when compared to the mature mice ($F_{(1,18)} = 7.53$, $p = 0.026$), however the activity levels was not different between the two ages during the testing phase ($F_{(1,18)} = 1.38$, $p = 0.256$; Fig. 3-2B).

To test whether this texture discrimination ability was dependent on whiskers, the mystacial vibrissae of mice were removed bilaterally 3 days prior to testing. Mice with intact whiskers were able to distinguish between novel and familiar textures ($t_{(13)} = 4.31$, $p = 0.001$) while the "whisker-less" mice were unable to discriminate the novel texture ($t_{(13)} = -0.26$, $p = 0.796$; Fig. 3-3A). Mice with intact whiskers were unable to discriminate between the novel texture and the learning phase texture when the textured surface of the objects was covered with a transparent plastic film to create "texture-less" objects ($t_{(10)} = 0.69$, $p = 0.509$). Neither removing the whiskers nor rendering the objects smooth with transparent plastic film affected exploration activity (learning phase: $F_{(2,38)} = 0.13$, $p = 0.876$; testing phase: $F_{(2,38)} = 1.51$, $p = 0.234$). One animal in the whisker-less group and two animals in the texture-less group were excluded from analysis due to lack of exploratory behaviour.

Figure 3-10: Performance of young and older mice in texture discrimination.

A) Male, 2-month-old and 6-month-old C57BL/6 mice were able to discriminate between novel and familiar textures separated by 25 μm in average particle size. B) Young mice explored the textured objects more than the older mice during the learning phase but not the testing phase. Dashed line represents chance level (50%); error bars represents the standard error of the mean; asterisks indicates statistical significance *vs* chance at $p < 0.05$.

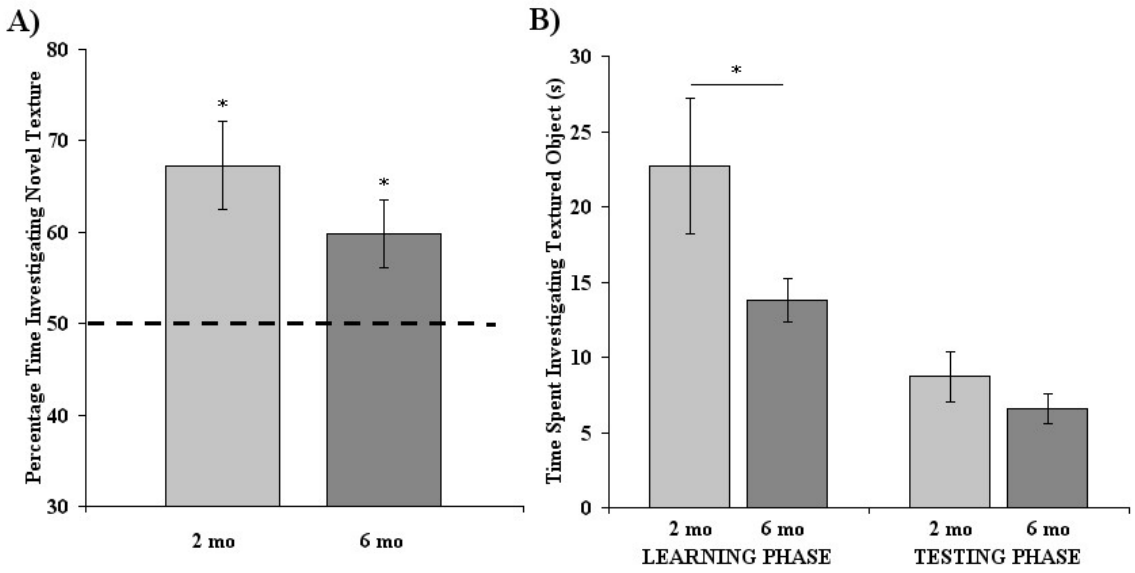
A)
Percentage Time Investigating Novel Texture
80
70
60
50
40
30
*
*
2 mo
6 mo
B)
Time Spent Investigating Textured Object (s)
30
25
20
15
10
5
0
*
2 mo
6 mo
2 mo
6 mo
LEARNING PHASE
TESTING PHASE

Figure 3-11: Whisker-dependent texture discrimination.

A) Mice were not able to discriminate between "texture-less" objects (textured objects with the textured surface covered with transparent plastic film) or between textured objects with 25 μm difference in roughness after the mystacial vibrissae were removed.B) The use of paws did not affect the ability of mice to discriminate between the textured objects.Dashed line represents chance level (50%); error bars represent the standard error of the mean; asterisks indicates statistical significance *vs* chance at $p < 0.05$.

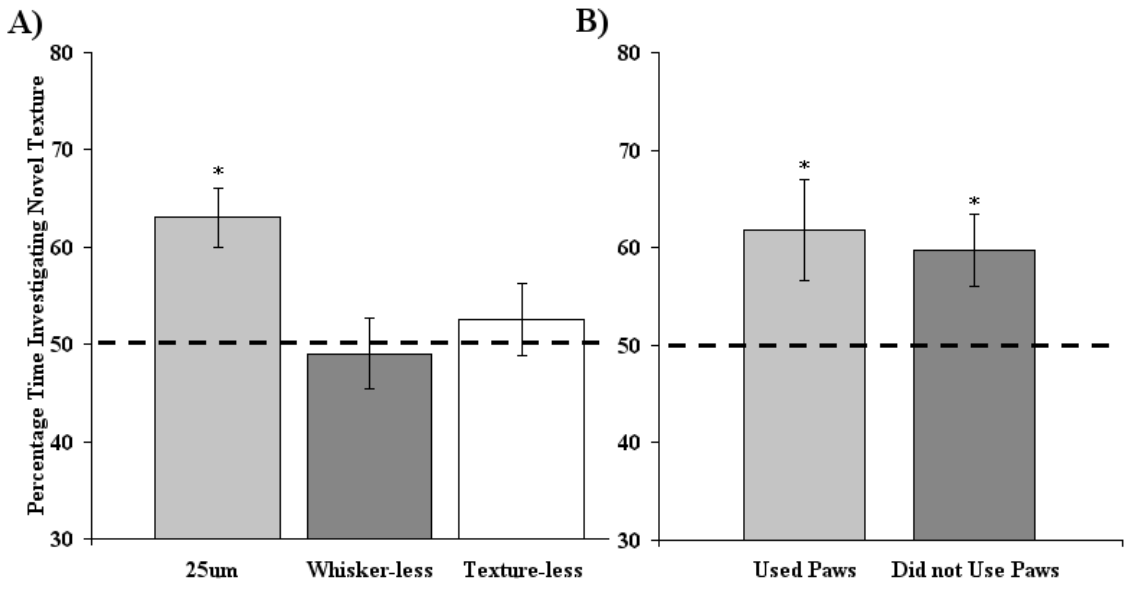
A)
B)
Percentage Time Investigating Novel Texture
80
70
60
50
40
30
*
*
*
25um
Whisker-less
Texture-less
Used Paws
Did not Use Paws

The number of times the mice placed their paws on the objects was recorded to determine the contribution of sensory cues from the paws to texture discrimination. Mice were categorized to have used their paws when both of the following conditions were met: 1. the mouse placed one or both of its forepaws on the any of the two objects at least once during the learning phase, and 2. the mouse placed one or both of its forepaws at least once on both the novel and familiar objects during the testing phase. The use of the paws was not associated with changes in exploratory activity (learning phase: $F_{(1,18)} = 2.56$, $p=0.128$; testing phase: $F_{(1,18)} = 0.01$, $p = 0.948$). Bilateral removal of the mystacial vibrissae did not predict the number of mice that used their paws ($c^2_{(1, N=55)} = 0.01$, $p = 0.949$, Cramer's V = 0.01). Finally, whiskered mice that used their paws ($t_{(10)} = 2.29$, $p = 0.045$) and those that did not ($t_{(7)} = 2.64$, $p = 0.033$) were both able to distinguish between novel and familiar textures that differed by only 25 μm (Fig. 3-3B).

This texture discrimination task can be used to assess the sensitivity of mice to different grades of sandpaper. Mice tested in the present study were able to distinguish between textures separated by a difference of 25 μm ($t_{(13)} = 4.31$, $p = 0.001$), 50 μm ($t_{(4)} = 3.96$, $p = 0.017$), and 125 μm ($t_{(12)} = 5.59$, $p < 0.001$) in average particle sizes (Fig. 3-4).

Figure 3-12: Percentage of testing time spent investigating the novel object.

Mice were able to discriminate between textures with 25 μm, 50 μm, and 125 μm difference in roughness. Dashed line represents chance level (50%); error bars represent the standard error of the mean; asterisks indicates statistical significance *vs* chance at $p < 0.05$.

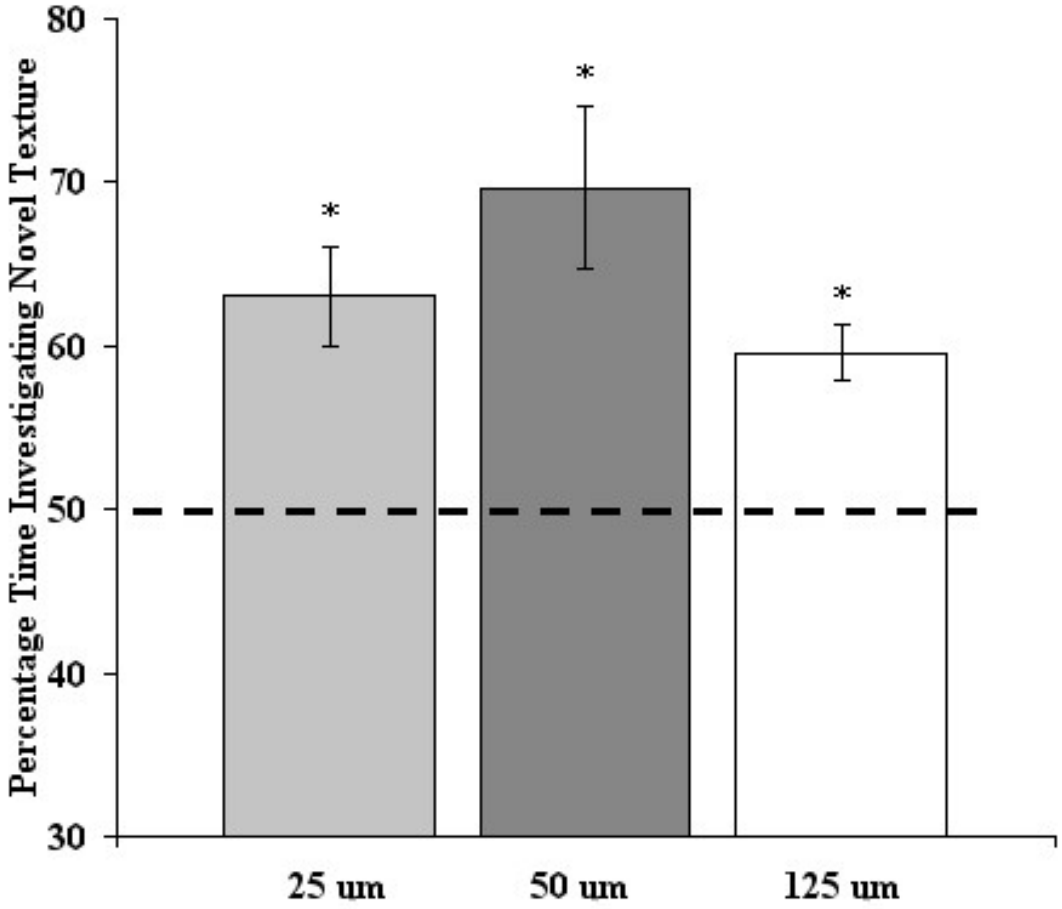
Percentage Time Investigating Novel Texture
80
70
60
50
40
30
*
*
*
25 um
50 um
125 um

3.5 Discussion

We have shown that mice were able to discriminate between objects based on texture alone. This texture discrimination ability is dependent upon intact mystacial vibrissae, as the removal of the vibrissae abolished the mouse's ability to discriminate between the presented textures. This is in line with observation made in rats, where it was found that the barrel cortex and mystacial vibrissae are essential to texture discrimination (Guic-Robles et al., 2010a,b). I have also obtained evidence to suggest that the full complement of mystacial vibrissae is required (Appendix A).

To assess contribution from visual sensory input to the discrimination task, texture cues were removed by shielding the objects with transparent film. The remaining subtle visual differences between the objects were not sufficient to enable the mice to discriminate between the two different textures.

Mice also receive sensory input from their paws. Mice prefer exploring objects that allows climbing and perform the novel object recognition task better with these objects (Chemero and Heyser, 2005). Although approximately 50 % of mice placed their paws on the textured objects in the present study the use of the paws did not influence their ability to discriminate based on texture. Loss of the mystacial vibrissae did not affect the frequency with which mice used their paws. The use of paws in mice lacking vibrissae was also not sufficient to enable texture discrimination. These results suggest that neither visual cues nor sensory input from the paws contributed to successful performance, whereas intact mystacial vibrissae are essential for successful texture discrimination.

Industrial sandpaper was used to provide the textured surface for discrimination. This allows the experimenter to test the sensitivity of mouse whiskers to a gradient of roughness using a readily available and cost-efficient material. The sensitivity of mice to these textures was measured as the ability to discriminate the difference in the average particle diameters between the sandpaper applied on the novel and the familiar objects. The average particle diameters of the grades of sandpaper used in the present study ranged from approximately 70 μm to 190 μm. The average separation between particles ranged from approximately 75 μm to 200 μm. These ranges are well above the minimum roughness of 30 μm particles spaced at 90 μm intervals rats are known to be able to identify (Carvell and Simons, 1990). Here, we demonstrated that mice are able to discriminate between textures separated by 125 μm, 50 μm, and 25 μm in average particle diameter.

One caveat to using industrial sandpaper is the lack of uniform visual appearance between the different grades of sandpaper that are available. The colour, density, and reflectiveness of sandpaper vary between grades. The sandpapers that were used in this study all had a red hue. Sandpaper grades with larger particle sizes tend to be darker and more reflective than grades with smaller particle sizes. The lights in the testing room were dimmed to minimize visual differences between the sandpaper. Regardless, we found that the mice were not able to discriminate between sandpaper grades used in this study using visual cues alone. However, the experimenter should be aware of visual differences between larger increments of sandpaper grade, as mice may be able to visually discriminate between sandpapers with greater differences in colour.

Experimenters are encouraged to include the control trials using transparent film-covered objects to assess for the effect of visual cues on the texture discrimination task.

We have also demonstrated that mature, 6-month-old, mice were able to discriminate between sandpapers of average particle-sizes differing by 25 μm, just as well as could the younger, 2-month-old mice. These results suggest that both adolescent and mature mice are able to perform this texture discrimination task equally well. However, additional studies utilizing mice at multiple ages are required to adequately examine the effects of age on texture discrimination.

Lastly, there is evidence to suggest that this novel texture discrimination task can be used to repeatedly assay the same subject without loss of exploration activity or novel preference on repeated exposure to the same test parameters (Appendix A). This opens up the possibility of using this task to assess for loss of function or gain of function within the same subject.

Approximately 1 in 6 mice was excluded from analyses due to lack of adequate exploration activity. The following equation can be used to determine the minimum sample size required for this task (Lachin, 1981):

$$n = \frac{(Z_\alpha + Z_\beta)^2 \sigma^2}{\Delta^2},$$

where Z_α is the standard normal deviate at significance levels (1.96 for α error of 5 %); Z_β is the constant associated with the selected power on a normal distribution curve(1.28 for

90% power);σ is the estimated standard deviation (10 %); Δ is the target difference between the mean and chance level of 50 %. With Δ set to a criterion of 15 %, 5 animals are required per group to achieve a power of 90 % at a significance level of 0.05. Accounting for approximately 20 % drop-out rate, the experimenter should plan to test a minimum of 6 animals per group.

The texture discrimination task we have described requires three days to perform and does not require food and water deprivation. The task relies only on the animal's innate curiosity and exploratory behaviour. Minimal handling of the mice is involved and the level of stress induced during testing is similar to observing the animals in an open-field condition. This task provides a quick and effective alternative for testing whisker function without extensive training paradigms, implications of motivation, and induction of higher levels of stress.

Chapter 4: Synaptic Zinc Modulates Whisker-Mediated Texture Discrimination

4.1 Abstract:

Zincergic terminals are found throughout the neocortex, concentrated in layers II/III, V, and VI. Synaptic zinc is a potent neuromodulator and may mediate inter-cortical integration of somatosensory information in the barrel cortex. Zinc Transporter-3 (ZnT3) is responsible for loading zinc into synaptic vesicles. ZnT3 KO mice lack synaptic zinc within the cortex and provide a useful model to examine the contribution of synaptic zinc to barrel cortex-dependent behaviour. In the present study, we demonstrated that ZnT3 KO mice display a marked decrease in spatial acuity for whisker-dependent texture discrimination. ZnT3 KO mice were not able to discriminate between rough and smooth textures separated by less than 300 μm in average particle diameter while control mice were able to discriminate between textures separated by 25 μm. *In vivo* voltage sensitive dye imaging revealed that single whisker deflection-evoked activity in layers II/III of the barrel cortex remain at a level above 50 % of peaking amplitude longer in ZnT3 KO mice. These results suggest that synaptic zinc is necessary for the integration of somatosensory information within the barrel cortex.

4.2 Introduction

Many rodents, such as mice and rats, rely extensively on their mystacial vibrissae to explore their environment. The barrel cortex, which comprises approximately 70 % of the primary somatosensory cortex of rodents, is devoted to processing sensory input from the

mystacial vibrissae (Woolsey and Van der Loos, 1970). The integrity of the barrel cortex and mystacial whiskers is essential for whisker-dependent discrimination of objects and textures (Guic-Robles et al., 1989; Guic-Robles et al., 1992). It has been demonstrated that NMDA receptor-mediated glutamatergic neurotransmission is vital to maintaining the spatiotemporal dynamics of sensory responses in the barrel cortex (Armstrong-James et al., 1993; Petersen et al., 2003; Moore, 2004). Whereas thalamic activation of layer IV neurons in the barrel cortex is mediated by non-NMDA receptors, propagation of somatosensory responses through layers II/III is almost entirely dependent on NMDA receptors (Armstrong-James et al., 1993).

A large population of glutamatergic neurons within the mammalian cerebral cortex contains synaptic vesicles concentrated with histochemically reactive, or "free", zinc (Beaulieu et al., 1992). This synaptic zinc is co-released with glutamate in an activity-dependent manner (Assaf and Chung, 1984; Qian and Noebels, 2005) and is a potent neuromodulator (see Nakashima and Dyck, 2009). Physiologically relevant concentrations of synaptic zinc can inhibit NMDA receptor activity in a concentration- and subunit-specific manner (Westbrook and Mayer, 1987; Christine and Choi, 1990; Chen et al., 1997). The laminar distribution of synaptic zinc within the barrel cortex mirrors the contribution of NMDA receptors to the processing of somatosensory information. That is, layer IV of the barrel cortex is largely devoid of synaptic zinc while layer II/III is densely populated with zincergic terminals (Czupryn and Skangiel-Kramska, 1997; Brown and Dyck, 2004). It has also been demonstrated that the density of zincergic synapses within the barrel cortex is modulated by sensory experience. Sensory deprivation induced by removal of mystacial whiskers results in an

increase in the density of zinc staining throughout the corresponding barrel field (Quaye et al, 1999; Czupryn and Skangiel-Kramska, 2001) that is detectable within hours (Brown and Dyck, 2002). It was further observed that this increase in zinc staining corresponds with and increase in the number and density of zincergic terminals (Nakashima and Dyck, 2010). With these factors taken into consideration, synaptic zinc is positioned to modulate sensory responses within the barrel cortex and may be essential to barrel cortex-dependent behavior.

The ZnT3 KO mouse is a useful model to examine the contribution of synaptic zinc to barrel cortex-dependent behavior. ZnT3 is responsible for sequestering zinc into synaptic vesicles within the cerebral cortex (Palmiter et al., 1996; Cole et al.,1999; Linkous et al., 2007). ZnT3 KO mice are available and lack histochemically reactive zinc within the cortex (Cole et al.,1999). Initial investigations were unable to describe a unique phenotype for ZnT3 KO mice (Cole et al., 2001). However, it has since been revealed that ZnT3 KO mice demonstrate deficiencies in a number of behavioral tasks, including contextual discrimination memory (Sindreu et al., 2011), fear memory (Kodirov et al, 2006; Martel et al., 2010), and pre-senile deficits in spatial memory (Adlard et al., 2010). We propose that the loss of synaptic zinc in ZnT3 KO mice will contribute to deficits in barrel cortex-mediated behavior as well. To test this hypothesis, we examined the performance of ZnT3 KO mice in a mystacial whisker-dependent, texture discrimination task (Wu et al., 2012). Barrel cortex activation was visualized through voltage-sensitive dye (VSD) imaging to identify the spatiotemporal characteristics of cortical activity that may be associated to deficits in the texture discrimination task.

4.3 Methods

4.3.1 Animals and treatment groups

Male ZnT3 $^{-/-}$ (KO) and $^{+/+}$ (WT) mice at the ages of 8 - 10 weeks and 12 months were used for this study. WT mice were obtained from the same breeding stock as the KO mice. All animals were maintained on standard laboratory diet and water *ad libitum* and kept in standard laboratory housing under a 12-hour light/dark cycle for the duration of the experiment. A "whisker-less" group of mice was produced to test the specificity of the texture-discrimination task to the mystacial vibrissae system. Whisker-less KO and whisker-less WT mice were produced, 3-days prior to start of behavioural testing, by carefully removing all of the mystacial vibrissae with tweezers while the mice were under isoflourane anaesthesia (5 % for induction; 1-2 % for whisker removal). All procedures were approved by the Animal Care Committee of the University of Calgary and conform to the guidelines set out by the Canadian Council for Animal Care.

4.3.2 Texture discrimination

Behavioural testing was performed approximately 1 hour after the beginning of the dark cycle. The texture discrimination task was described previously (Chapter 3). Briefly, the mice were first habituated to the testing arena for two consecutive days. During each of the two days, each mouse was allowed to explore the empty, 40 x 40 cm arena for 10 min. The testing day consisted of learning, retention, and testing phases (Fig. 1). During the learning phase, the mouse was placed in the testing arena for 5 min with plaques covered with sandpaper of two identical textures placed at the centre of the arena. The mouse was then held in an empty cage for a retention interval of 5 min. The two objects

in the arena were replaced with a third, identical object as well as a novel plaque overed with sandpaper of a different texture. The mouse was then returned to the testing arena for 3 min. The roughness of the textures used was sorted such that an equal number of mice was presented with a novel texture that was smoother than the familiar texture and vice versa. The testing arena, textured plaques, and transport cage were cleaned with 70 % ethanol between each testing session and between each animal to mask olfactory cues.

The amount of time mice spent investigating the textures during the learning phase was interpreted as a measure of general exploration activity. The discrimination measure was calculated as the percentage of time mice spent investigating the novel texture versus the familiar texture during the testing phase. Investigation was defined as directing the nose towards the texture with a distance of less than 2 cm from the nose to the texture or touching the nose to the texture. Resting, grooming, and digging next to, or sitting on, the texture was not considered as investigation. Mice that explored only one of the two textures during the testing phase or had a total exploration time less than 2 sec during either of the two phases were excluded from the study for lack of adequate exploratory activity. The difference between the average particle diameters of the familiar and novel textures was varied to determine the threshold at which discrimination could be made. One-sample t-tests against a chance level of 50 % were used to determine whether performance of the discrimination task was significantly better than chance.

To determine if other inherent behavioural deficits in the ZnT3 KO mice affected performance in the texture discrimination task, ZnT3 KO mice were tested on the standard novel object preference task (Ennaceur and Delacour, 1988) as well. The discrimination targets used in the standard novel object preference task consist of

porcelain or glass figurines roughly 4 x 4 x 4 cm in size, with varying shapes, textures, and colours.

Figure 4-13: Schematic of the discrimination tasks.

Top row: the standard novel object preference task; Bottom row: texture discrimination task; a, a', a": 3 identical objects; b: novel object of a different shape, colour, and texture to a"; A, A', and A": 3 identical textures; B: novel texture with a different texture to A".

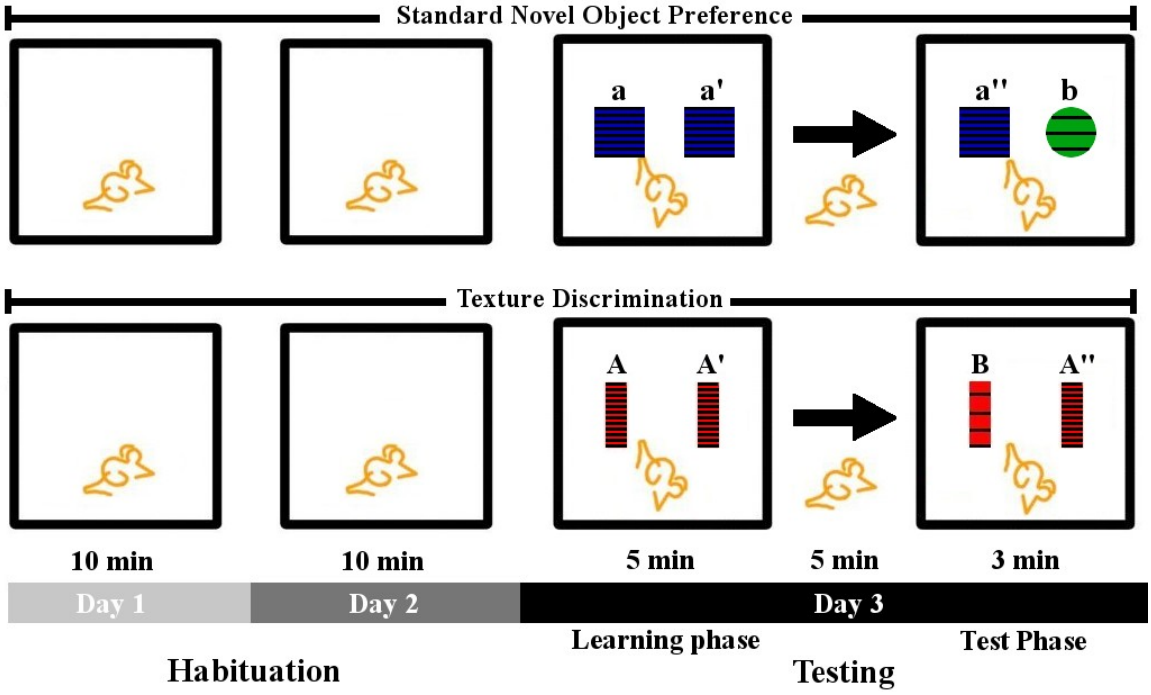
Standard Novel Object Preference
a
a'
a''
b
Texture Discrimination
A
A'
B
A''
10 min
10 min
5 min
5 min
3 min
Day 1
Day 2
Day 3
Learning phase
Test Phase
Habituation
Testing

4.3.3 Voltage Sensitive Dye (VSD) Imaging

For *in vivo* VSD imaging, mice were anaesthetized with isoflourane (5 % in oxygen for induction; 3 % for surgery; 1.0-1.5% for dye incubation and imaging). A custom-made metallic head plate was affixed to the exposed skull with instant glue. Dental cement was used to seal the contact between the skull and head plate and create a well approximately 1 mm deep to retain artificial cerebral spinal fluid (ACSF) and dye. A craniotomy window approximately 4 mm in diameter, centered on the C2 barrel (approximately 1.15 mm posterior and 3 mm lateral to Bregma), was created with a high-speed drill. The cisterna magna was punctured with a 27 gauge needle to relieve pressure in preparation for craniotomy. The skull and dura were carefully removed under ACSF (135.0 mM NaCl, 5.4 mM KCl, 1.8 mM $CaCl_2$, 1.0 mM $MgCl_2$, and 5.0 mM Na-HEPES) to expose the barrel cortex. Voltage-sensitive dye RH-1692 (0.5 mg/ml in ACSF; Optical Imaging, Rehovot, Israel) was applied to the exposed barrel cortex for 90 min. The blue, RH-1692, VSD dye used in has an absorption spectrum far away from the peak of haemoglobin absorption, and, therefore, is not affected by heartbeat- and other blood circulation-induced artefact (Shoham et al., 1999). Fresh dye was reapplied every 15 min. Penetration of the voltage-sensitive dye has been reported to extend past layers II/III and allow for the imaging of voltage-sensitive dye fluorescence in layers II/III with subcolumnar resolution (Ferezou et al., 2006). After dye incubation, excess dye was washed out with ACSF. The exposed brain was covered with agarose (low melt; 1.3 % in ACSF) and sealed with a custom-cut glass cover (Fig. 4-2).

Figure 4-14: Schematic of *in vivo* voltage-sensitive dye imaging setup.

.Dotted box: representation of craniotomy window over the mouse barrel cortex. The piezoelectric stimulator, light source, and high speed camera were controlled by a computer running data acquisition software (Brain Vision Analyser version 1201; SciMedia, California, USA).

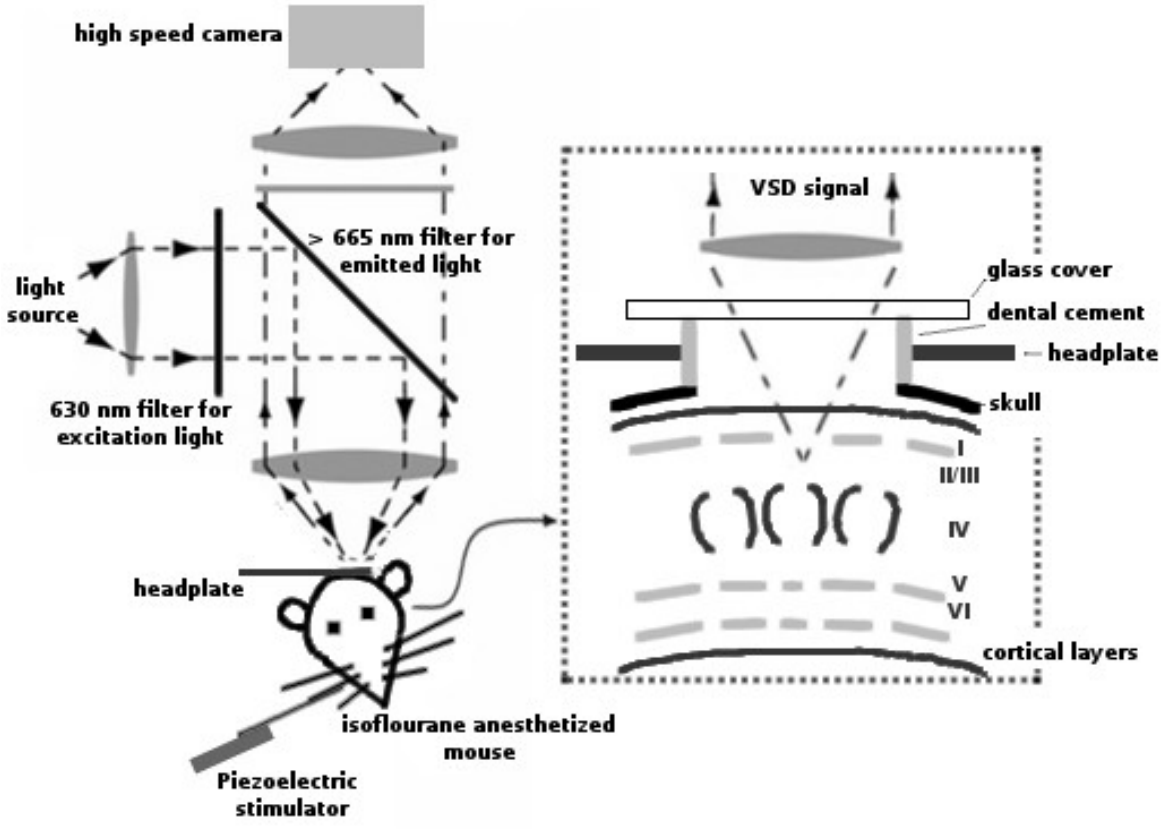
high speed camera
> 665 nm filter for emitted light
light source
630 nm filter for excitation light
headplate
isoflourane anesthetized mouse
Piezoelectric stimulator
VSD signal
glass cover
dental cement
headplate
skull
I
II/III
IV
V
VI
cortical layers

VSD imaging data were collected with a high speed CCD camera (MICAM02-HR; SciMedia, California, USA). VSD was excited with 630 nm wavelength light (MHAB-150W; Moritex, Tokyo, Japan) focused approximately 200 μm below the surface (Planapo 1.0 x and 0.63 x lenses; Leica, Solms, Germany). Excitation light at 630 nm has been reported to penetrate cortical layers I, II, and III (Ferezou et al., 2006). Cortical response was measured as VSD emission at wavelengths > 665 nm. Image frames 4 ms in duration were captured 200 ms prior to, and 800 ms after, a single 2 ms mechanical deflection of the contralateral C2 mystacial whisker with a piezoelectric actuator (approximately 200 μm amplitude, 2 mm away from the base of the whisker; CMBP05 piezo bender actuator; Noliac, Kvistgaard, Denmark). The response to whisker stimulation was taken as the average of 15 stimulation trials. To account for photo-bleaching of the dye, each trial consisted of the difference in evoked cortical response between a stimulation trial and a null stimulation trial. The amplitude of measured responses were expressed as the percentage change in fluorescence signal ($\Delta F/F_o$), where the signal recorded during each frame after the stimulation was divided by the average of the signal recorded during the 200 ms prior to the stimulation. The barrel fields were located by means of stereotaxic co-ordinates and comparison with post-mortem histochemical localization (Cresyl Violet staining of tangential sections of the barrel cortex).

Peak amplitude of VSD signal was represented as the max percentage change in fluorescence signal from baseline ($\Delta F/F_o$) across the duration of recording for each

mouse. Response time, or initialization of stimulation-evoked response, was calculated as the time where percentage change in fluorescence signal increased above 10 % of peak amplitude. Time to reach peak amplitude was represented as the duration from stimulation to peak amplitude of VSD signal. Duration of activation was represented as the duration where the VSD signal is above 50 % of peak amplitude. Lastly, area of activation was represented as the maximum area where the VSD signal is above 50 % of peak amplitude.

4.4 Results

4.4.1 Texture Discrimination

ZnT3 WT ($t_{(5)} = 4.72$, $p < 0.01$) and KO mice ($t_{(6)} = 10.17$, $p < 0.001$) at 2-months-of-age were both able to perform the standard novel object preference task (Fig. 4-3A). WT mice were also able to discriminate between two textures with different roughness in the texture discrimination task (difference in average particle diameter = 215 μm; average particle diameter of the 2 textures were 350 μm and 135 μm, as well as 270 μm and 55 μm; $t_{(8)} = 4.44$, $p < 0.002$). ZnT3 KO mice, however, failed to discriminate between textures (215 μm; $t_{(6)} = -0.40$, $p = 0.70$). Bilateral removal of mystacial vibrissae did not affect the ability of WT ($t_{(4)} = 5.53$, $p < 0.01$) and KO ($t_{(6)} = 2.80$, $p < 0.04$) to perform the standard novel object preference task (Fig. 4-2B). However, whisker-less WT mice lost the ability to discriminate between textures (215 μm; $t_{(5)} = 0.65$, $p = 0.54$). Whisker-less KO mice performed no differently than whisker-intact KO mice at the texture discrimination task (215 μm; $t_{(6)} = 1.60$, $p = 0.16$).

Age did not have a significant impact on texture discrimination (Fig. 4-3C). One year old ZnT3 WT mice remained able to perform the novel object preference task ($t_{(5)}$ = 4.78, $p < 0.005$) as well as discriminate between textures (215 μm ; $t_{(6)} = 4.88$, $p < 0.003$). One year old ZnT3 KO mice also remained able to perform the novel object preference task ($t_{(5)} = 5.15$, $p < 0.004$) and unable to discriminate between textures (215 μm ; $t_{(8)}$ = -.37, $p = 0.72$).

ZnT3 KO mice were not able to discriminate between textures separated by average particle diameters of 215 μm (reported above) or 280 μm ($t_{(6)} = 0.91$, $p = 0.40$; Fig. 4-4). The KO mice were able to discriminate between textures when the separation between average particle diameters was increased to 310 μm ($t_{(5)} = 6.37$, $p < 0.01$) and 360 μm ($t_{(8)} = 2.32$, $p < 0.05$). ZnT3 WT mice were able to discriminate between textures separated by as little as 25 μm in average particle diameter ($t_{(5)} = 5.30$, $p < 0.01$).

Five mice were excluded from analyses for a lack of exploration activity. General exploratory activity was not different ($t_{(4)} = 0.09$, $p = 0.93$) between ZnT3 WT (n = 39; 6.81% ± 4.19%) and KO (n = 44; 6.89% ± 3.71) mice.

Figure 4-15: Percentage of testing time spent investigating the novel object.

Both 2 month- and 1 year-old ZnT3 KO mice were able to perform the standard novel object preference task, but were unable to discriminate between novel and familiar textures. The ability of WT mice to discriminate between textures was dependent on intact mystacial vibrissae. A: 2 month-old mice with intact whiskers; B: 2 month-old mice with bilateral removal of mystacial vibrissae; C: 1 year-old mice with intact whiskers; Textured surfaces: average particle diameter = 215 μm; Dashed line: chance level (50 %); Error bars: standard error of the mean; Asterisks: significance *vs* chance at $p < 0.05$; n = 6-9.

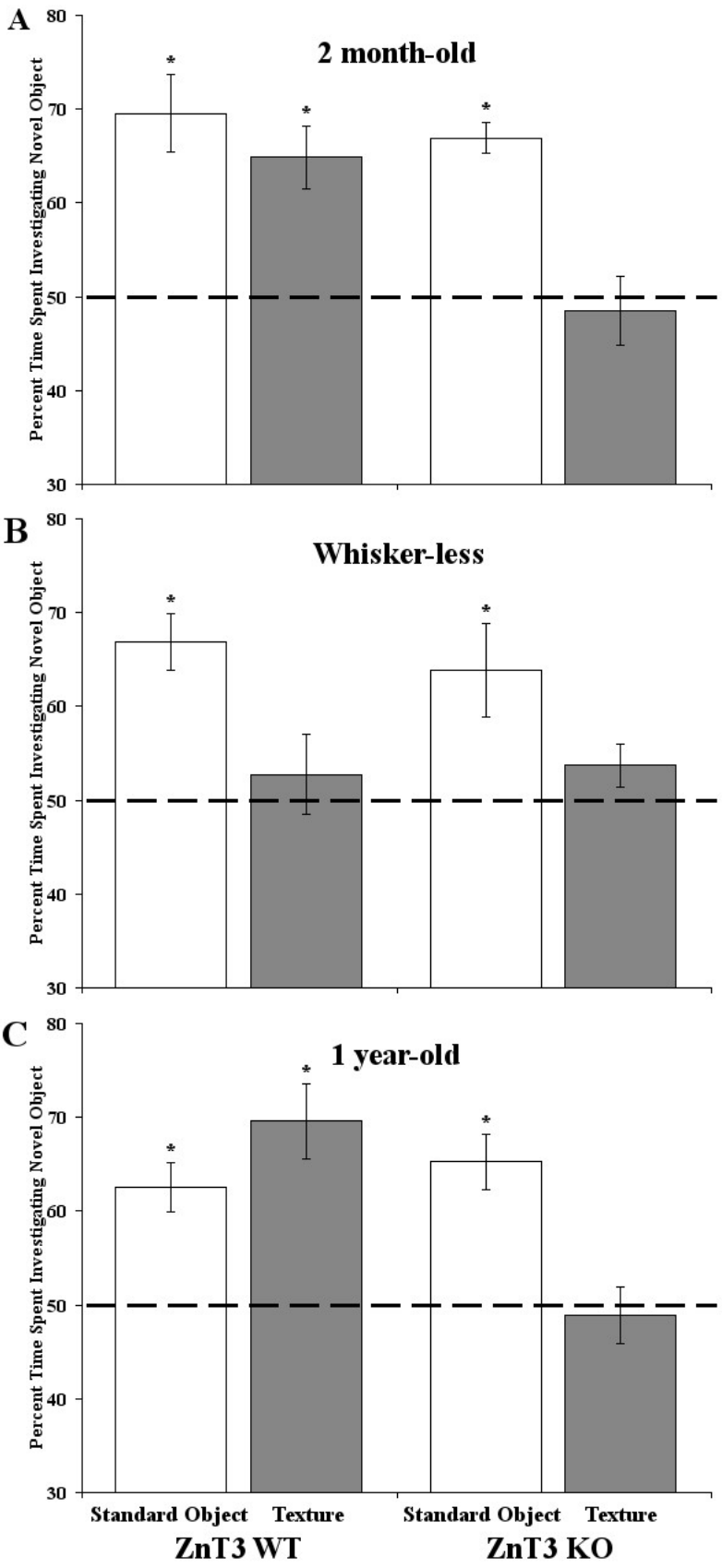
A
2 month-old
B
Whisker-less
C
1 year-old
Percent Time Spent Investigating Novel Object
80
70
60
50
40
30
*
Standard Object
Texture
Standard Object
Texture
ZnT3 WT
ZnT3 KO

Figure 4-16: Threshold for texture discrimination.

ZnT3 WT mice were able to discriminate between textures separated by 25 μm in average particle diameter. ZnT3 KO mice were only able to discriminate between textures more than 300 μm apart. Dashed line: chance level (50%); Error bars: standard error of the mean; Asterisks: significance *vs* chanceat $p < 0.05$; $n = 6\text{-}9$.

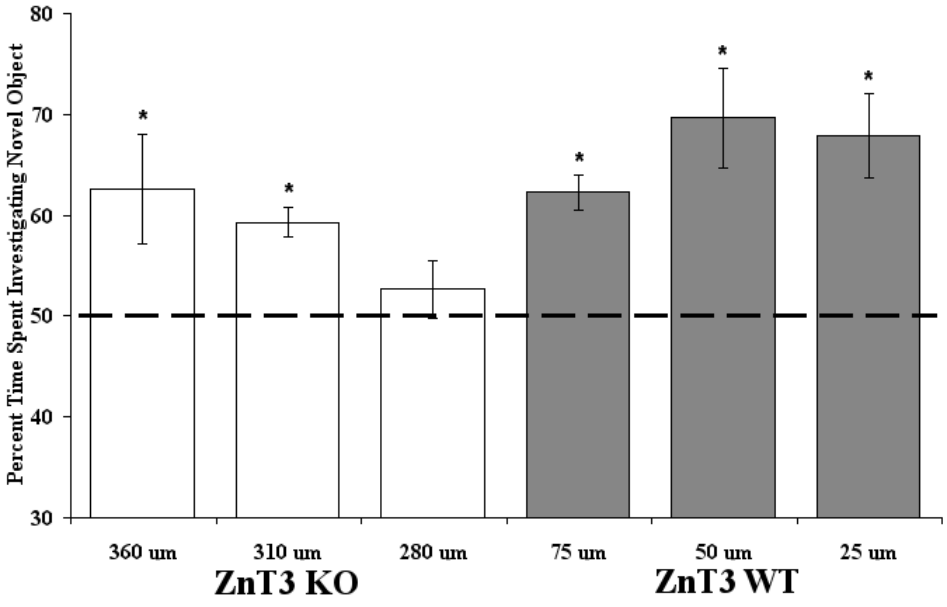
Percent Time Spent Investigating Novel Object
80
70
60
50
40
30
*
*
*
*
*
360 um
310 um
280 um
75 um
50 um
25 um
ZnT3 KO
ZnT3 WT

4.4.2 VSD Imaging

The spatiotemporal characteristics of stimulation-evoked barrel cortex activity were examined in ZnT3 KO mice (Fig. 4-5A). A number of the properties of cortical response were not different between ZnT3 WT and KO mice. Mechanical deflection of contralateral C2 whisker initiated activity within the C2 barrel field that was detectable following a 16-20 ms delay. The cortical response spread across the barrel cortex and reached peak amplitude within 50 ms of whisker deflection (Fig. 4-5B). There were no significant differences in the initialization (time to reach 10 % of peak amplitude), peak amplitude (maximum amplitude of VSD signal), and area (maximum area where activation is above 50 % of peak amplitude) of cortical responses between ZnT3 WT and KO mice.

The duration of sensory evoked cortical activity within the principal barrel field (duration of activity above 50 % of peak amplitude) was significantly longer in ZnT3 KO mice ($t_{(4)} = 2.12$, $p < 0.04$; Fig. 4-5C, D). Evoked cortical response dropped below 50 % of maximum response amplitude within approximately 150 ms of initial activation in ZnT3 WT mice. In KO mice, cortical response within the C2 barrel field remained above 50 % of peak amplitude approximately 100 ms longer.

Figure 4-17: VSD image of stimulation-evoked cortical response in the barrel cortex.

A: Comparison of the cortical response to C2 whisker deflection between ZnT3 WT and ZnT3 KO mice. Images consist of averaged data from 15 stimulation- versus null-stimulation sweeps for 2 representative samples. Outline in the first panel: barrel fields; Black outline: C row barrel fields; Shaded black outline: C2 barrel field;

B: Cortical response to C2 whisker deflection within C row barrel fields across time. Responses were normalized to the peak amplitude evoked in ZnT3 WT mice and averaged (n = 5) across row C. Linescan plot (time on the y-axis and space on the x-axis) was used here to visualize the propagation of cortical response across C row barrel fields;

C: Cortical response to C2 whisker deflection within the C2 barrel field only;

D: Quantified comparisons of cortical response characteristics within the C2 barrel field between ZnT3 WT and KO mice. Area of activation plot consists of data from the entire VSD imaging field. Error bars: standard error of the mean.

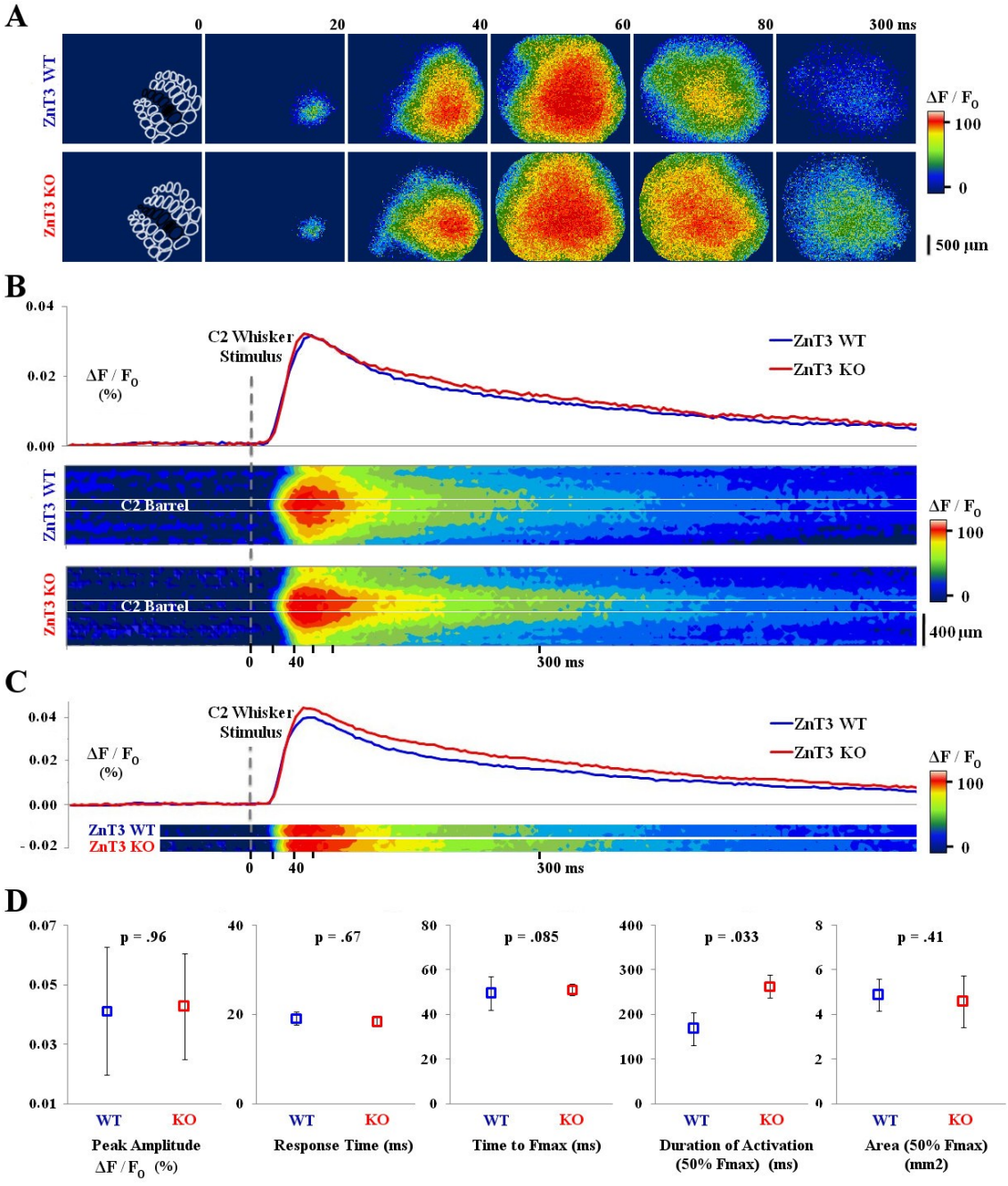
A
0
20
40
60
80
300 ms
ZnT3 WT
ZnT3 KO
ΔF / F0
100
0
500 µm
B
0.04
0.02
0.00
C2 Whisker Stimulus
ΔF / F0 (%)
ZnT3 WT
ZnT3 KO
C2 Barrel
C2 Barrel
400 µm
0
40
300 ms
C
0.04
0.02
0.00
- 0.02
C2 Whisker Stimulus
ΔF / F0 (%)
ZnT3 WT
ZnT3 KO
0
40
300 ms
D
p = .96
p = .67
p = .085
p = .033
p = .41
WT
KO
Peak Amplitude ΔF / F0 (%)
Response Time (ms)
Time to Fmax (ms)
Duration of Activation (50% Fmax) (ms)
Area (50% Fmax) (mm2)

4.5 Discussion

In the present experiment, we sought to examine whether the loss of synaptic zinc in the barrel cortex of ZnT3 KO mice contributes to deficits in whisker-dependent texture discrimination. Prior to interpreting the performance of ZnT3 KO mice in the texture discrimination task, we must first account for the possibility of false negative results. In addition to the cerebral cortex, the amygdala and hippocampus are also densely populated with synaptic zinc (Brown and Dyck, 2004; Shen et al., 2007). The loss of synaptic zinc in ZnT3 KO mice contributes to deficits in contextual fear memory (Kodirov et al., 2006; Kadeda et al., 2010) and premature deterioration in spatial learning (Adlard et al., 2010). It is therefore necessary, when measuring barrel cortex function in ZnT3 KO mice, to utilize a test that is specific to the vibrissal sensory system, relies minimally on unaltered amygdaloid and hippocampal function, and is not affected by age. The texture discrimination task used in the present experiment is minimally stressful, requires no food or water motivation, and is independent of hippocampal function (Hammond, 2004). In further support of the specificity and validity of this texture discrimination task, we observed that the levels of explorative activity were identical between ZnT3 WT and KO mice. KO mice were also able to discriminate between familiar and novel objects in the standard novel object preference task regardless of age. Therefore, deficits reported in ZnT3 KO mice were specific for the vibrissal system and not secondary to motivation, memory, or aging effects.

We demonstrated that ZnT3 WT mice were able to discriminate between textures separated by a difference in average particle diameter as low as 25 μm. Comparable

levels of sensitivity were reported previously in C57BL/6 mice (Wu et al., 2012) and observed in rats as well (Carvell and Simons, 1990). This level of whisker-dependent texture sensitivity was notably absent in ZnT3 KO mice. ZnT3 KO mice could not differentiate between textures with less than 300 μm difference in average particle diameter. This observation suggests that synaptic zinc participates in regulating barrel cortex-mediated behaviour.

Two caveats to this interpretation of the results must be considered. The first is that the absence of synaptic zinc from birth in ZnT3 KO mice may affect the development of the barrel cortex. The deficits observed in this study may be a phenotype of altered barrel cortex development and not a direct consequence of the loss of synaptic zinc in the barrel cortex *at the time of testing*. Further studies that manipulate the levels of synaptic zinc within the barrel cortex *in vivo*, such as through microdialysis of zinc chelators, are required to directly delineate the contribution of synaptic zinc to barrel cortex-mediated behaviour. However, the deficit in whisker-dependent texture discrimination observed in ZnT3 KO mice was one of decreased sensitivity and not the complete loss of the ability. If barrel cortex organization is grossly altered in ZnT3 KO mice, more overt effects on barrel cortex-dependent behaviour might be expected (Guic-Robles et al., 1992). We have also found no reliable differences between the barrel cortex maps of ZnT3 WT and KO mice. Therefore, it is unlikely that the development of the barrel cortex is compromised in ZnT3 KO mice.

The second caveat is that the loss of synaptic zinc in the ZnT3 KO mouse is not restricted to the cortex. Although the thalamus is largely devoid of synaptic zinc, ZnT3 is

expressed in the follicles of mystacial whiskers, neurons of the spinal sensory ganglion, and the facial nucleus of the brain stem (Wang, 2002; Wang, 2003). The loss of synaptic zinc in components of the whisker somatosensory pathway caudal to the barrel cortex may contribute to observed deficits in whisker-dependent texture discrimination. However, neither zinc nor the zinc chelator TPEN affects the firing pattern of mechanosensory nerve terminals in isolated rat sinus hair preparation (Cahusac et al., 2005). Qualitative observations suggested that whisking behaviour was unaltered in ZnT3 KO animals and we were also unable to detect synaptic zinc within the mystacial whisker pads of ZnT3 WT mice (Fig. 4-6). Lastly, VSD imaging results revealed that the timing and amplitude of stimulation-evoked cortical responses in layers II/III of the barrel cortex were not different between ZnT3 KO and WT mice, which suggests that sensory input was unaltered. The values recorded in the present experiment are also comparable to those reported in studies that visualized barrel cortex activity through VSD imaging during active whisker touch (Ferezou et al., 2006) or through electrophysiological recordings following single whisker deflection (O'Connor et al., 2010). Although involvement of the sensory pathway upstream of the sensory cortex cannot be completely ruled out, it is highly likely that the deficits observed in ZnT3 KO mice are cortical in origin. Further studies, such as high speed video analyses of whisking behaviour and electrophysiological recording of whisker sensory driving responses in associated brainstem and thalamic neurons, are required to further support this conclusion.

Figure 4-18: Tangental 20 µm section of the whisker pad stained for Nissl substance.

(A) and synaptic zinc (B). Zinc staining was light and restricted to the periphery of the vibrissa follicle. A: Creysl Violet stained section; B: Zinc stained section using a modified selenium autometallographic staining procedure ; Arrows: vibrissa follicles.

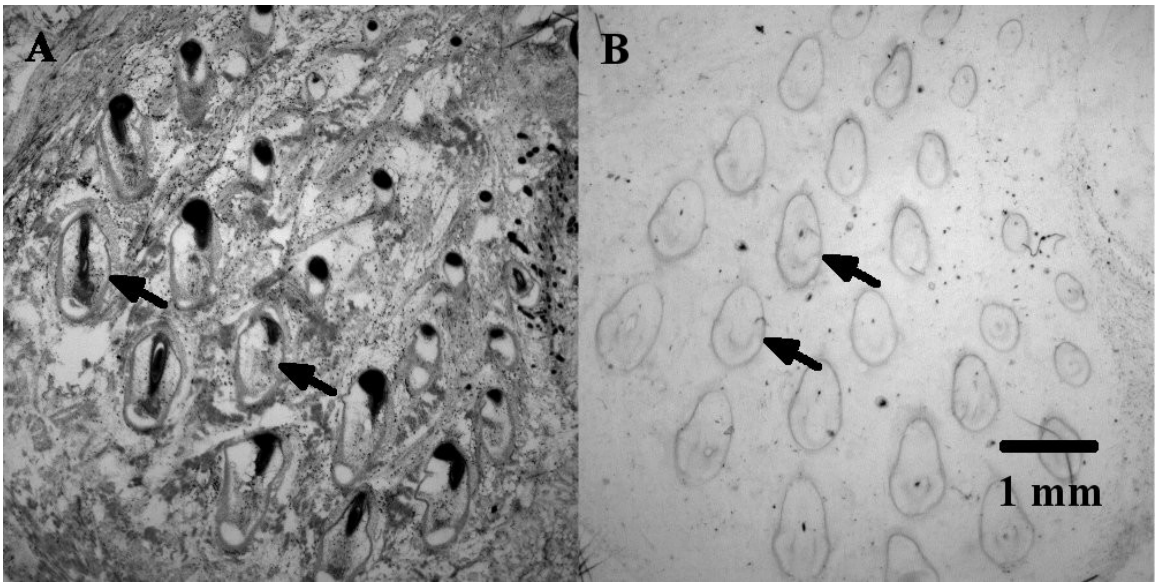
A
B
1 mm

The barrel cortex is necessary for texture discrimination (Guic-Robles et al., 1992; Kleinfeld et al., 2006). The level of sensitivity in texture discrimination depends on the integration of sensory information from multiple whiskers (Armstrong-James, 1993). Rats with one spared whisker retain the ability to discriminate between textures but are outperformed by rats with 2 or more whiskers in the level of sensitivity to which this discrimination can be made. The loss of synaptic zinc in ZnT3 KO mice decreased texture discrimination sensitivity but did not abolish the ability. There is also evidence to suggest that removal of a subset of whiskers in mice abolishes texture discrimination ability (Appendix A). These results sustain the proposal that synaptic zinc participates in the integration of sensory input from multiple whiskers.

Layer II/III of the barrel cortex is populated by inter-barrel projections. Propagation of sensory driven responses across the barrel cortex initiates in layers II/III and is dependent on NMDA receptors (Armstrong-James et al., 1993; Cahusac et al., 2005). Pharmacologically inhibiting NMDA receptors disrupts the transmission and integration of sensory information within the barrel cortex (Armstrong-James et al., 1992). There is a high density of zincergic terminals in layers II/III of the barrel cortex (Brown and Dyck, 2004). Synaptic zinc is also a potent inhibitor of NMDA receptors (Chen et al., 1997; Paoletti et al., 1997). Therefore, synaptic zinc is positioned to modulate the propagation of NMDA receptor-dependent sensory driven responses in layers II/III of the barrel cortex and regulate the integration of somatosensory information between whiskers. The VSD imaging data recorded from layers II/III of the barrel cortex (Fig. 4-4) supports this hypothesis. It was observed that the duration of the cortical activity evoked through a single deflection of the whisker is prolonged within ZnT3 KO

mice. This suggests that the temporal resolution of stimulation-evoked activity within the barrel cortex of ZnT3 KO mice is decreased, potentially reducing the amount of information that can be extracted and integration from somatosensory input.

A major consideration of the VSD imaging results is that the VSD response is not restricted to reflect neuronal activity. As with other amphiphilic dyes, the VSD used in this study, RH-1692, does not distinguish between neuron and glia; dye molecule present in the tissue are bound to neuronal membrane, glial membrane, as well as remain in extracellular matrix (Shoham et al., 1999). Furthermore, VSD signal reflects all change in membrane potential, including both depolarizing and hyperpolarizing synaptic potentials. Since dendrites present a large membrane area when compared to axonal membrane, only a fraction of the VSD signal may originate from neuronal activity (Shoham et al., 1999). Although dividing the vibrissa stimulation-evoke VSD signal by the average of the baseline VSD signal recorded prior to stimulation enhances the signal-to-noise ratio, change in membrane potential because of EPSPs and IPSPs following stimulation can still contribute to the observed VSD response. As such, the prolonged, whisker deflection-induced cortical response reported in this study may reflect a subthreshold change in neuronal membrane potential, and not neuronal activity. Electrophysiological recording from single neurons are required to confirm the conclusion drawn from the VSD imaging results. Nonetheless, it was demonstrated in this study that there is a significant alteration in vibrissa stimulation-evoked VSD response within ZnT3 KO mice.

NMDA receptor expression within the cerebral cortex is dominated by those containing either NR2A or NR2B subunits (Watanabe et al., 1992). Synaptic zinc is a

high affinity (5 - 80 nM) inhibitor of NR2A, while NR2B containing receptors are inhibited by higher (4 – 79 μM) levels of zinc (William, 1996). The concentration of circulating extracellular zinc is estimated to be sufficient to induce tonic inhibition of NR2A-containing receptors (Palmiter et al., 1996), while active release of synaptic zinc may provide phasic modulation of NR2B-containing receptors (see Nakashima and Dyck, 2009). The absence of synaptic zinc in ZnT3 KO mice could result in a lowered threshold of activation for NMDA receptors in layers II/III of the barrel cortex and finally manifest into prolonged stimulation-evoked activity, decreased complexity in somatosensory integration, and reduced sensitivity in texture discrimination. Further studies that investigate the subunit-specific contribution of NMDA receptors to whisker-dependent texture discrimination are required to test this hypothesis.

The association between synaptic zinc and barrel cortex plasticity has been robustly established across multiple laboratories in the past decade (See Nakashima and Dyck, 2009). We have provided evidence that synaptic zinc also contributes to barrel cortex-dependent behaviour. The present experiment sustains the assumption that synaptic zinc regulates the integration of vibrissal sensory information in the barrel cortex and is necessary for fine whisker-mediated texture discrimination.

Chapter 5: General Discussion

5.1 Main findings

The experiments reported in this thesis have provided additional evidence on the role of synaptic zinc as a neuromodulator in the cerebral cortex. In Chapter 2, it was shown that the laminar distribution of synaptic zinc in the visual cortex of mice was mediated by visual experience. Increases in synaptic zinc levels within the primary visual cortex were detectable following 24 hours to 3 months of monocular deprivation. This experience-dependent regulation of synaptic zinc levels is dynamic and lamina-specific. Short-term deprivation resulted in a marked increase of synaptic zinc levels in layer IV of the deprived-eye domains, while long-term deprivation resulted in an increase of synaptic zinc within layers II/III, V, and VI. These findings are consistent with observations made in the visual cortex of cats and monkeys and the barrel cortex of mice. Further, preliminary findings from a pilot study that manipulated the acoustic environment suggest that synaptic zinc levels in the auditory cortex of mice are mediated by auditory experience as well.

In Chapter 3, a novel whisker-dependent texture discrimination task was described. Currently available models and techniques do not allow for efficient and targeted manipulation of synaptic zinc levels *in vivo* without affecting zincergic signalling systemically. To investigate the role of synaptic zinc within the barrel cortex to the production of barrel cortex-dependent behaviour, the sensitivity of the employed behavioural test should be maximally restricted to barrel cortex function and require minimal involvement of other systems. Texture and roughness discrimination by vibrissae requires intact barrel cortex function (Guic-Robles et al., 1988). It was demonstrated in

Chapter 3 that the described novel texture discrimination task requires intact mystacial vibrissae and that visual and olfactory cues were not sufficient to replace somatosensory cues from the vibrissae. The task itself is minimally stressful, does not require additional motivation paradigms to be employed, and can be performed without intact hippocampi. In Chapter 4, the texture discrimination task was used to investigate barrel cortex function in ZnT3 KO mice. The ZnT3 KO mouse remains the most direct model available to study the effect of the removal of synaptic zinc in the cortex. However, ZnT3 KO mice have been found to display behavioural deficits attributable to loss of synaptic zinc in the hippocampus and the amygdala (Martel et al., 2010; Sindreu et al., 2011). The development of the barrel cortex dependent texture discrimination task allowed for the examination of barrel cortex function in ZnT3 KO mice with minimal contamination from the loss of synaptic zinc in other cortical structures.

It was demonstrated in Chapter 4 that ZnT3 KO mice were not able to discriminate between textures with the same degree of sensitivity as ZnT3 WT and C57BL/6 mice. This decrease in the sensitivity of barrel cortex-mediated texture discrimination was observed in both young (3 months) and older (6 months) ZnT3 KO mice. It is also important to note that the deficit observed in ZnT3 KO mice was a decrease in sensitivity and not an inability to discriminate between textures through vibrissal somatosensation. Therefore, early-onset senescence-related and hippocampus-dependent deficits in spatial memory, reported in ZnT3 KO mice in other studies, did not play a role in the deficit in texture discrimination observed here. *In vivo* VSD imaging data further demonstrated that vibrissal stimulation-evoked propagation of cortical activity in the barrel cortex of ZnT3 KO is altered. The duration of the

propagation of evoked activity in the barrel cortex was increased in ZnT3 KO mice; however, the initiation, amplitude, and area of propagation of evoked barrel cortex activity were not different between ZnT3 KO and WT mice.

5.2 Considerations

5.2.1 Zinc histochemistry

Autometallographic staining remains the most direct method to histochemically visualize vesicular zinc. There are, however, two notable caveats to using this method to measure synaptic zinc density. Firstly, the overall intensity of staining cannot be precisely controlled. The methodological nuances for zinc staining that fail to control for individual differences in the subjects and require subjective input from the experimenter were discussed in detail within Chapter 2. Briefly, autometallographic staining of vesicular zinc relies on systemic circulation of selenium within the subject, and development of the zinc-selenium crystals requires subjective determination of the end point. As such, zinc staining intensities may not be directly comparable between subjects and, in the most extreme examples, even adjacent sections of tissue from the same animal that are stained in different batches may not match each other in overall zinc staining intensity. The latter discrepancy can be compensated for by normalizing the staining intensity readings, between sections, to the readings from a neutral reference structure. However, no appropriate candidates for the neutral reference exist since the reference structure must be present within all relevant sections of tissue and must be proven to have a homogeneous distribution of vesicular zinc. Between-subject comparisons could not benefit from the use of a reference, either, since it cannot be easily determined whether the experimental manipulation has affected zinc density within the reference structure. Under these

circumstances, within-subject comparisons of relative changes in zinc staining intensity between structures on the same section will most accurately represent manipulation-induced differences. Therefore, comparing measurements of vesicular zinc density derived from zinc histochemistry is most relevant in compartmentalized systems, where adjacent domains that perform similar functions can be individually manipulated. The isomorphically organized vibrissae-barrel field system in the barrel cortex and ocular dominance fields in the visual cortex are examples. Even within these well-characterized systems, the experimenter must be cautious. The left and right binocular visual fields in mice receive disproportionate amounts of visual input from both eyes such that monocular deprivation-induced changes in zinc staining intensities are difficult to interpret. There is also some evidence to suggest that regulation of synaptic zinc levels in the barrel cortex is not completely compartmentalized (Appendix B).

The second caveat is that autometallographic staining only identifies histochemically reactive zinc that is within vesicles. Zinc loosely bound to metallothioneins and free zinc in the cytoplasm and extracellular space are lost during tissue preparation and staining. Histochemical observations are not sufficient to correlate vesicular zinc levels with zinc release. The majority of evidence, including electron micrographic observations of an increase in the ratio of zincergic terminals in the barrel cortex following sensory deprivation, suggest that zinc *is* released from these synaptic vesicles and that sensory deprivation increases the amount of zinc released (Section 1.1.1). Although it is very likely, imaging zinc release *in vivo* or *in vitro* with techniques such as zinc fluorescence imaging is required to confirm that there is an increase in zinc

release that accompanies the sensory deprivation-induced upregulation of vesicular zinc levels.

5.2.2 ZnT3 knockout mice

ZnT3 KO mice provide the opportunity to investigate the effects of a complete absence of synaptic zinc on nervous system function. Where *mocha* and SAMP10 strains of mice have reduced levels of synaptic zinc, other physiological processes unrelated to synaptic zinc are affected as well (see Section 1.5.3). The advantage to the genetic deletion of the ZnT3 gene is specificity in targeting synaptic zinc. Functional deficits observed in ZnT3 KO mice are more directly attributable to the loss of synaptic zinc. However, since the ZnT3 gene is inactive from conception in ZnT3 KO mice, the possibility that the absence of synaptic zinc may affect the neurodevelopment of ZnT3 KO mice must be considered.

Initial examination of the ZnT3 KO mouse failed to record any overt behaviourally or physiologically mutant phenotypes (Cole et al., 1999). Although this is not proof that neural development is not altered in ZnT3 KO mice, the absence of obvious behavioural deficits does suggest that the structure of the nervous system in ZnT3 KO mice is not systemically or grossly different from that in WT animals. Early electrophysiological examination also reported no gross alterations in function. Evoked field-potential response, paired-pulse evoked responses, NMDA or 'non-NMDA' receptor-mediated postsynaptic responses, and $GABA_A$ or $GABA_B$ receptor-mediated responses within the mossy fibre synapse of ZnT3 KO mice were not different in WT mice (Lopantsev et al., 2003). The only difference observed in the otherwise synaptic zinc-rich mossy fibre terminals was the attenuation of $GABA_A$-mediated inhibitory

postsynaptic potentials during tetanic stimulation. More recent experiments revealed deficits in spatial learning, contextual fear memory, and early senescence-related learning deficits (Adlard et al., 2010; Martel et al., 2010; Sindreu et al., 2011). It was also found that presynaptic mossy fibre-LTP is abolished in ZnT3 KO mice (Pan et al., 2011). These results suggest that the absence of synaptic zinc in ZnT3 KO mice have very targeted effects that can be divergent, depending on the region of the brain and specific attribute of function examined.

Although the possibility that the deficit in texture-discrimination observed in Chapter 4 is caused by altered development of the barrel cortex in ZnT3 KO mice cannot be completely ruled out, several lines of evidences suggest otherwise. Anatomically, barrel cortex map development is not altered in ZnT3 KO mice. On the behavioural level, the deficit observed in ZnT3 KO was one of loss of spatial acuity, and not loss of discrimination altogether. Lastly, stimulation-evoked activity within the superficial layers of the barrel cortex was not grossly different between ZnT3 KO and WT mice. These observations suggest that the ZnT3 KO mouse is a valid model with which to examine the impact of the loss of synaptic zinc on barrel cortex function. Regardless of the caveats inherent in transgenic KO models, the ZnT3 KO mice provide important insight into synaptic zinc function. Subsequent studies that selectively reintroduce synaptic zinc to ZnT3 KO miceor chelate synaptic zinc in control mice, through microinfusion, are required to conclusively demonstrate that the behavioural deficits and alteration in barrel cortex neurotransmission reported in this thesis are directly associated with the loss of synaptic zinc in the barrel cortex.

5.3 Role of zinc in modulating neurotransmission

5.3.1 Experience dependent plasticity

It is apparent that synaptic zinc contributes to the modulation of sensory processing within the cerebral cortex. Together with the observations made within this thesis, experience-dependent alteration of the concentration and laminar distribution pattern of synaptic zinc in the primary sensory cortex have been described in four different laboratory animals and across two different sensory systems. deprivation of sensory input corresponds with increase in synaptic zinc levels within the deprived domains of the primary sensory cortex. There is further evidence that synaptic zinc levels in the auditory cortex of mice is altered by change in the auditory sensory environment (Appendix C).

It is unlikely that this increase in synaptic zinc levels is an epiphenomenon of decreased signalling. The most dramatic increase in synaptic zinc levels was observed in layer IV of the deprived primary sensory cortical domains. Throughout the cerebral cortex, and particularly prominent in the primary sensory cortices, layer IV of naive animals is characteristically devoid of synaptic zinc. Build-up of synaptic zinc due to decrease in activation and release cannot explain the increase in synaptic zinc density here. Moreover, the increase in synaptic zinc density consists of an increase in the number and ratio of zincergic synapses throughout layers II to V of the deprived barrel field (Nakashima and Dyck, 2010). This suggests that novel zincergic synapses were formed, or that synapses previously devoid of zinc come to house synaptic zinc. Either way, synaptic zinc levels are dynamically regulated by sensory input.

This experience-dependent regulation of synaptic zinc levels may be considered as a form of plasticity itself. Since the fundamental function of the nervous system is to constantly integrate sensory information from the changing environment to generate appropriate responses, experience-dependent plasticity can be considered as an extension of natural sensory processing where sensory input is deprived or activated for an extended period of time. The conservative nature of biological systems suggests that neuromodulators that mediate experience-dependent plasticity induced by sensory deprivation are, therefore, also expected to participate in the regulation of neurotransmission under 'normal' control environments. An example is glutamate activation of NMDA receptor. Studies examining the biochemical properties that underlie synaptic plasticity have focused on glutamatergic signalling and postsynaptic activation of NMDA receptors. Well characterized forms of LTP/LTD are dependent on NMDA receptor activation (see Nicoll and Roche, 2013). At the same time, NMDA receptor activation is also crucial for neurotransmission in the barrel cortex under control environments (Armstrong-James et al., 1992, 1993). Whereas the vibrissa-stimulation-evoked responses in layer IV of the barrel cortex is dependent on AMPA receptor activation, propagation of sensory driven responses across layers II/III of the barrel cortex is almost entirely dependent on NMDA receptors (Armstrong-James et al., 1993; Cahusac et al., 2005). The role of synaptic zinc in experience-dependent plasticity can be considered as the extension of the modulation of neurotransmission by synaptic zinc during natural sensory experience.

5.3.2 Sensory processing

The co-localization of zinc with glutamate and its potent regulatory effects on glutamate receptors suggest that synaptic zinc plays a role in the regulation of excitatory neurotransmission. Layers II/III of the cerebral cortex are particularly populated with zincergic terminals that are intracortical in origin, while the primary thalamocortical input layer, layer IV, is devoid of zinc under control environments (Brown and Dyck 2004, 2005). By extension, synaptic zinc may mediate intracortical propagation of excitatory neurotransmission but not the thalamic relay of sensory input into the cortex. Observations made in Chapter 4 support this theory. *In vivo* VSD imaging results suggest that the propagation of stimulation-evoked activity to the superficial layers of the barrel cortex was not impaired in the absence of zinc. The timing of stimulation-evoked activity in layers II/III of the barrel cortex was not different in ZnT3 KO mice. This supports the notion that both thalamocortical input into layer IV of the barrel cortex and propagation of stimulation-evoked activity from layer IV to layer II/III are not regulated by synaptic zinc. The increase in the duration of stimulation-evoked activity observed in ZnT3 KO mice suggests that intercortical propagation of excitatory neurotransmission was altered in the absence of zinc. Intracortical integration of sensory information is required for the sensitivity with which rodents use their mystacial vibrissae to distinguish between textures. A rat with 2 intact mystacial vibrissae can discern finer details in texture than a rat with 1 remaining vibrissa (Armstrong-James, 1993). The absence of synaptic zinc decreased spatial acuity but did not abolish the ability for ZnT3 KO mice to discriminate between textures.

As already described, synaptic zinc is also a potent inhibitor of NMDA receptors. Under normal physiological conditions, the concentration of zinc within the synapse is estimated to be in the nanomolar range (Paoletti et al., 1997). 1~10 nM of zinc is sufficient to inhibit NR2A containing NMDA receptors in a voltage-independent manner (Chen et al., 1997). The inhibition of NR2A receptors becomes concentration- and voltage-dependent at 1~100 μM of zinc, while NR2B receptors are almost completely deactivated in a voltage independent manner at this concentration (Chen et al., 1997; Rachline et al., 2005). The dynamic regulation of NMDA receptor activity may provide the mechanism by which synaptic zinc modulates neurotransmission within the barrel cortex. A model to this effect is proposed as follows: At rest, spontaneous release of synaptic zinc maintains tonic inhibition of NR2A receptors to prevent generalization of spontaneous activity; during natural sensory stimulation, the concentration of synaptic zinc rises and dynamically modulates NR2A receptor activity to facilitate intracortical integration of sensory information; in response to sensory deprivation, the density of vesicular zinc and zincergic terminals rise, and correspondingly, an increased amount of zinc is released spontaneously, inhibiting both NR2A and NR2B receptors to promote synaptic depression.

The model proposed above would account for the sensory deprivation-induced increase in synaptic zinc levels within layers II/III but not layer IV. Sensory deprivation, through trimming or plucking of vibrissae (3-7 days), causes depression of responses to stimulation of the regrown vibrissae, mainly in layers II/III (Glazewski et al., 1998). This depression is generated by lateral inhibition from neighbouring spared vibrissae domains as well as by a reduction of layer IV to II/III activity (Glazewski and Fox, 1996; Fox,

2002). While thalamocortical input into in layer IV is unaffected by sensory deprivation, there is a reduction in the size of the layer IV cortical domain (Skibinska et al., 2000). That is, short latency (5-8 ms) stimulation-evoked responses in layer IV are not sensitive to sensory deprivation, while a large number of neurons expected to respond at longer latencies (9-14 ms) are silenced following deprivation (Glazewski et al., 1998). The dramatic deprivation-induced increase in synaptic zinc levels may mediate this depression of intracortical activity within layer IV.

Synaptic zinc may modulate the layer IV responses via a variety of mechanisms. As mentioned, synaptic zinc may inhibit NMDA receptor activity and prevent experience-dependent modulation of synaptic efficacy (Peters et al., 1987; Rema et al., 1998; Paoletti and Neyton, 2007). AMPA receptor mediated thalamocortical responses would not be attenuated by increased levels synaptic zinc since micromolar concentrations of zinc can potentiate AMPA receptors activity. Calcium-permeable AMPA and NMDA, and voltage-gated calcium channels may facilitate entry of zinc into the postsynaptic neuron (Hollmann et al 1991; Koh and Choi, 1994; Yin et al 1998; Sensi et al., 1999). This allows the increase in the level of zinc in the synaptic cleft to potentially activate a number of signalling pathways, including those mediated by CaMKII, PKC, and cAMP (Baba et al., 1991; Legyel et al., 2000; Klein et al., 2002). CaMKII is of particular interest. T286A mutant mice lack functional CaMKII, and do not show the decrease in principal whisker response expected following sensory deprivation (Glazewski et al., 1998).

Recently, it has been demonstrated that synaptic zinc may activate a potential postsynaptic zinc receptor, GPR-39. Within the cochlear nucleus, zinc activation of

GPR39 can initiate the synthesis of the endocannabinoid 2-AG and subsequently inhibit presynaptic glutamate release (Perez-Rosello et al., 2013). Research examining the role of endogenous cannabinergic neurotransmission in the barrel cortex is sparse, but existing data do suggest that suppression of endocannabinoid receptor 1 (CB1) in the barrel cortex results in increased cortical activity in response to vibrissa stimulation (Patel et al., 2002). Synaptic zinc may mediate endocannabinoid signalling within the barrel cortex to regulate presynaptic glutamate release.

5.4 Future directions

To address the limitation associated with using ZnT3 KO mice as a model for the absence of synaptic zinc, *in vivo* manipulation of synaptic zinc levels is required to demonstrate that zinc indeed modulates barrel cortex-dependent behaviour. Preliminary evidence suggests that systemic circulation of the zinc chelator clioquinol in mice decreases synaptic zinc concentration throughout the neocortex and impairs texture-discrimination (unpublished data). However, a more targeted and acute approach to removing synaptic zinc in the barrel cortex is necessary. This can be achieved with implantation of osmotic mini-pumps that deliver zinc chelating compounds to the barrel cortex. The texture-discrimination task described in Chapter 3 allows for repeated assessment of the same animal without contamination from previous exposure (Appendix A). Texture discrimination ability can be assayed prior to installation of osmotic pumps, during delivery of zinc chelators, and following the depletion of osmotic pump stores of zinc chelators to assess for the loss and recovery of sensitivity. Recent development in the design of zinc chelators has provided compounds suitable for *in vivo* manipulation of zinc levels. ZX1 is a novel extracellular zinc chelator that can sequester synaptic zinc with

sufficient affinity and speed to block zincergic signalling (Pan et al., 2011; Radford and Lippard 2013). The efficacy of ZX1 has been demonstrated in a hippocampal slice preparation, and has been found to be sufficient to prevent zincergic activation of presynaptic LTP in mossy fibre terminals (Pan et al., 2011).

To establish the mechanism through which synaptic zinc affects barrel cortex function, texture discrimination performance can be assayed following application of agonists and antagonists of potential synaptic zinc targets. CB1 receptor antagonist SR141716 can be applied to disrupt zinc activation of endocannabinoid signalling pathways (Terranova et al., 1996). Preliminary assessment of CB1 KO mice suggest that endocannabinoid signalling plays a similar role as synaptic zinc in allowing for fine discrimination of vibrissal sensory input. Further, Ifenprodil, a NR2B antagonist, and NVP-AAM007, a NR2A antagonist, can be used to assess the effect of zinc on NMDA receptor activity in the barrel cortex. Although artificial application of NMDA antagonists is not expected to replace the potentially dynamic release of synaptic zinc and subsequent selective inhibition of NR2A receptors *in vivo*, the hypothesis that synaptic zinc dynamically inhibits NR2A and NR2B receptors to facilitate sensory integration in the barrel cortex can be tested. Low level inhibition of NR2A receptors that simulates its tonic inhibition by synaptic zinc may increase texture discrimination sensitivity in ZnT3 KO mice. NR2B inhibition across the entire barrel cortex may simulate increased synaptic zinc release in response to sensory deprivation and result in depression of cortical activity and loss of texture discrimination ability.

VSD imaging with the manipulations proposed above – application of ZX1 zinc chelator and NR2A, NR2B, and CB1 antagonists on ZnT3 KO and WT mice – can be

used to support behavioural data and further examine the role of synaptic zinc in the propagation of stimulation-evoked activity in the barrel cortex. Chelating extracellular zinc in WT mice is expected to prolong the evoked responses similar to what was reported in ZnT3 KO mice. Inhibition of CB1 receptors in WT mice or application of its agonist to KO mice will reveal the involvement of endocannabinoids in zinc signalling. Application of NR2A and NR2B antagonists in ZnT3 KO mice will reveal if NMDA receptor inhibition by zinc contributes to the altered cortical responses observed in Chapter 4.

Electrophysiological examination of barrel cortex slice preparations under different zinc conditions is required to further understand the significance of experience-dependent regulation of synaptic zinc levels in the barrel cortex. The amount of vesicular zinc in the barrel cortex can be manipulated genetically, chemically, and behaviourally. Increased levels of synaptic zinc can be induced by removing the whiskers of mice for a duration prior to testing, or by the addition of zinc into the bath media. Removal of zinc from the barrel cortex can be achieved through using ZnT3 KO mice or the addition of membrane permeable or impermeable zinc chelators. The development of fluorescent zinc probes that are extremely sensitive (pKa ~ pM levels; Kwon et al., 2012) and ones that can transiently detect mobile extracellular zinc (Radford et al., 2013) will allow for visualization of zinc release and examination of the relationship between vesicular zinc concentration and amount of zinc released. The source of zincergic terminals in layer IV following sensory deprivation can be located by observing zinc-induced fluorescence in layer IV following stimulation of afferent neurons. LTP/LTD induction and maintenance, and depression of layer IV – II/III responses that

typically results from sensory deprivation can be examined following manipulation of synaptic zinc levels. Lastly, the mechanism through which synaptic zinc may regulate barrel cortex responses can be examined through observing the effects of glutamatergic and endocannabinoid antagonists on the propagation of stimulation-evoked responses throughout the barrel cortex.

Responses to sensory deprivation within the visual cortex are similar to those measured in the somatosensory cortex. Deprivation results in an immediate depression of cortical activity in the deprived domains, followed by the potentiation of responses in spared, active domains. The experience-dependent alteration of synaptic zinc levels is expressed in both the visual and barrel cortices as well. This would suggest that synaptic zinc performs similar functions within both primary sensory cortices. Given that the results in this thesis suggest that synaptic zinc mediates the integration of vibrissal sensory input in the barrel cortex, synaptic zinc may regulate the acuity with which the visual cortex processes visual information as well. To test for this possibility, a computer-based, two-alternative, forced-choice visual discrimination task (Prusky et al., 1998) can be performed to assess the threshold of visual spatial acuity in mice following manipulation of synaptic zinc levels within the visual cortex.

5.5 Conclusion

What may be considered as a unique characteristic of biological systems is that repeated presentation of an identical stimulus does not elicit identical responses from an organism. "Hebbian" forms of plasticity predict that activity itself alters the synaptic efficacy of connections within the stimulated network. Homeostatic, and other non-Hebbian, forms of plasticity, where neuronal excitability is regulated by intrinsic functions, also exist.

Since the pioneering studies of visual cortex plasticity in the 1960s, it is now obvious that cortical plasticity, even in adults, is an inherent property of the nervous system. The brain is constantly processing sensory information from the environment and adapting to it to produce the optimal response. Understanding the myriad of modulators and mechanisms that govern sensory processing and plasticity is essential to understanding brain function.

The results of this thesis add to the body of evidence that indicate that synaptic zinc is a potent neuromodulator. The distribution and concentration of synaptic zinc is dynamically modulated by experience in the primary sensory cortices examined. The absence of synaptic zinc leads to alterations in cortical processing of sensory stimulation and associated behavioural deficits were observed. Although the precise role for synaptic zinc in, and mechanisms by which it can affect, neurotransmission in the cortex is only beginning to be elucidated, it is apparent that synaptic zinc is an integral component of cortical circuitry. Novel behavioural and chemical, methods and tools are now available for detailed examination of zincergic function in the cortex. The next decade of research in zinc neurophysiology is expected to be very exciting.

References

Adlard, P.A., Parncutt, J.M., Finkelstein, D.I., and Bush, A.I. (2010). Cognitive Loss in Zinc Transporter-3 Knock-Out Mice: A Phenocopy for the Synaptic and Memory Deficits of Alzheimer's Disease? J. Neurosci. 30, 1631–1636.

Allen, C.B., Celikel, T., and Feldman, D.E. (2003). Long-term depression induced by sensory deprivation during cortical map plasticity in vivo. Nat. Neurosci. 6, 291–299.

Antonini, A., Fagiolini, M., and Stryker, M.P. (1999). Anatomical correlates of functional plasticity in mouse visual cortex. J. Neurosci. 19, 4388–4406.

Armstrong-James, M., Fox, K., and Das-Gupta, A. (1992). Flow of excitation within rat barrel cortex on striking a single vibrissa. J. Neurophysiol. 68, 1345–1358.

Armstrong-James, M., Welker, E., and Callahan, C.A. (1993). The contribution of NMDA and non-NMDA receptors to fast and slow transmission of sensory information in the rat SI barrel cortex. J. Neurosci. 13, 2149–2160.

Assaf, S.Y., and Chung, S.-H. (1984). Release of endogenous Zn2+ from brain tissue during activity. Nature 308, 734–736.

Aydemir, T.B., Blanchard, R.K., and Cousins, R.J. (2006). Zinc supplementation of young men alters metallothionein, zinc transporter, and cytokine gene expression in leukocyte populations. Proc. Natl. Acad. Sci. U.S.A. 103, 1699–1704.

Barth, A.L., McKenna, M., Glazewski, S., Hill, P., Impey, S., Storm, D., and Fox, K. (2000). Upregulation of cAMP response element-mediated gene expression during experience-dependent plasticity in adult neocortex. J. Neurosci. 20, 4206–4216.

Bear, M.F., and Kirkwood, A. (1993). Neocortical long-term potentiation. Curr. Opin. Neurobiol. 3, 197–202.

Beaulieu, C., Dyck, R., and Cynader, M. (1992). Enrichment of glutamate in zinc-containing terminals of the cat visual cortex. Neuroreport 3, 861–864.

Bell, S.G., and Vallee, B.L. (2009). The Metallothionein/Thionein System: An Oxidoreductive Metabolic Zinc Link. Biochem 10, 55–62.

Besser, L., Chorin, E., Sekler, I., Silverman, W.F., Atkin, S., Russell, J.T., and Hershfinkel, M. (2009). Synaptically released zinc triggers metabotropic signaling via a zinc-sensing receptor in the hippocampus. J. Neurosci 29, 2890–2901.

Bhalerao, S., and Kadam, P. (2010). Sample size calculation. Int. J. Ayurveda Res. 1, 55.

Bienenstock, E.L., Cooper, L.N., and Munro, P.W. (1982). Theory for the development of neuron selectivity: orientation specificity and binocular interaction in visual cortex. J. Neurosci. 2, 32–48.

Bitanihirwe, B.K.Y., and Cunningham, M.G. (2009). Zinc: The brain's dark horse. Synapse 63, 1029–1049.

Blasie, C.A., and Berg, J.M. (2002). Structure-based thermodynamic analysis of a coupled metal binding-protein folding reaction involving a zinc finger peptide. Biochemistry 41, 15068–15073.

Brecht, M. (2007). Barrel cortex and whisker-mediated behaviors. Curr. Opin. Neurobiol. 17, 408–416.

Brecht, M., Preilowski, B., and Merzenich, M. (1997). Functional architecture of the mystacial vibrissae. Behav. Brain Res. 84, 81–97.

Bresink, I., Ebert, B., Parsons, C.G., and Mutschler, E. (1996). Zinc changes AMPA receptor properties: results of binding studies and patch clamp recordings. Neuropharmacology 35, 503–509.

Brown, C.E., and Dyck, R.H. (2002). Rapid, experience-dependent changes in levels of synaptic zinc in primary somatosensory cortex of the adult mouse. J. Neurosci 22, 2617–2625.

Brown, C.E., and Dyck, R.H. (2003). Experience-dependent regulation of synaptic zinc is impaired in the cortex of aged mice. Neuroscience 119, 795–801.

Brown, C.E., and Dyck, R.H. (2004). Distribution of zincergic neurons in the mouse forebrain. J. Comp. Neurol. 479, 156–167.

Brown, C.E., and Dyck, R.H. (2005). Retrograde tracing of the subset of afferent connections in mouse barrel cortex provided by zincergic neurons. J. Comp. Neurol. 486, 48–60.

Cahusac, P., Senok, S., Hitchcock, I., Genever, P., and Baumann, K. (2005). Are unconventional NMDA receptors involved in slowly adapting type I mechanoreceptor responses? Neurosci. 133, 763–773.

Caldwell, D.F., Oberleas, D., Clancy, J.J., and Prasad, A.S. (1970). Behavioral impairment in adult rats following acute zinc deficiency. Proc. Soc. Exp. Biol. Med. 133, 1417–1421.

Carder, R.K., and Hendry, S.H. (1994). Neuronal characterization, compartmental distribution, and activity-dependent regulation of glutamate immunoreactivity in adult monkey striate cortex. J. Neurosci. 14, 242–262.

Carvell, G.E., and Simons, D.J. (1990). Biometric analyses of vibrissal tactile discrimination in the rat. J. Neurosci. 10, 2638–2648.

Carvell, G.E., and Simons, D.J. (1996). Abnormal tactile experience early in life disrupts active touch. J. Neurosci. 16, 2750–2757.

Casanovas-Aguilar, C., Christensen, M.K., Reblet, C., Martínez-García, F., Pérez-Clausell, J., and Bueno-López, J.L. (1995). Callosal neurones give rise to zinc-rich boutons in the rat visual cortex. Neuroreport 6, 497–500.

Catalano, S.M., Chang, C.K., and Shatz, C.J. (1997). Activity-dependent regulation of NMDAR1 immunoreactivity in the developing visual cortex. J. Neurosci. 17, 8376–8390.

Chemero, A., and Heyser, C. (2005). Object Exploration and a Problem with Reductionism. Synthese 147, 403–423.

Chen, N., Moshaver, A., and Raymond, L.A. (1997). Differential sensitivity of recombinant N-methyl-D-aspartate receptor subtypes to zinc inhibition. Mol. Pharmacol 51, 1015–1023.

Choi, Y.B., and Lipton, S.A. (1999). Identification and mechanism of action of two histidine residues underlying high-affinity Zn2+ inhibition of the NMDA receptor. Neuron 23, 171–180.

Chow, S.-C., Shao, J., and Wang, H. (2002). A note on sample size calculation for mean comparisons based on noncentral statistics. J. Biopharm. Stat. 12, 441–456.

Chowanadisai, W., Kelleher, S.L., and Lönnerdal, B. (2005). Maternal zinc deficiency reduces NMDA receptor expression in neonatal rat brain, which persists into early adulthood. J. Neurochem. 94, 510–519.

Christine, C.W., and Choi, D.W. (1990). Effect of zinc on NMDA receptor-mediated channel currents in cortical neurons. J. Neurosci 10, 108–116.

Cohen-Kfir, E., Lee, W., Eskandari, S., and Nelson, N. (2005). Zinc inhibition of gamma-aminobutyric acid transporter 4 (GAT4) reveals a link between excitatory and inhibitory neurotransmission. Proc. Natl. Acad. Sci. U.S.A. 102, 6154–6159.

Cole, T., Martyanova, A., and Palmiter, R.D. (2001). Removing zinc from synaptic vesicles does not impair spatial learning, memory, or sensorimotor functions in the mouse. Brain Res. 891, 253–265.

Cole, T.B., Wenzel, H.J., Kafer, K.E., Schwartzkroin, P.A., and Palmiter, R.D. (1999). Elimination of zinc from synaptic vesicles in the intact mouse brain by disruption of the ZnT3 gene. Proc. Natl. Acad. Sci. U.S.A 96, 1716–1721.

Cole, T.B., Robbins, C.A., Wenzel, H.J., Schwartzkroin, P.A., and Palmiter, R.D. (2000). Seizures and neuronal damage in mice lacking vesicular zinc. Epilepsy Res. 39, 153–169.

Colvin, R.A., Fontaine, C.P., Laskowski, M., and Thomas, D. (2003). Zn2+ transporters and Zn2+ homeostasis in neurons. Eur. J. Pharmacol. 479, 171–185.

Cousins, R.J., Liuzzi, J.P., and Lichten, L.A. (2006). Mammalian zinc transport, trafficking, and signals. J. Biol. Chem. 281, 24085–24089.

Di Cristo, G., Berardi, N., Cancedda, L., Pizzorusso, T., Putignano, E., Ratto, G.M., and Maffei, L. (2001). Requirement of ERK activation for visual cortical plasticity. Science 292, 2337–2340.

Czupryn, A., and Skangiel-Kramska, J. (1997). Distribution of synaptic zinc in the developing mouse somatosensory barrel cortex. J. Comp. Neurol. 386, 652–660.

Czupryn, A., and Skangiel-Kramska, J. (2001). Deprivation and denervation differentially affect zinc-containing circuitries in the barrel cortex of mice. Brain Res. Bull 55, 287–295.

Danscher, G., Haug, F., and Fredens, K. (1973). Effect of diethyldithiocarbamate (DEDTC) on sulphide silver stained boutons: reversible blocking of Timm's sulphide silver stain for "heavy" metals in DEDTC. Exp. Brain Res. 16, 521-532.

Danscher, G., Hall, E., Fredens, K., Fjerdingstad, E., and Fjerdingstad, E. J. (1975). Heavy metals in the amygdala of the rat: zinc, lead and copper. Brain Res. 94, 167-172.

Danscher, G. (1982). Exogenous selenium in the brain. Histochemistry 76, 281–293.

Danscher, G., Howell, G., Perez-Clausell, J., and Hertel, N. (1985). The dithizone, Timm's sulphide silver and the selenium methods demonstrate a chelatable pool of zinc in CNS: a proton activation (PIXE) analysis of carbon tetrachloride extracts from rat brains and spinal cords intravitally treated with dithizone. Histochem. 83, 419-422.

Danscher, G. (1996). The autometallographic zinc-sulfide method: a new approach in vivo creation of nanometer sized zinc sulfide crystal lattices in zinc-enriched synaptic and secretory vesicles. J. Histochem. 28:363-373

Darian-Smith, C., and Gilbert, C.D. (1994). Axonal sprouting accompanies functional reorganization in adult cat striate cortex. Nature 368, 737–740.

Dineley, K.E., Richards, L.L., Votyakova, T.V., and Reynolds, I.J. (2005). Zinc causes loss of membrane potential and elevates reactive oxygen species in rat brain mitochondria. Mitochondrion 5, 55–65.

Dräger, U.C. (1978). Observations on monocular deprivation in mice. J. Neurophysiol. 41, 28–42.

Dyck, R.H. (2003). Experience-dependent Regulation of the Zincergic Innervation of Visual Cortex in Adult Monkeys. Cerebral Cortex 13, 1094–1109.

Dyck, R.H., and Cynader, M.S. (1993). An interdigitated columnar mosaic of cytochrome oxidase, zinc, and neurotransmitter-related molecules in cat and monkey visual cortex. Proc. Natl. Acad. Sci. U.S.A. 90, 9066–9069.

Dyck, R., Beaulieu, C., and Cynader, M. (1993). Histochemical localization of synaptic zinc in the developing cat visual cortex. J. Comp. Neurol. 329, 53–67.

Ebadi, M., Iversen, P.L., Hao, R., Cerutis, D.R., Rojas, P., Happe, H.K., Murrin, L.C., and Pfeiffer, R.F. (1995). Expression and regulation of brain metallothionein. Neurochem. Int. 27, 1–22.

Ennaceur, A., and Delacour, J. (1988). A new one-trial test for neurobiological studies of memory in rats. 1: Behavioral data. Behav. Brain Res. 31, 47–59.

Erickson, J.C., Hollopeter, G., Thomas, S.A., Froelick, G.J., and Palmiter, R.D. (1997). Disruption of the metallothionein-III gene in mice: analysis of brain zinc, behavior, and neuron vulnerability to metals, aging, and seizures. J. Neurosci. 17, 1271–1281.

Etoh, S., Baba, A., and Iwata, H. (1991). NMDA induces protein kinase C translocation in hippocampal slices of immature rat brain. Neurosci. Lett. 126, 119–122.

Fagiolini, M., and Hensch, T.K. (2000). Inhibitory threshold for critical-period activation in primary visual cortex. Nature 404, 183–186.

Feldman, D.E. (2005). Map Plasticity in Somatosensory Cortex. Science 310, 810–815.

Feldmeyer, D., Brecht, M., Helmchen, F., Petersen, C.C.H., Poulet, J. F. A., Staiger, J. F., Luhmann, H. J., and Schwarz, C. (2013). Barrel cortex function. Prog. Neurobio. 103, 3-27.

Ferezou, I., Bolea, S., and Petersen, C.C.H. (2006). Visualizing the cortical representation of whisker touch: voltage-sensitive dye imaging in freely moving mice. Neuron 50, 617–629.

Fischer, Q.S., Beaver, C.J., Yang, Y., Rao, Y., Jakobsdottir, K.B., Storm, D.R., McKnight, G.S., and Daw, N.W. (2004). Requirement for the RIIbeta isoform of PKA, but not calcium-stimulated adenylyl cyclase, in visual cortical plasticity. J. Neurosci. 24, 9049–9058.

Forwood, S.E., Winters, B.D., and Bussey, T.J. (2005). Hippocampal lesions that abolish spatial maze performance spare object recognition memory at delays of up to 48 hours. Hippocampus 15, 347–355.

Fox, K. (2002). Anatomical pathways and molecular mechanisms for plasticity in the barrel cortex. Neuroscience 111, 799–814.

Frederickson, C.J. (1989). Neurobiology of zinc and zinc-containing neurons. Int. Rev. Neurobiol. 31, 145–238.

Frederickson, C.J., and Moncrieff, D.W. (1994). Zinc-containing neurons. Biol. Signals 3, 127–139.

Frederickson, C., Gibliniii, L., Rengarajan, B., Masalha, R., Frederickson, C., Zeng, Y., Lopez, E., Koh, J., Chorin, U., and Besser, L. (2006). Synaptic release of zinc from brain slices: Factors governing release, imaging, and accurate calculation of concentration. J. Neurosci. Meth. 154, 19–29.

Frederickson, C.J., Cuajungco, M.P., and Frederickson, C.J. (2005). Is zinc the link between compromises of brain perfusion (excitotoxicity) and Alzheimer's disease? J. Alzheimers Dis. 8, 155–160; discussion 209–215.

Frederickson, R.E., Frederickson, C.J., and Danscher, G. (1990). In situ binding of bouton zinc reversibly disrupts performance on a spatial memory task. Behav. Brain Res. 38, 25–33.

Frenkel, M.Y., and Bear, M.F. (2004). How Monocular Deprivation Shifts Ocular Dominance in Visual Cortex of Young Mice. Neuron 44, 917–923.

Gaither, L.A., and Eide, D.J. (2001). Eukaryotic zinc transporters and their regulation. Biometals 14, 251–270.

Galasso, S.L., and Dyck, R.H. (2007). The role of zinc in cerebral ischemia. Mol. Med. 13, 380–387.

Gilbert, C.D., and Wiesel, T.N. (1992). Receptive field dynamics in adult primary visual cortex. Nature 356, 150–152.

Glazewski, S., and Fox, K. (1996). Time course of experience-dependent synaptic potentiation and depression in barrel cortex of adolescent rats. J. Neurophysiol. 75, 1714–1729.

Glazewski, S., McKenna, M., Jacquin, M., and Fox, K. (1998). Experience-dependent depression of vibrissae responses in adolescent rat barrel cortex. Eur. J. Neurosci. 10, 2107–2116.

Gordon, J.A., and Stryker, M.P. (1996). Experience-dependent plasticity of binocular responses in the primary visual cortex of the mouse. J. Neurosci. 16, 3274–3286.

Guic-Robles, E., Jenkins, W.M., and Bravo, H. (1992). Vibrissal roughness discrimination is barrelcortex-dependent. Behav. Brain Res. 48, 145–152.

Guić-Robles, E., Valdivieso, C., and Guajardo, G. (1989). Rats can learn a roughness discrimination using only their vibrissal system. Behav. Brain Res. 31, 285–289.

Gustafson, J.W., and Felbain-Keramidas, S.L. (1977). Behavioral and neural approaches to the function of the mystacial vibrissae. Psychol Bull 84, 477–488.

Halas, E.S., and Sandstead, H.H. (1975). Some effects of prenatal zinc deficiency on behavior of the adult rat. Pediatr. Res. 9, 94–97.

Halas, E.S., Eberhardt, M.J., Diers, M.A., and Sandstead, H.H. (1983). Learning and memory impairment in adult rats due to severe zinc deficiency during lactation. Physiol. Behav. 30, 371–381.

Hammond, R. (2004). On the delay-dependent involvement of the hippocampus in object recognition memory. Neurobiol. Learn. Mem. 82, 26–34.

Haug, F.M. (1967). Electron microscopical localization of the zinc in hippocampal mossy fibre synapses by a modified sulfide silver procedure. Histochemie 8, 355–368.

Haug, F. M. (1975). On the normal histochemistry of trace metals in the brain. J. Hirnforsch. 16, 151-162.

Hershfinkel, M., Moran, A., Grossman, N., and Sekler, I. (2001). A zinc-sensing receptor triggers the release of intracellular Ca2+ and regulates ion transport. Proc. Natl. Acad. Sci. U.S.A. 98, 11749–11754.

Heynen, A.J., Yoon, B.-J., Liu, C.-H., Chung, H.J., Huganir, R.L., and Bear, M.F. (2003). Molecular mechanism for loss of visual cortical responsiveness following brief monocular deprivation. Nat. Neurosci. 6, 854–862.

Hofer, S.B., Mrsic-Flogel, T.D., Bonhoeffer, T., and Hübener, M. (2005). Prior experience enhances plasticity in adult visual cortex. Nat. Neurosci. 9, 127–132.

Hofer, S.B., Mrsic-Flogel, T.D., Bonhoeffer, T., and Hübener, M. (2006). Lifelong learning: ocular dominance plasticity in mouse visual cortex. Curr. Opin. Neurobiol. 16, 451–459.

Hollmann, M., Hartley, M., and Heinemann, S. (1991). Ca2+ permeability of KA-AMPA--gated glutamate receptor channels depends on subunit composition. Science 252, 851–853.

Howell, G.A., Welch, M.G., and Frederickson, C.J. (1984). Stimulation-induced uptake and release of zinc in hippocampal slices. Nature 308, 736–738.

Hubel, D.H., and Wiesel, T.N. (1964). Effects of monocular deprivation in kittens. Naunyn-Schmiedebergs Archiv Fur Experimentelle Pathologie Und Pharmakologie 248, 492–497.

Hubel, D.H., Wiesel, T.N., and LeVay, S. (1977). Plasticity of ocular dominance columns in monkey striate cortex. Philos. Trans. R. Soc. Lond., B, Biol. Sci. 278, 377–409.

Kaas, J.H. (1991). Plasticity of Sensory and Motor Maps in Adult Mammals. Ann. Rev. of Neurosci. 14, 137–167.

Kaas, J.H., Merzenich, M.M., and Killackey, H.P. (1983). The Reorganization of Somatosensory Cortex Following Peripheral Nerve Damage in Adult and Developing Mammals. Ann. Rev. of Neurosci. 6, 325–356.

Kantheti, P., Qiao, X., Diaz, M.E., Peden, A.A., Meyer, G.E., Carskadon, S.L., Kapfhamer, D., Sufalko, D., Robinson, M.S., Noebels, J.L., et al. (1998). Mutation in AP-3 delta in the mocha mouse links endosomal transport to storage deficiency in platelets, melanosomes, and synaptic vesicles. Neuron 21, 111–122.

Kay, A.R. (2003). Evidence for chelatable zinc in the extracellular space of the hippocampus, but little evidence for synaptic release of Zn. J. Neurosci. 23, 6847–6855.

Khalil, R., and Levitt, J.B. (2013). Zinc histochemistry reveals circuit refinement and distinguishes visual areas in the developing ferret cerebral cortex. Brain Struct. Funct. 218, 1293–1306.

Kim, T.-Y., Hwang, J.-J., Yun, S.H., Jung, M.W., and Koh, J.-Y. (2002). Augmentation by zinc of NMDA receptor-mediated synaptic responses in CA1 of rat hippocampal slices: mediation by Src family tyrosine kinases. Synapse 46, 49–56.

Kirkwood, A., Dudek, S.M., Gold, J.T., Aizenman, C.D., and Bear, M.F. (1993). Common forms of synaptic plasticity in the hippocampus and neocortex in vitro. Science 260, 1518–1521.

Klein, C., Heyduk, T., and Sunahara, R.K. (2004). Zinc inhibition of adenylyl cyclase correlates with conformational changes in the enzyme. Cell. Signal. 16, 1177–1185.

Kleinfeld, D., Ahissar, E., and Diamond, M.E. (2006). Active sensation: insights from the rodent vibrissa sensorimotor system. Curr. Opin. Neurobio. 16, 435–444.

Kodirov, S.A., Takizawa, S., Joseph, J., Kandel, E.R., Shumyatsky, G.P., and Bolshakov, V.Y. (2006). Synaptically released zinc gates long-term potentiation in fear conditioning pathways. P. Natl. A. Sci. 103, 15218–15223.

Koh, J.Y., and Choi, D.W. (1994). Zinc toxicity on cultured cortical neurons: involvement of N-methyl-D-aspartate receptors. Neurosci. 60, 1049–1057.

Komatsu, K., Kikuchi, K., Kojima, H., Urano, Y., and Nagano, T. (2005). Selective zinc sensor molecules with various affinities for Zn2+, revealing dynamics and regional distribution of synaptically released Zn2+ in hippocampal slices. J. Am. Chem. Soc. 127, 10197–10204.

Krupa, D.J., Matell, M.S., Brisben, A.J., Oliveira, L.M., and Nicolelis, M.A. (2001). Behavioral properties of the trigeminal somatosensory system in rats performing whisker-dependent tactile discriminations. J. Neurosci. 21, 5752–5763.

Kwon, J.E., Lee, S., You, Y., Baek, K.-H., Ohkubo, K., Cho, J., Fukuzumi, S., Shin, I., Park, S.Y., and Nam, W. (2012). Fluorescent Zinc Sensor with Minimized Proton-Induced Interferences: Photophysical Mechanism for Fluorescence Turn-On Response and Detection of Endogenous Free Zinc Ions. Inorg. Chem. 51, 8760–8774.

Lee, J.-M., Kim, Y.-J., Ra, H., Kang, S.-J., Han, S., Koh, J.-Y., and Kim, Y.-H. (2008). The involvement of caspase-11 in TPEN-induced apoptosis. FEBS Lett. 582, 1871–1876.

Lengyel, I., Fieuw-Makaroff, S., Hall, A.L., Sim, A.T., Rostas, J.A., and Dunkley, P.R. (2000). Modulation of the phosphorylation and activity of calcium/calmodulin-dependent protein kinase II by zinc. J. Neurochem. 75, 594–605.

Lickey, M.E., Pham, T.A., and Gordon, B. (2004). Swept contrast visual evoked potentials and their plasticity following monocular deprivation in mice. Vis. Res. 44, 3381–3387.

Linkous, D.H., Flinn, J.M., Koh, J.Y., Lanzirotti, A., Bertsch, P.M., Jones, B.F., Giblin, L.J., and Frederickson, C.J. (2007). Evidence That the ZNT3 Protein Controls the Total Amount of Elemental Zinc in Synaptic Vesicles. J. Histochem. Cytochem. 56, 3–6.

Lobner, D., Canzoniero, L.M., Manzerra, P., Gottron, F., Ying, H., Knudson, M., Tian, M., Dugan, L.L., Kerchner, G.A., Sheline, C.T., et al. (2000). Zinc-induced neuronal death in cortical neurons. Cell. Mol. Biol. (Noisy-Le-Grand) 46, 797–806.

Lopantsev, V., Wenzel, H.J., Cole, T.B., Palmiter, R.D., and Schwartzkroin, P.A. (2003). Lack of vesicular zinc in mossy fibers does not affect synaptic excitability of CA3 pyramidal cells in zinc transporter 3 knockout mice. Neurosci. 116, 237–248.

MacDonald, R.S. (2000). The role of zinc in growth and cell proliferation. J. Nutr. 130, 1500S–8S.

Martel, G., Hevi, C., Friebely, O., Baybutt, T., and Shumyatsky, G.P. (2010). Zinc transporter 3 is involved in learned fear and extinction, but not in innate fear. Learn. Memory 17, 582–590.

Massey, P.V. (2004). Differential Roles of NR2A and NR2B-Containing NMDA Receptors in Cortical Long-Term Potentiation and Long-Term Depression. J. Neurosci. 24, 7821–7828.

Mayer, M.L., and Vyklicky, L., Jr (1989). The action of zinc on synaptic transmission and neuronal excitability in cultures of mouse hippocampus. J. Physiol. (Lond.) 415, 351–365.

Meeusen, J.W., Nowakowski, A., and Petering, D.H. (2012). Reaction of metal-binding ligands with the zinc proteome: zinc sensors and N,N,N',N'-tetrakis(2-pyridylmethyl)ethylenediamine. Inorg Chem 51, 3625–3632.

Mioche, L., and Singer, W. (1989). Chronic recordings from single sites of kitten striate cortex during experience-dependent modifications of receptive-field properties. J. Neurophysiol. 62, 185–197.

Mitchell, C.L., and Barnes, M.I. (1993). Proconvulsant action of diethyldithiocarbamate in stimulation of the perforant path. Neurotoxicol Teratol 15, 165–171.

Moore, C.I. (2004). Frequency-dependent processing in the vibrissa sensory system. J. Neurophysiol 91, 2390–2399.

Mott, D.D., Benveniste, M., and Dingledine, R.J. (2008). pH-dependent inhibition of kainate receptors by zinc. J. Neurosci. 28, 1659–1671.

Murphy, K.P., Reid, G.P., Trentham, D.R., and Bliss, T.V. (1997). Activation of NMDA receptors is necessary for the induction of associative long-term potentiation in area CA1 of the rat hippocampal slice. J. Physiol. (Lond.) 504 (Pt 2), 379–385.

Nakashima, A.S., and Dyck, R.H. (2008). Enhanced plasticity in zincergic, cortical circuits after exposure to enriched environments. J. Neurosci. 28, 13995–13999.

Nakashima, A.S., and Dyck, R.H. (2009). Zinc and cortical plasticity. Brain Res. Rev. 59, 347–373.

Nakashima, A.S., and Dyck, R.H. (2010). Dynamic, experience-dependent modulation of synaptic zinc within the excitatory synapses of the mouse barrel cortex. Neuroscience 170, 1015–1019.

Nicoll, R.A., and Roche, K.W. (2013). Long-term potentiation: peeling the onion. Neuropharmacology 74, 18–22.

O'Connor, D.H., Clack, N.G., Huber, D., Komiyama, T., Myers, E.W., and Svoboda, K. (2010a). Vibrissa-based object localization in head-fixed mice. J. Neurosci. 30, 1947–1967.

O'Connor, D.H., Peron, S.P., Huber, D., and Svoboda, K. (2010b). Neural activity in barrel cortex underlying vibrissa-based object localization in mice. Neuron 67, 1048–1061.

Ou, H. (2000). Noise damage in the C57BL/CBA mouse cochlea. Hear. Res. 145, 111–122.

Outten, C.E., Tobin, D.A., Penner-Hahn, J.E., and O'Halloran, T.V. (2001). Characterization of the metal receptor sites in Escherichia coli Zur, an ultrasensitive zinc(II) metalloregulatory protein. Biochemistry 40, 10417–10423.

Palmiter, R.D. (1998). The elusive function of metallothioneins. Proc. Natl. Acad. Sci. U.S.A. 95, 8428–8430.

Palmiter, R.D., and Huang, L. (2004). Efflux and compartmentalization of zinc by members of the SLC30 family of solute carriers. Pflugers Arch. 447, 744–751.

Palmiter, R.D., Cole, T.B., Quaife, C.J., and Findley, S.D. (1996). ZnT-3, a putative transporter of zinc into synaptic vesicles. Proc. Natl. Acad. Sci. U.S.A 93, 14934–14939.

Pan, E., Zhang, X., Huang, Z., Krezel, A., Zhao, M., Tinberg, C.E., Lippard, S.J., and McNamara, J.O. (2011). Vesicular Zinc Promotes Presynaptic and Inhibits

Postsynaptic Long-Term Potentiation of Mossy Fiber-CA3 Synapse. Neuron 71, 1116–1126.

Paoletti, P., and Neyton, J. (2007). NMDA receptor subunits: function and pharmacology. Curr Opin Pharmacol 7, 39–47.

Paoletti, P., Ascher, P., and Neyton, J. (1997). High-affinity zinc inhibition of NMDA NR1-NR2A receptors. J. Neurosci 17, 5711–5725.

Paoletti, P., Vergnano, A.M., Barbour, B., and Casado, M. (2009). Zinc at glutamatergic synapses. Neuroscience 158, 126–136.

Patel, S., Gerrits, R., Muthian, S., Greene, A.S., and Hillard, C.J. (2002). The CB1 receptor antagonist SR141716 enhances stimulus-induced activation of the primary somatosensory cortex of the rat. Neurosci. Lett. 335, 95–98.

Perez-Clausell, J., and Danscher, G. (1985). Intravesicular localization of zinc in rat telencephalic boutons: a histochemical study. Brain Res. 337, 91-98.

Perez-Rosello, T., Anderson, C.T., Schopfer, F.J., Zhao, Y., Gilad, D., Salvatore, S.R., Freeman, B.A., Hershfinkel, M., Aizenman, E., and Tzounopoulos, T. (2013). Synaptic Zn2+ inhibits neurotransmitter release by promoting endocannabinoid synthesis. J. Neurosci. 33, 9259–9272.

Peters, D.P. (1978). Effects of prenatal nutritional deficiency on affiliation and aggression in rats. Physiol. Behav. 20, 359–362.

Peters, D.P. (1979). Effects of prenatal nutrition on learning and motivation in rats. Physiol. Behav. 22, 1067–1071.

Peters, S., Koh, J., and Choi, D.W. (1987). Zinc selectively blocks the action of N-methyl-D-aspartate on cortical neurons. Science 236, 589–593.

Petersen, C.C.H., Grinvald, A., and Sakmann, B. (2003). Spatiotemporal dynamics of sensory responses in layer 2/3 of rat barrel cortex measured in vivo by voltage-sensitive dye imaging combined with whole-cell voltage recordings and neuron reconstructions. J. Neurosci 23, 1298–1309.

Pham, T.A. (2004). A semi-persistent adult ocular dominance plasticity in visual cortex is stabilized by activated CREB. Learn. Memory 11, 738–747.

Polley, D.B., Kvasnák, E., and Frostig, R.D. (2004). Naturalistic experience transforms sensory maps in the adult cortex of caged animals. Nature 429, 67–71.

Prasad, A.S., Miale, A., Jr, Farid, Z., Sandstead, H.H., and Schulert, A.R. (1963). Zinc metabolism in patients with the syndrome of iron deficiency anemia, hepatosplenomegaly, dwarfism, and hypognadism. J. Lab. Clin. Med. 61, 537–549.

Prusky, G.T., West, P.W.., and Douglas, R.M. (2000). Behavioral assessment of visual acuity in mice and rats. Vis. Res. 40, 2201–2209.

Qian, J., and Noebels, J.L. (2005). Visualization of transmitter release with zinc fluorescence detection at the mouse hippocampal mossy fibre synapse. J. Physiol. (Lond.) 566, 747–758.

Qian, J., and Noebels, J.L. (2006). Exocytosis of Vesicular Zinc Reveals Persistent Depression of Neurotransmitter Release during Metabotropic Glutamate

Receptor Long-Term Depression at the Hippocampal CA3-CA1 Synapse. J. Neurosci. 26, 6089–6095.

Quaye, V.L., Shamalla-Hannah, L., and Land, P.W. (1999). Experience-dependent alteration of zinc-containing circuits in somatosensory cortex of the mouse. Brain Res. Dev. Brain Res 114, 283–287.

Quinta-Ferreira, M.E., and Matias, C.M. (2004). Hippocampal mossy fiber calcium transients are maintained during long-term potentiation and are inhibited by endogenous zinc. Brain Res. 1004, 52–60.

Rachline, J., Perin-Dureau, F., Le Goff, A., Neyton, J., and Paoletti, P. (2005). The micromolar zinc-binding domain on the NMDA receptor subunit NR2B. J. Neurosci. 25, 308–317.

Radford, R.J., Chyan, W., and Lippard, S.J. (2013). Peptide-based targeting of fluorescent zinc sensors to the plasma membrane of live cells. Chem. Sci. 4, 3080.

Raulin, J. (1869) Etudes cliniques sur la vegetation. Ann. Sci. Nat. Bot. Biol. Veg. 11,

Rema, V., Armstrong-James, M., and Ebner, F.F. (1998). Experience-dependent plasticity of adult rat S1 cortex requires local NMDA receptor activation. J. Neurosci. 18, 10196–10206.

Salazar, G., Love, R., Werner, E., Doucette, M.M., Cheng, S., Levey, A., and Faundez, V. (2004). The zinc transporter ZnT3 interacts with AP-3 and it is preferentially targeted to a distinct synaptic vesicle subpopulation. Mol. Biol. Cell 15, 575–587.

Sandstead, H.H. (2000). Causes of iron and zinc deficiencies and their effects on brain. J. Nutr. 130, 347S–349S.

Sawtell, N.B., Frenkel, M.Y., Philpot, B.D., Nakazawa, K., Tonegawa, S., and Bear, M.F. (2003). NMDA Receptor-Dependent Ocular Dominance Plasticity in Adult Visual Cortex. Neuron 38, 977–985.

Sensi, S.L., Yin, H.Z., Carriedo, S.G., Rao, S.S., and Weiss, J.H. (1999). Preferential Zn2+ influx through Ca2+-permeable AMPA/kainate channels triggers prolonged mitochondrial superoxide production. Proc. Natl. Acad. Sci. U.S.A. 96, 2414–2419.

Shatz, C.J., and Stryker, M.P. (1978). Ocular dominance in layer IV of the cat's visual cortex and the effects of monocular deprivation. J. Physiol. (Lond.) 281, 267–283.

Shen, H., Wang, F., Zhang, Y., Xu, J., Long, J., Qin, H., Liu, F., and Guo, J. (2007). Zinc distribution and expression pattern of ZnT3 in mouse brain. Biol Trace Elem Res 119, 166–174.

Shepherd, G.M.G., Pologruto, T.A., and Svoboda, K. (2003). Circuit analysis of experience-dependent plasticity in the developing rat barrel cortex. Neuron 38, 277–289.

Shoham, D., Glaser, D.E., Arieli, A., Kenet, T., Wijnbergen, C., Toledo, Y., Hildesheim, R., Grinvald, A. (1999). Imaging cortical dynamics at high spatial and temporal resolution with novel blue voltage-sensitive dyes. Neuron 24, 791-802.

Şık, A., van Nieuwehuyzen, P., Prickaerts, J., and Blokland, A. (2003). Performance of different mouse strains in an object recognition task. Behavioural Brain Res. 147, 49–54.

Simons, D.J., and Woolsey, T.A. (1979). Functional organization in mouse barrel cortex. Brain Res. 165, 327–332.

Sindreu, C., Palmiter, R.D., and Storm, D.R. (2011). From the Cover: Zinc transporter ZnT-3 regulates presynaptic Erk1/2 signaling and hippocampus-dependent memory. Proc. Nat. A. Sci.s 108, 3366–3370.

Sindreu, C.B., Varoqui, H., Erickson, J.D., and Pérez-Clausell, J. (2003). Boutons containing vesicular zinc define a subpopulation of synapses with low AMPAR content in rat hippocampus. Cereb. Cortex 13, 823–829.

Skibinska, A., Glazewski, S., Fox, K., and Kossut, M. (2000). Age-dependent response of the mouse barrel cortex to sensory deprivation: a 2-deoxyglucose study. Exp Brain Res 132, 134–138.

Slomianka, L., Danscher, G., and Frederickson, C.J. (1990). Labeling of the neurons of origin of zinc-containing pathways by intraperitoneal injections of sodium selenite. Neuroscience 38, 843–854.

Spanswick, S.C., and Sutherland, R.J. (2010). Object/context-specific memory deficits associated with loss of hippocampal granule cells after adrenalectomy in rats. Learn. Memory 17, 241–245.

Stiebler, I., Neulist, R., Fichtel, I., and Ehret, G. (1997). The auditory cortex of the house mouse: left-right differences, tonotopic organization and quantitative analysis of frequency representation. J Comp. Physio. A 181, 559–571.

Stoltenberg, M., Nejsum, L.N., Larsen, A., and Danscher, G. (2004). Abundance of zinc ions in synaptic terminals of mocha mutant mice: zinc transporter 3 immunohistochemistry and zinc sulphide autometallography. J. Mol. Histol. 35, 141–145.

Stüttgen, M.C. (2010). Toward behavioral benchmarks for whisker-related sensory processing. J. Neurosci. 30, 4827–4829.

Tagawa, Y., Kanold, P.O., Majdan, M., and Shatz, C.J. (2005). Multiple periods of functional ocular dominance plasticity in mouse visual cortex. Nat. Neurosci. 8, 380–388.

Taha, S., Hanover, J.L., Silva, A.J., and Stryker, M.P. (2002). Autophosphorylation of alphaCaMKII is required for ocular dominance plasticity. Neuron 36, 483–491.

Takeda, A., Hirate, M., Tamano, H., Nisibaba, D., and Oku, N. (2003). Susceptibility to kainate-induced seizures under dietary zinc deficiency. J. Neurochem. 85, 1575–1580.

Takeda, A., Minami, A., Yamaide, R., and Oku, N. (2004). Involvement of amygdalar extracellular zinc in rat behavior for passive avoidance. Neurosci. Lett. 358, 119–122.

Takeda, A., Tamano, H., Tochigi, M., and Oku, N. (2005). Zinc homeostasis in the hippocampus of zinc-deficient young adult rats. Neurochem. Int. 46, 221–225.

Takeda, A., Tamano, H., Imano, S., and Oku, N. (2010). Increases in extracellular zinc in the amygdala in acquisition and recall of fear experience and their roles in response to fear. Neuroscience 168, 715–722.

Takeda, T., Hosokawa, M., and Higuchi, K. (1997). Senescence-accelerated mouse (SAM): a novel murine model of senescence. Exp. Gerontol. 32, 105–109.

Terranova, J.-P., Storme, J.-J., Lafon, N., Pério, A., Rinaldi-Carmona, M., Le Fur, G., and Soubrié, P. (1996). Improvement of memory in rodents by the selective CB1 cannabinoid receptor antagonist, SR 141716. Psychopharmacology 126, 165–172.

Tupler, R., Perini, G., and Green, M.R. (2001). Expressing the human genome. Nature 409, 832–833.

Turner, T.Y., and Soliman, M.R. (2000). Effects of zinc on spatial reference memory and brain dopamine (D1) receptor binding kinetics in rats. Prog. Neuropsychopharmacol. Biol. Psychiatry 24, 1203–1217.

Vallee, B.L. (1995). The function of metallothionein. Neurochem. Int. 27, 23–33.

Vallee, B.L., and Falchuk, K.H. (1993). The biochemical basis of zinc physiology. Physiol. Rev. 73, 79–118.

Van Brussel, L., Gerits, A., and Arckens, L. (2009). Identification and localization of functional subdivisions in the visual cortex of the adult mouse. J. Comp. Neurol. 514, 107–116.

Veran, J., Kumar, J., Pinheiro, P.S., Athané, A., Mayer, M.L., Perrais, D., and Mulle, C. (2012). Zinc potentiates GluK3 glutamate receptor function by stabilizing the ligand binding domain dimer interface. Neuron 76, 565–578.

Vogt, K., Mellor, J., Tong, G., and Nicoll, R. (2000). The actions of synaptically released zinc at hippocampal mossy fiber synapses. Neuron 26, 187–196.

Wallace, H., Glazewski, S., Liming, K., and Fox, K. (2001). The role of cortical activity in experience-dependent potentiation and depression of sensory responses in rat barrel cortex. J. Neurosci. 21, 3881–3894.

Wang, Z. (2002). Localization of zinc-enriched neurons in the mouse peripheral sympathetic system. Brain Res. 928, 165–174.

Wang, Z. (2003). Zinc transporter 3 and zinc ions in the rodent superior cervical ganglion neurons. Neuroscience 120, 605–616.

Watanabe, M., Inoue, Y., Sakimura, K., and Mishina, M. (1992). Developmental changes in distribution of NMDA receptor channel subunit mRNAs. Neuroreport 3, 1138–1140.

Westbrook, G.L., and Mayer, M.L. (1987). Micromolar concentrations of Zn2+ antagonize NMDA and GABA responses of hippocampal neurons. Nature 328, 640–643.

Wiesel, T.N., and Hubel, D.H. (1963). Singel-cell responses in striate cortex of kittens deprived of visionin one eye. J. Neurophysiol. 26, 1003–1017.

Wiesel, T.N., and Hubel, D.H. (1965). Comparison of the effects of unilateral and bilateral eye closure on cortical unit responses in kittens. J. Neurophysiol. 28, 1029–1040.

Williams, K. (1996). Separating dual effects of zinc at recombinant N-methyl-D-aspartate receptors. Neurosci. Lett. 215, 9–12.

Willott, J.F., Aitkin, L.M., and McFadden, S.L. (1993). Plasticity of auditory cortex associated with sensorineural hearing loss in adult C57BL/6J mice. J Comp Neurol 329, 402–411.

Wong-Riley, M. (1979). Changes in the visual system of monocularly sutured or enucleated cats demonstrable with cytochrome oxidase histochemistry. Brain Res. 171, 11–28.

Woolsey, T.A., and Van der Loos, H. (1970). The structural organization of layer IV in the somatosensory region (SI) of mouse cerebral cortex. The description of a cortical field composed of discrete cytoarchitectonic units. Brain Res. 17, 205–242.

Wu, H.-P.P., Ioffe, J.C., Iverson, M.M., Boon, J.M., and Dyck, R.H. (2013). Novel, whisker-dependent texture discrimination task for mice. Behavioural Brain Res. 237, 238–242.

Yang, Y., Kawataki, T., Fukui, K., and Koike, T. (2007). Cellular Zn2+ chelators cause “dying-back” neurite degeneration associated with energy impairment. J. Neurosci. Res. 85, 2844–2855.

Yasuda, S., Miyazaki, T., Munechika, K., Yamashita, M., Ikeda, Y., and Kamizono, A. (2007). Isolation of Zn2+ as an endogenous agonist of GPR39 from fetal bovine serum. J. Recept. Signal Transduct. Res. 27, 235–246.

Yin, H.Z., Ha, D.H., Carriedo, S.G., and Weiss, J.H. (1998). Kainate-stimulated Zn2+ uptake labels cortical neurons with Ca2+-permeable AMPA/kainate channels. Brain Res. 781, 45–56.

APPENDIX A: TEXTURE DISCRIMINAION SUPPLEMENTAL RESULTS

A.1. Test-retest

While previous exposure to a behavioural assay is known to affect subsequent performance on the same task by the same subject, the ability to use the same behavioural task to assess loss of and recovery of function within one subject is nonetheless an asset to the experimenter. To examine the test-retest performance of mice on the novel texture discrimination task described in Chapter 3, C57BL/6 mice at 2 months of age were assayed with the same texture discrimination parameters on 2 sequential testing days.

The mice were first habituated to the testing arena for 2 days at 10 min each day. This was followed by 2 testing days separated by 24 hours (Fig 3-1; the testing day, day 3 is repeated again on day 4 with the same parameters). The total time the mice spent investigating the target textured objects during the learning and test phases of each of the 2 testing days were record to assess for changes in general level of exploration activity on retest. The percentage time the mice spent investigating the novel texture was recorded to assess for the ability to discriminate between the presented textures. As all of the textured objects are no longer novel on the second testing day, the novel object in the second test phase was defined as the object with a texture different to the texture presented on during the second learning phase.

Previous exposure did not affect general exploration activity (Fig A1-1). Previous exposure to the same texture discrimination task also did not affect the preference for the novel texture on the second testing session (Fig. A1-2). These results suggest the sensory information obtained from the previous testing session were lost 24 hours later. The

frame of reference with which mice used to assess the novelty an object is refreshed within 24 hours. Tests using shorter durations between the 2 testing days are required to determine the minimum threshold separating that is required for test-retest. However, the results reported here is sufficient to encourage repeated use of the novel texture discrimination task.

Figure A19-1: The effect of test-retest on general exploration activity

There was no significant difference in the time spent investigating textured objects between trials 1 and 2. Mice spent equal amounts of time in exploration between the first and second learning phases as well as the first and second testing phases. n = 12; error bars: standard error of the mean.

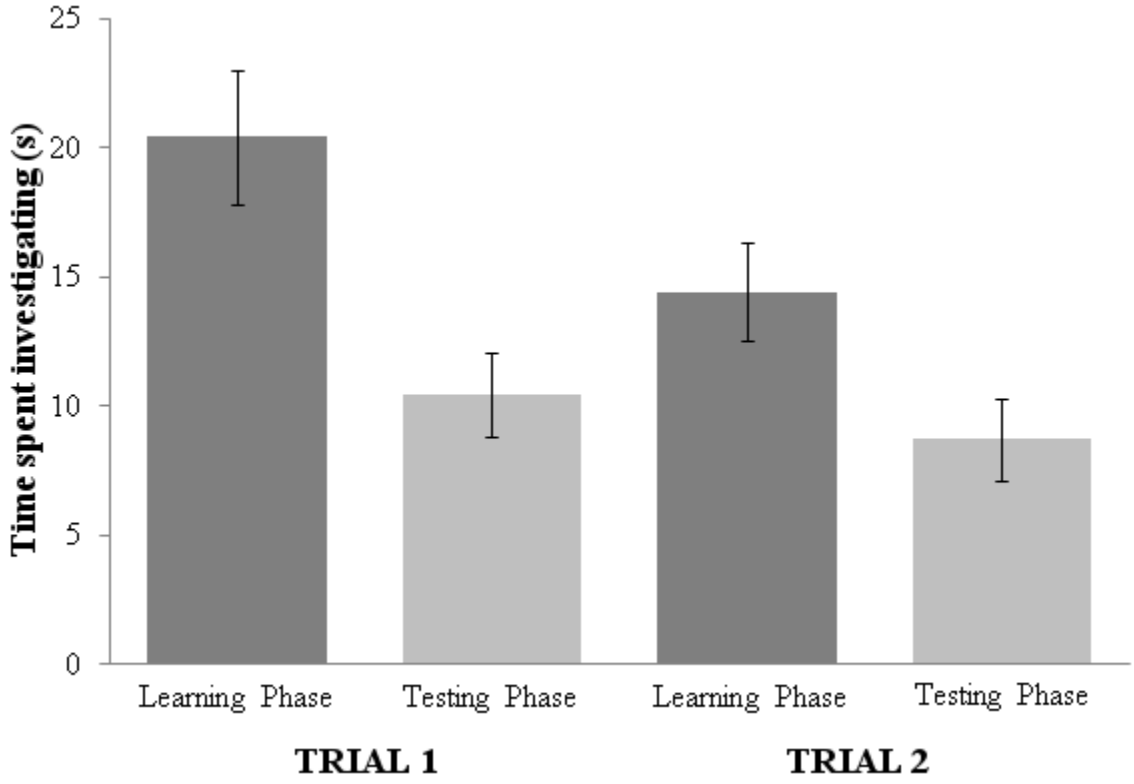
25
20
15
10
5
0
Time spent investigating (s)
Learning Phase
Testing Phase
Learning Phase
Testing Phase
TRIAL 1
TRIAL 2

Figure A1-2: The effect of test-retest on texture discrimination

Mice were able to discriminate between textures with 125 μm separation in roughness on both testing days. Repeated exposure to the same textures did not affect novel preference. n = 10; error bars represent standard error of the mean; dashed horizontal line represents chance level (50 %).

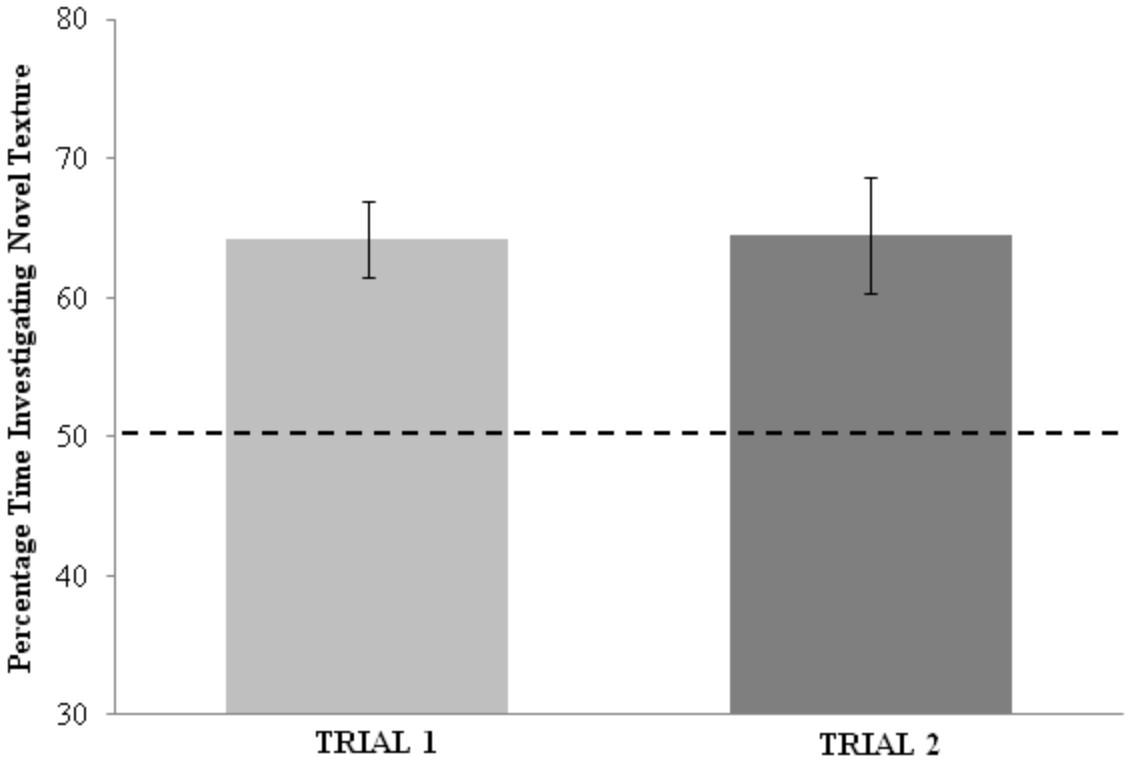
Percentage Time Investigating Novel Texture
80
70
60
50
40
30
TRIAL 1
TRIAL 2

A.2. Differential contribution by mystacial vibrissa to texture discrimination

The full complement of mouse mystacial vibrissae includes vibrissae of varying thicknesses, from the longer and thicker principle vibrissae on the caudal arc of the mystacial whisker pad to the shorter and finer vibrissae on the rostral arcs. There is evidence to suggest that vibrissae of specific lengths and widths are optimal for identification of specific attributes of an object. Macro vibrissae are critically involved in special tasks while micro vibrissae were critical for object recognition. (Brecht et al., 1997).

Integration of somatosensation from multiple mystacial vibrissae is required for the sensitivity with which mice can discriminate between textures (Guic-Robles et al., 1992). Due to the possible differential contribution by macro versus micro vibrissae to texture discrimination, the decrease in texture discrimination sensitivity observed in ZnT3 KO mice within Chapter 4 were examined in further detail. The loss of sensitivity observed in ZnT3 KO mice may be due to a loss of integration of relevant sensory input between the micro vibrissae, between the macro vibrissae, or between all mystacial vibrissae.

To examine the contribution of micro versus macro vibrissa to texture discrimination, 2-6 month old C57BL/6 mice were placed under isoflourane anesthesia and the rostral 2 arcs and/or the caudal 2 arcs of mystacial vibrissae were removed bilaterally with tweezers. Care was taken to ensure that the plucking of whiskers did not damage the whisker follicles and induce bleeding. Three days following removal of a subset of whiskers, the mice were assayed with the novel texture discrimination task described in Chapter 2.

Removal of the rostral micro vibrissae – or the caudal macro vibrissae, or only sparing of the middle arcs of mystacial vibrissae – all abolished the ability to discriminate between textures separated by 125 μm in roughness (Fig. A2-1). Further testing is required to determine if a number of other factors affect texture discrimination. Texture discrimination may rely on a minimum number of intact whiskers irregardless of type, texture discrimination sensitivity may be proportional to the number of intact whiskers, and micro versus macro vibrissae may be necessary for identification of and discrimination between specific grades of roughness. The preliminary results presented here suggest that texture discrimination is a complex ability that requires the full completement of mystacial vibrissae. One caveat, the possibility that trauma from removal of the whiskers would impair discrimination acuity, must be accounted for before definitive conclusions can be made.

Figure A2-1: The contribution of micro versus macro vibrissae on texture discrimination

Mice were not able to discriminate between textures separate by 125 μm in roughness when the rostral 2 arcs of micro vibrissa, the caudal 2 arcs of marco vibrissae, or both the rostral and caudal arcs were removed. n = 10; error bars represent standard error of the mean; dashed horizontal line represents chance level (50%).

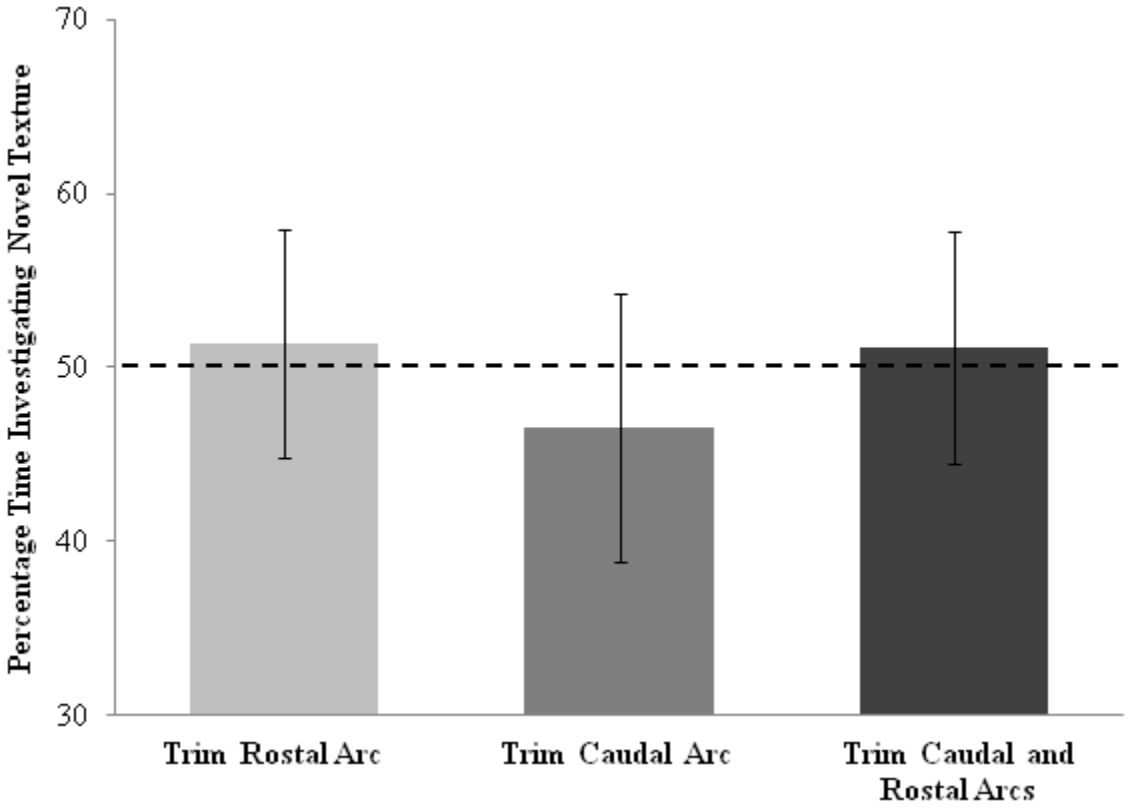
70
60
50
40
30
Percentage Time Investigating Novel Texture
Trim Rostal Arc
Trim Caudal Arc
Trim Caudal and Rostal Arcs

APPENDIX B: EXPERIENCE DEPENDENT REGULATION OF SYNAPTIC ZINC IN THE BARREL CORTEX.

Deprivation of sensory stimulation to the mystacial vibrissa is a typical method used to induce plasticity with the barrel cortex. Trimming or removing a subset of these vibrissae is thought to ultimately increase the behavioural salience of spared vibrissae via mechanisms that depress cortical response in deprived barrel fields and potentiate responses in the spared, active barrels. Removal of the mystacial vibrissae also results in a robust increase in synaptic zinc levels within layer IV of corresponding barrels (Quaye et al., 1999; Czupryn and Skangiel-Kramska, 2001a; Brown and Dyck, 2002). This experience-dependent modulation of synaptic zinc levels in the barrel cortex has been well documented and suggests that synaptic zinc plays a role in the modulation of barrel cortex plasticity (Section 1.4.2.2).

There are, however, a few inconsistencies between the electrophysiological characteristics of barrel cortex plasticity and the histochemical observation of experience-dependent regulation of synaptic zinc levels. The magnitude of response depression in deprived barrels will increase with proximity to spared barrels due to lateral competition between active and inactive vibrissae (Glazewski and Fox, 1996; Allen et al., 2003; Shepherd et al., 2003). The potentiation of stimulation-evoked cortical response in intact barrels also increases in magnitude with proximity to deprived barrels. With the assumption that synaptic zinc is intimately involved with barrel cortex plasticity, one would suspect that synaptic zinc levels within a particular barrel would be affected by the activity of neighbouring barrels. However, the experience dependent modulation of synaptic zinc levels appears to be contained within the deprived barrels (Brown and

Dyck, 2002). That is, there is a lack of observable gradient in synaptic zinc levels across the barrel fields regardless of proximity to deprived or spared barrels.

To re-explore experience dependent regulation of synaptic zinc levels within the barrel cortex, C57BL/6 mice at 2-months-of-age were separated into the following two groups: C2 spared, where all mystacial vibrissae except for C2 were removed while the mice was under isoflourane anaesthesia (n = 4), and C2 plucked, where only the C2 vibrissa was removed (n = 4). The mice were housed in standard laboratory cages under a 12 h light/dark cycle and provided standard laboratory diet and water *ad libitum*. The mice were killed three days after vibrissae removal and the brains were extracted, sectioned in the tangential plane, and processed for zinc histochemistry (Section 2.3.2). Densitometric analysis of synaptic zinc staining intensity consisted of computing the percentage difference in staining intensities between the C2 barrel and the barrels within immediately adjacent rows, immediately adjacent arcs, barrels 2 rows away, and barrels 2 arcs away.

There were no statistically significant differences ($p > 0.078$) between the groups measured. However, observable trends suggest that proximity to spared, active barrels may enhance deprivation induced increase in synaptic zinc levels (Fig. B1-1, B1-2, B1-3). These results suggest that experience dependent regulation of synaptic zinc levels within a barrel field may be affected by the activity of neighbouring barrels. Further research with more subjects and with the use of other vibrissae removal patterns are required to describe this phenomena.

Figure B1-1: Synaptic zinc stained tangential section through the barrel cortex
Sample synaptic zinc stained section of the barrel cortex of a mouse with all mystacial vibrissae except for C2 removed. Deprived barrel fields neighbouring the spared C2 barrel appear more densely stained than regions 2 barrels away from C2. Black arrow: spared C2 barrel; Grey arrow: barrel field in one of the 2 arcs neighbouring C2; White arrow: barrel field in one of the 2 rows neighbouring C2.

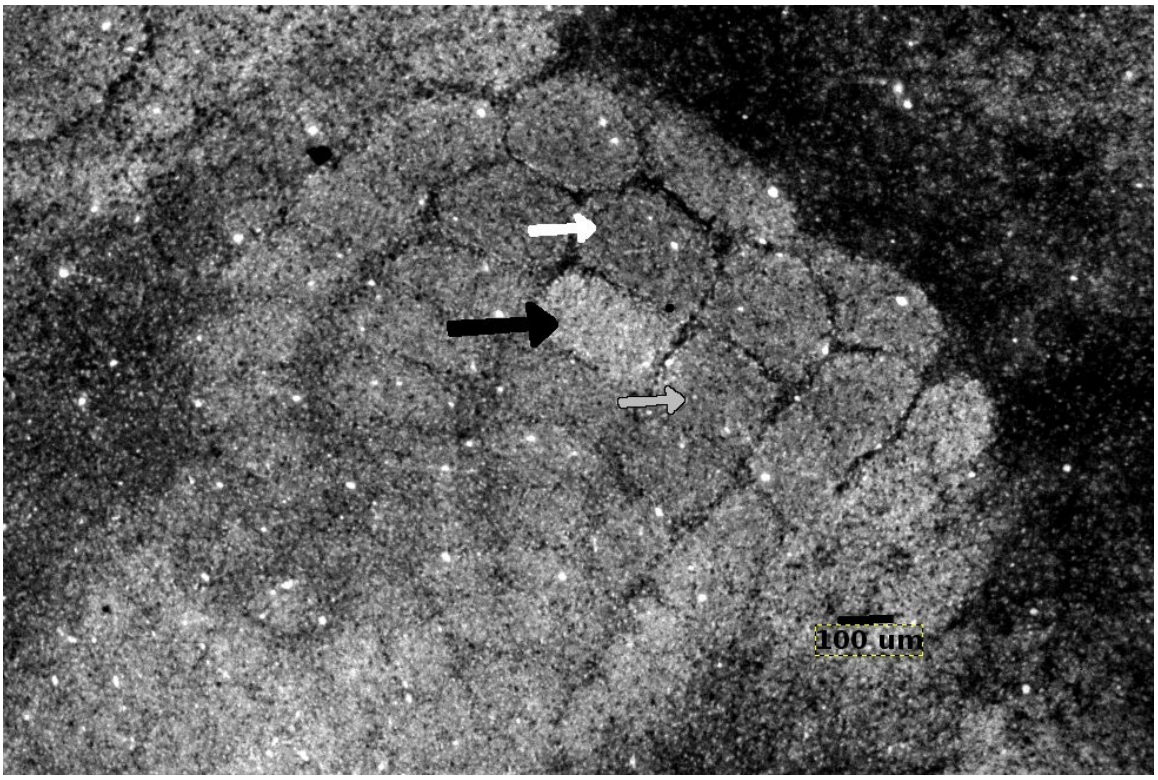
100 um

Figure B1-2: Percent change in zinc staining intensity in C2 plucked mice. There were no statistically significant differences when the increase in synaptic zinc staining intensity in the deprived C2 barrel was compared with barrels in the neighbouring row, neighbouring arc, 2 rows away, or 2 arcs away. n = 4: Error bars represent standard error of the mean.

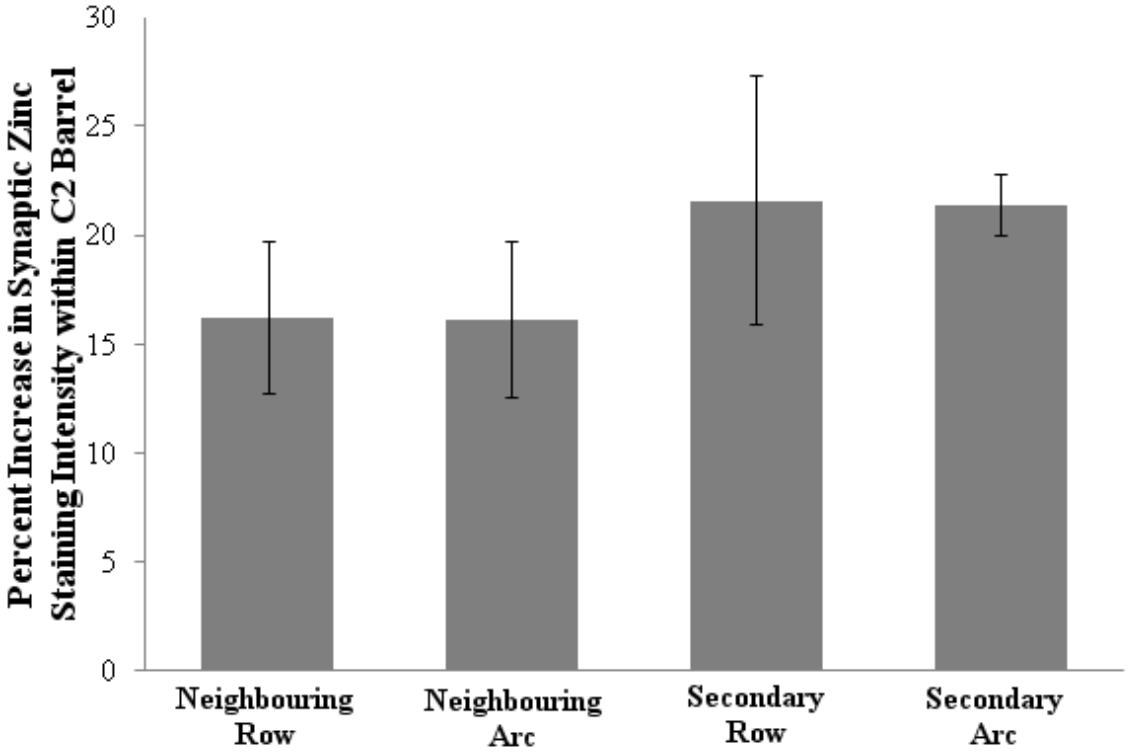
Percent Increase in Synaptic Zinc Staining Intensity within C2 Barrel
30
25
20
15
10
5
0
Neighbouring Row
Neighbouring Arc
Secondary Row
Secondary Arc

Figure B1-3: Percent change in zinc staining intensity in C2 spared mice.
There were no statistically significant differences when synaptic zinc staining intensity in the spared C2 barrel was compared with deprived barrels in the neighbouring row, neighbouring arc, 2 rows away, or 2 arcs away. n = 4: Error bars represent standard error of the mean.

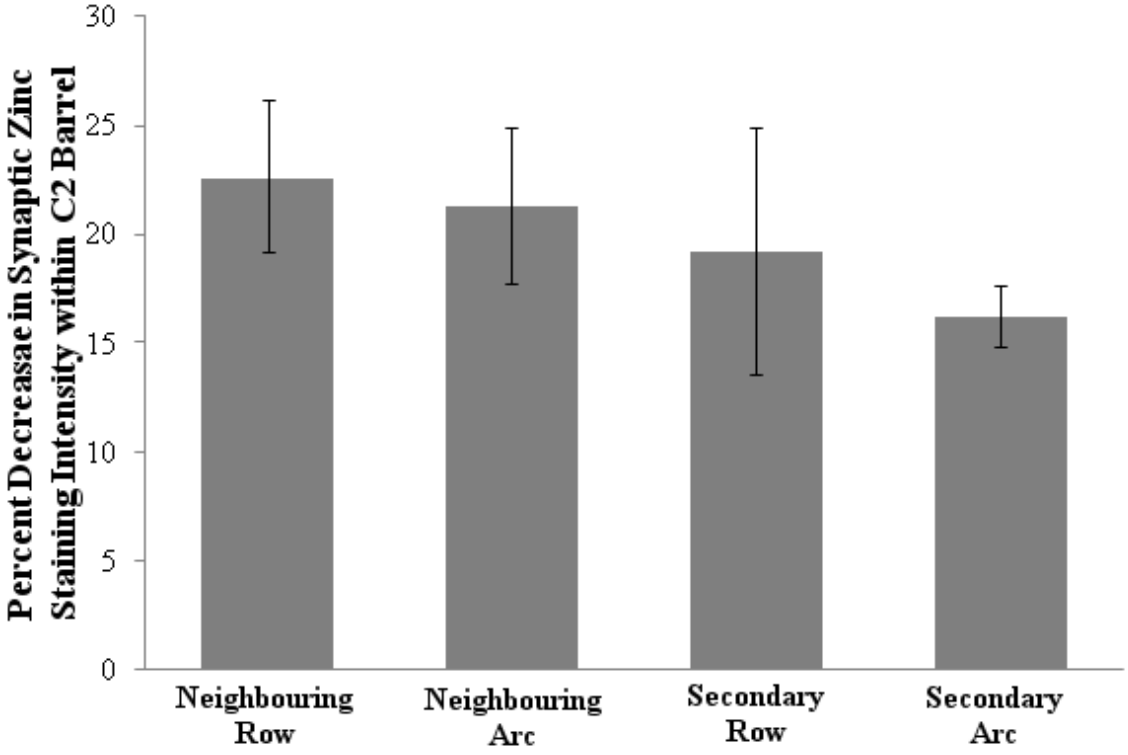
Percent Decreasae in Synaptic Zinc Staining Intensity within C2 Barrel
30
25
20
15
10
5
0
Neighbouring Row
Neighbouring Arc
Secondary Row
Secondary Arc

APPENDIX C: EXPERIENCE DEPENDENT REGULATION OF SYNAPTIC ZINC IN THE PRIMARY AUDITORY CORTEX OF MICE

The distribution of synaptic zinc in the barrel cortex and visual cortex of is regulated by sensory experience. Deprivation of vibrissal somatosensation and visual sensation leads to an increase in synaptic zinc levels within the corresponding deprived barrel and visual cortex domains. These results let to the speculation that synaptic zinc levels are dependent on sensory experience within all of the primary sensory cortices. To test this theory, the effects acoustic stimulation on synaptic zinc distribution within the primary auditory cortex (A1) of mice were examined.

The mouse A1 can be represented tonotopically through best frequency responses measured using multi-unit electrophysiological recordings (Stiebler et al., 1997). The A1 is approximately 1.5 mm in length and angled along a dorsorostral to ventrocaudal axis. The tonotopic map is organized in a gradient with best frequencies of approximately 40 kHz located on the dorsorostral tip of the A1 and 5 kHz located on the ventrocaudal end (Fig. B1-1). The following pilot study exploited the tonotopic organization of the mouse A1 to describe the effect of acoustic deprivation and stimulation on synaptic zinc levels.

C57BL/6 mice between 6 – 7 weeks of age were used. This age group was selected to avoid the natural loss of high frequency hearing observed in C57BL/6 mice greater than 2 months of age (Willott et al., 1993). The mice were maintained on a 12-hour diurnal light-dark cycle and provided with water and standard laboratory chow *ad libitum* for the duration of the experiment. The mice were housed in acoustically permeable cages positioned within in an acoustically isolated chamber. Treatment consisted of 7 days of exposure to 70 dB white noise with different frequency ranges

filtered out. 70 dB is below the typical 100 – 120 dB acoustic overstimulation used to induce trauma in mice (Ou, 2000) and should not damage the auditory sensory organs. The mice either exposed to 10-20 kHz noise (10 – 20 kHz band pass filtered white noise, n = 7), 1 – 10 kHz and 20 – 40 kHz noise (10 – 20 kHz notch filtered white noise, n = 8), or no auditory manipulations (n = 6). The animals were killed within 1 hour of the end of treatment and the brains extracted, sectioned in the coronal plane, and processed for vesicular zinc histochemistry (Section 2.3.2). Densitometric assessment of synaptic zinc distribution was performed (Section 2.3.3). The A1 was divided into thirds for assessment. The divisions are the high frequency sensitive dorsorostral third, the low frequency sensitive ventrocaudal third, and the mid frequency sensitive middle third. 10 – 20 kHz band pass filtered noise was designed to stimulate the middle third while the 10 – 20 kHz notch filtered noise was designed to stimulate the dorsorostral and ventrocaudal thirds of A1 (Fig. C1).

The distribution of synaptic zinc in A1 mirrors the pattern observed in the somatosensory and visual cortices. Layers V and VI are most densely populated with zincergic terminals and are closely followed by layer II/III, while layer IV is largely devoid of synaptic zinc. Exposure to 10 – 20 kHz noise did not alter synaptic zinc distribution in the dorsorostral and ventrocaudal thirds of A1 when compared to the control mice and mice exposed to 1 – 10 kHz and 20 – 40 kHz noise. Synaptic zinc density was noticeably lower in layer IV of middle third, 1 – 10 kHz and 20 – 40 kHz noise group when compared with control sections (Fig. C2). However, this comparison was not statistically different from each other.

Figure C1: Tonotopic organization of the mouse A1

Mouse A1 can be mapped by electrophysiological response to specific frequency bands. High frequencies are represented on the dorsorostral portion of A1 and lower frequencies on the ventrocaudal portion. Shaded area represents the area of A1 stimulated by 10 – 20 kHz pass band white noise. 5 – 10 kHz and 20 – 40 kHz noise was designed to stimulate regions of A1 outside of the shaded area.

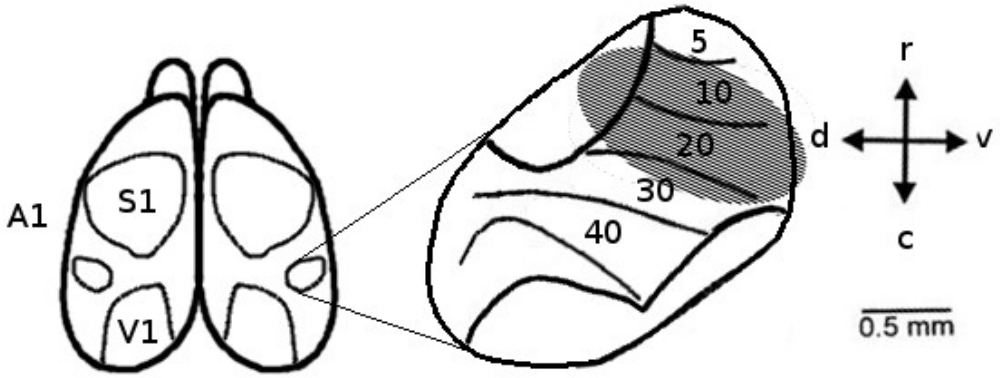
A1
S1
V1
5
10
20
30
40
d
r
v
c
0.5 mm

Figure C2: Synaptic zinc staining intensity profile for the middle third of A1

There was a lowered density of zincergic terminals in layer IV of the middle third of A1 exposed to 5 – 10 kHz and 20 – 40 kHz noise (grey solid line) when compared to control sections (black solid line). This difference was not statistically significant ($p = 0.081$). Error bars represent 95 % confidence ranges.

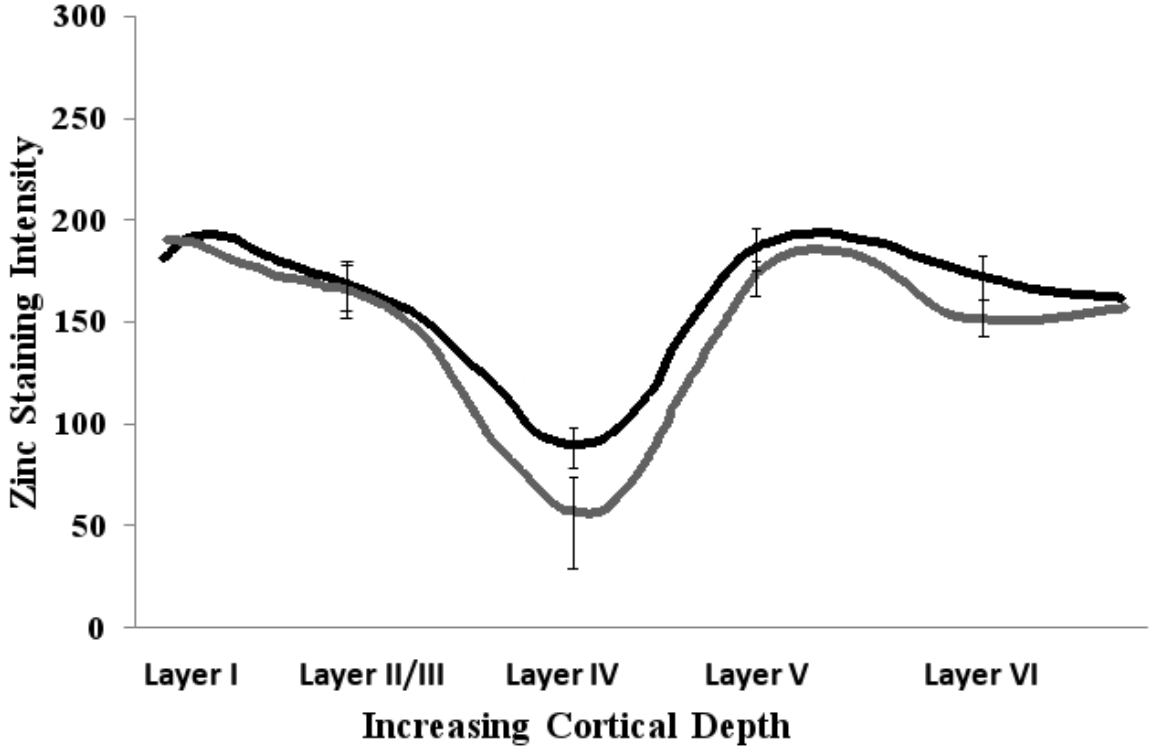
300
250
200
150
100
50
0
Zinc Staining Intensity
Layer I
Layer II/III
Layer IV
Layer V
Layer VI
Increasing Cortical Depth

The assumption was that synaptic zinc levels within A1 would respond in an experience dependent manner similar to what has been demonstrated in the barrel and visual cortices. Stimulation was expected to decrease synaptic zinc levels while deprivation increase it. However, the observable, though statistically not significant, difference in synaptic zinc levels induced in A1 was a decrease in zinc staining within the 10 – 20 kHz sensitive area of A1 following exposure to white noise with frequencies outside of this 10 – 20 kHz band.

This contradictory result illustrates the difference between the acoustic sensory deprivation/stimulation manipulation employed here and the sensory deprivation methods used in barrel and visual cortex studies. Whereas somatosensory and visual sensory manipulations consisted of deprivation through removal or occlusion of the sense organ, the auditory manipulation applied in this pilot study consisted of the presence or absence of constant simulation. The resulting trend where lack of constant stimulation in the 10-20 kHz band decreased the synaptic zinc levels within the region of A1 sensitive to these frequencies may reflect an increase in cortical activity in this area to process auditory information that is not drowned out by the constant noise outside of this frequency band. That is, 'tuning in' to the frequency band not filled by noise. This conclusion, however, is speculation and premature due to the lack of statistic significance in the findings. Methodological caveats already described in sections 2.5 and 5.2.1 also prevent further concrete conclusions from being made.

With these considerations in mind, the results of this study indicate that synaptic zinc distribution in the auditory cortex of mice is similar to those in other primary

sensory cortices. Further studies are required to determine whether experience dependent regulation of synaptic zinc levels also occurs in the auditory cortex.